

# Triggered dihadron correlations in Pb-Pb collisions from the ALICE experiment

---

**Andrew Adare**

Yale University

on behalf of

The ALICE collaboration

**Quark Matter 2011**

Annecy, FR - 24 May 2011

Yale University



# Some analysis details

## Dataset

**Pb-Pb at 2.76 TeV**

**13.5 M events after physics selection in 0-90%**

**pp reference at 2.76 TeV**

## Centrality

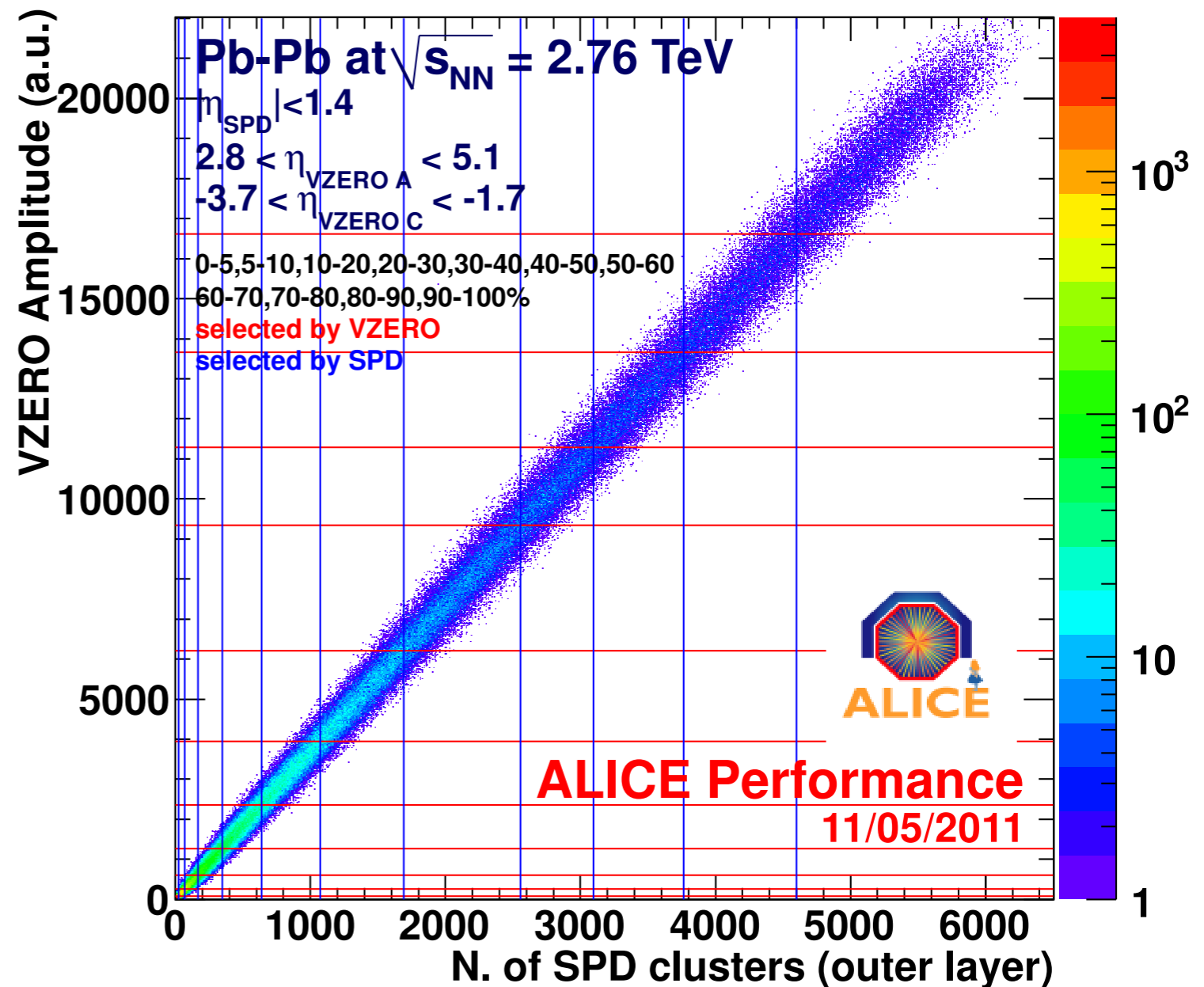
**VZERO**

**Enables 1% binning**

## Tracking

**TPC points + ITS vertex**

**= optimum acceptance + precision for correlations**



# Two-particle correlations

## Same and mixed event pair distributions

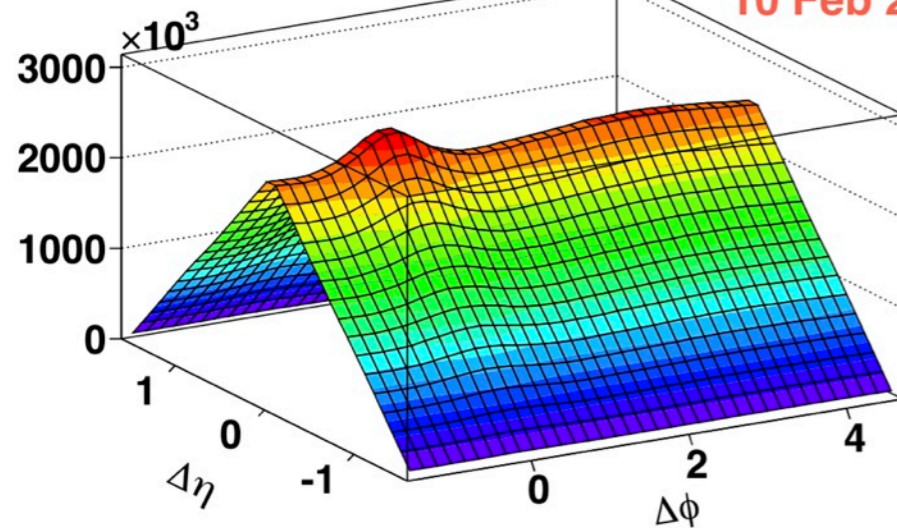
$$\Delta\phi = \phi_A - \phi_B$$

$$\Delta\eta = \eta_A - \eta_B$$

SameEv  $3.0 < p_{T,trig} < 4.0$   $2.0 < p_{T,assoc} < 3.0$  0-20%

ALICE  
performance  
10 Feb 2011

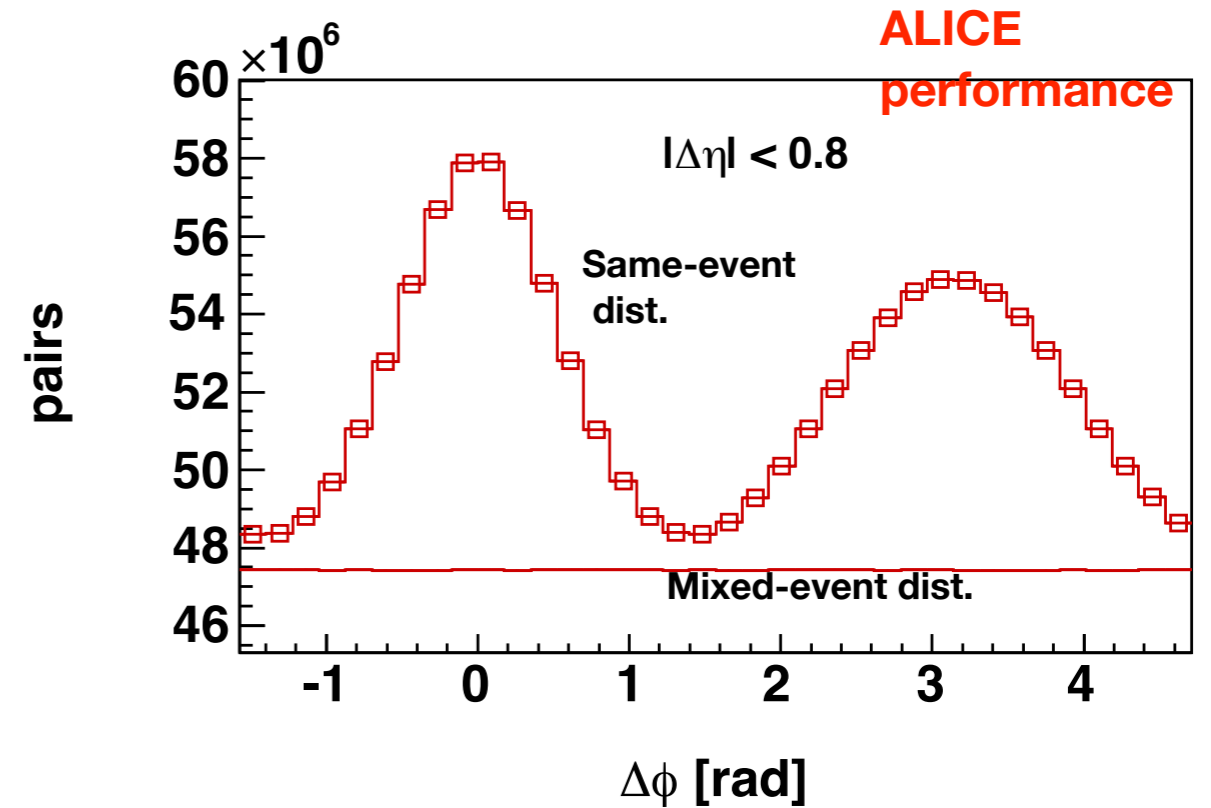
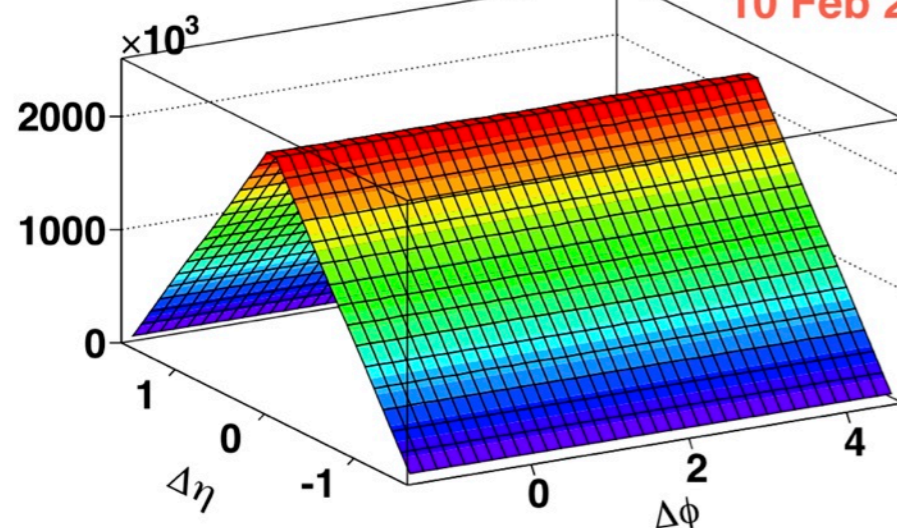
$$N_{same}^{AB}(\Delta\phi, \Delta\eta)$$



MixBkg  $3.0 < p_{T,trig} < 4.0$   $2.0 < p_{T,assoc} < 3.0$  0-20%

ALICE  
performance  
10 Feb 2011

$$N_{mixed}^{AB}(\Delta\phi, \Delta\eta)$$



## Simplest observable: correlation function

$$C(\Delta\phi) \equiv \frac{N_{mixed}^{AB}}{N_{same}^{AB}} \cdot \frac{dN_{same}^{AB}/d\Delta\phi}{dN_{mixed}^{AB}/d\Delta\phi}$$

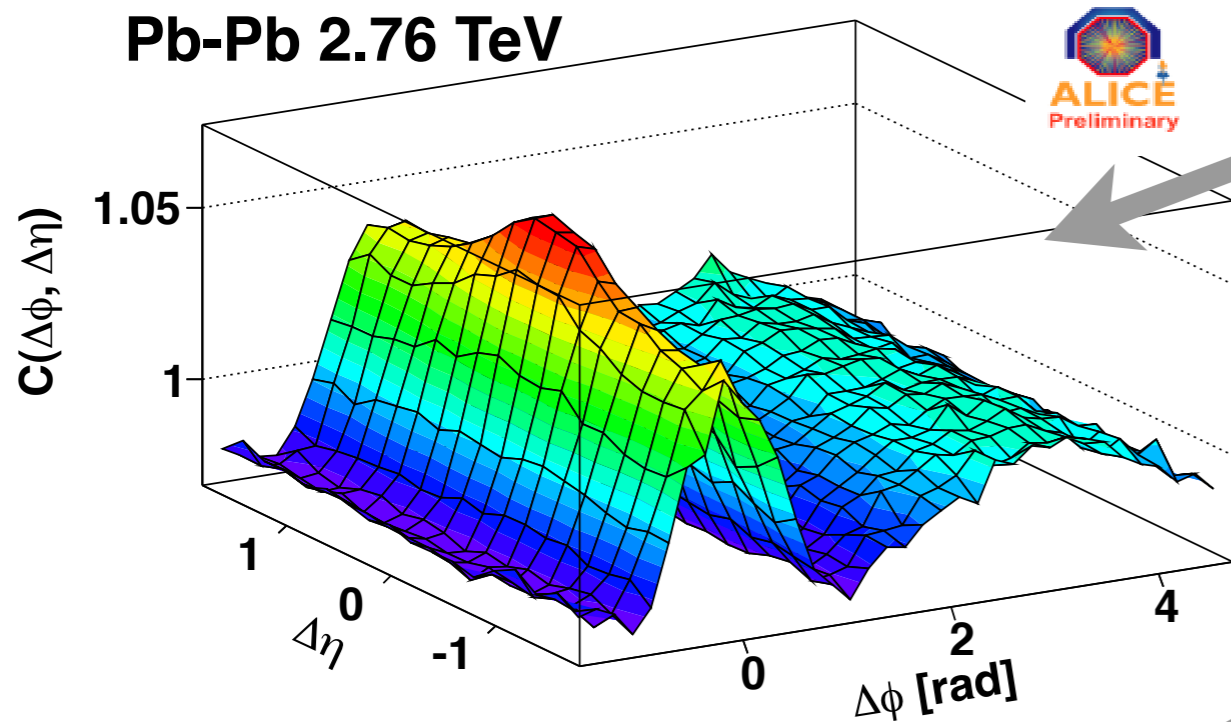
Conditional yield:  $Y \propto C(\Delta\phi) / \text{trigger particle.}$

$I_{AA}$ : the 2-particle version of  $R_{AA}$

$$I_{AA}(p_{T,trig}; p_{T,assoc}) = \frac{Y^{AA}(p_{T,trig}; p_{T,assoc})}{Y^{pp}(p_{T,trig}; p_{T,assoc})}$$

# Event structure evolution

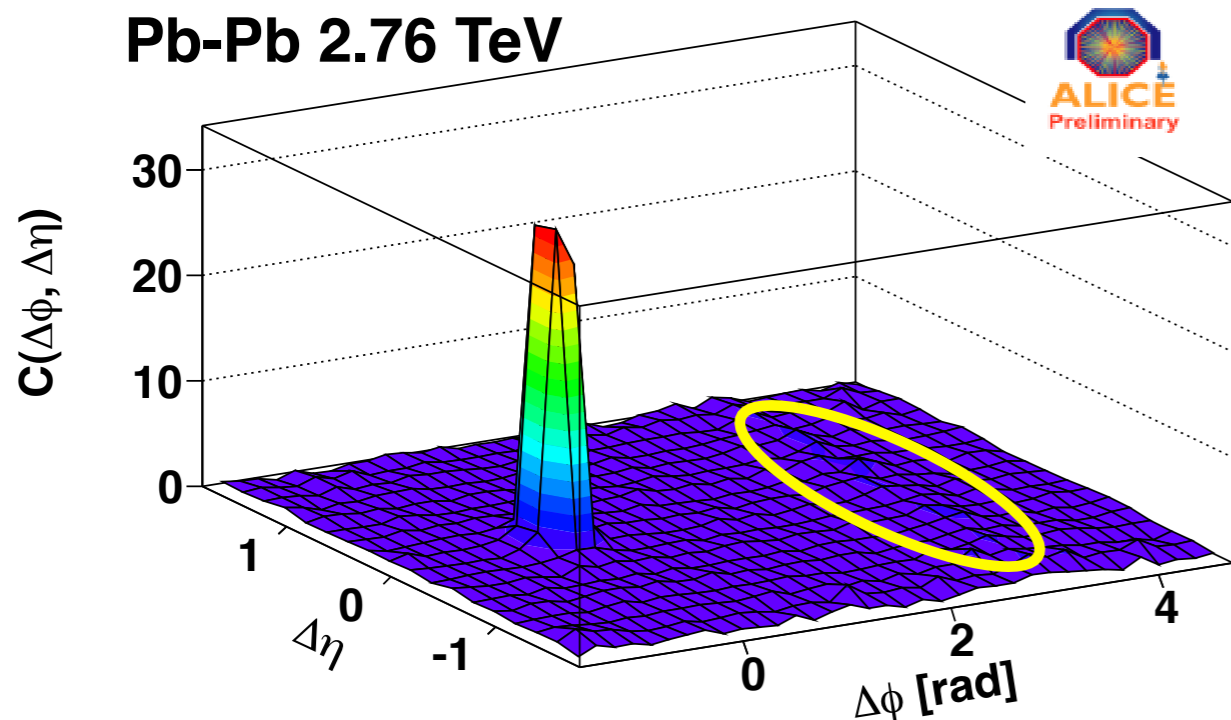
$p_T^t$  2.5-3,  $p_T^a$  2-2.5, 0-10%  
Pb-Pb 2.76 TeV



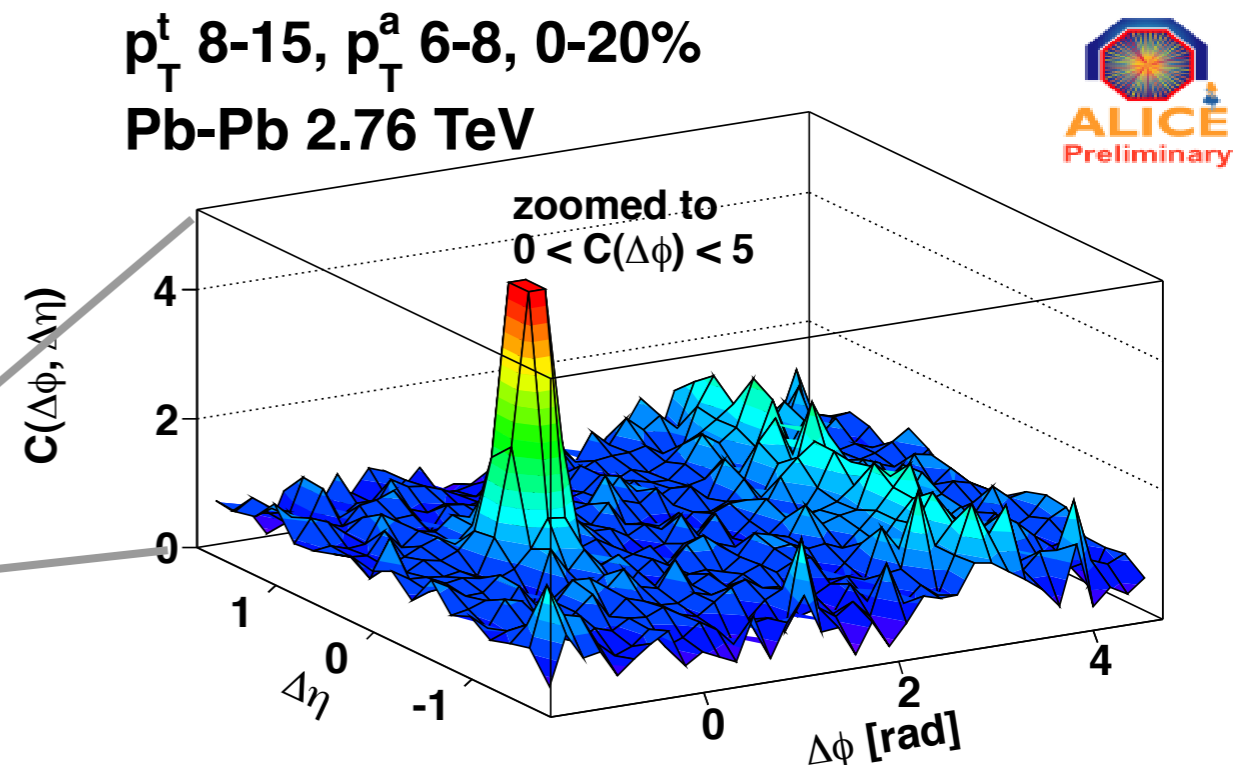
**Low-intermediate  $p_T$**   
**Distinct near-side ridge**  
**Broad away side**

**High  $p_T$ :**  
**Near side jet dominates**  
**ridge indistinct from background**  
**Elongated away-side structure**  
**from swinging recoil jet**

$p_T^t$  8-15,  $p_T^a$  6-8, 0-20%  
Pb-Pb 2.76 TeV

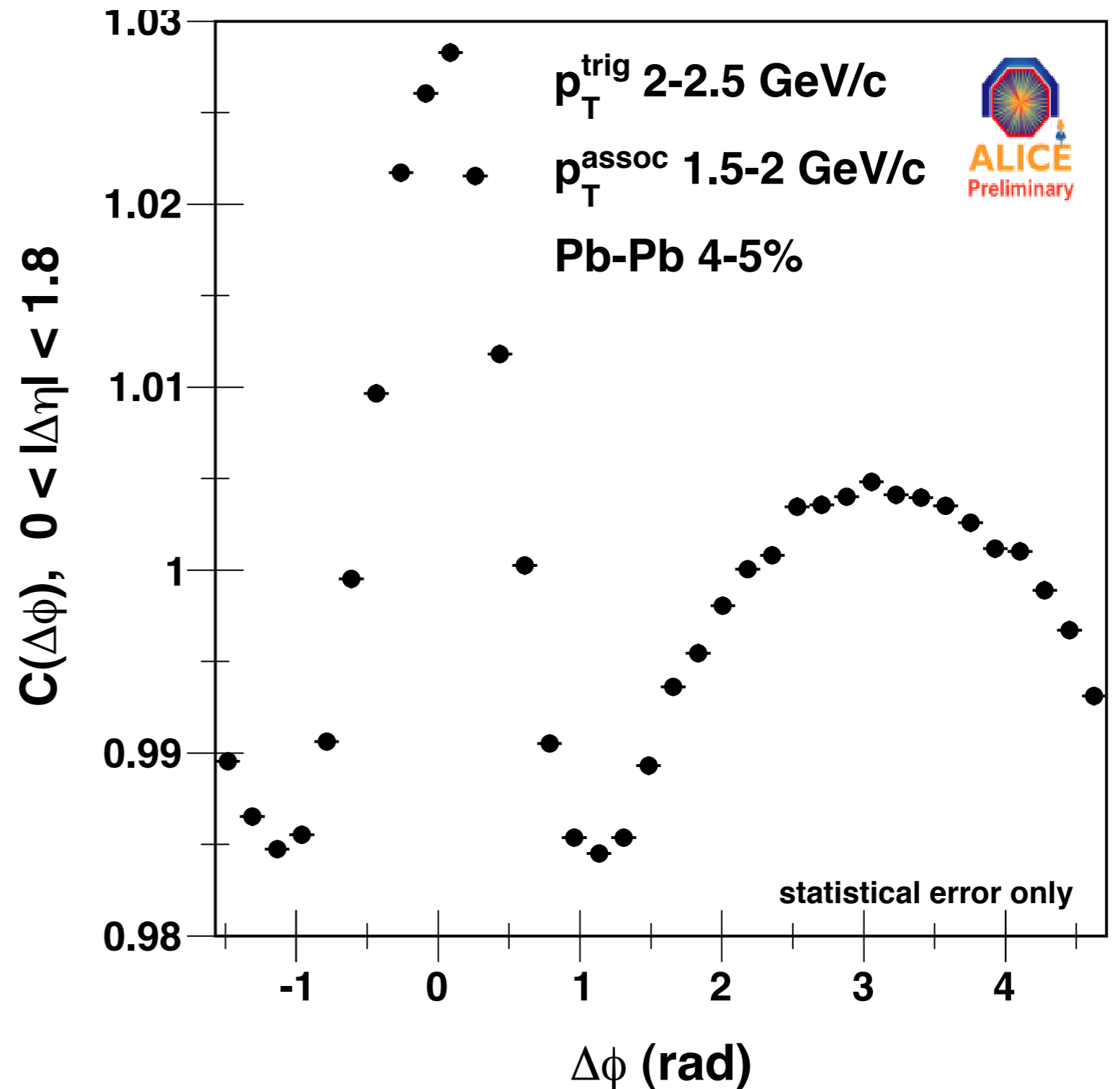


$p_T^t$  8-15,  $p_T^a$  6-8, 0-20%  
Pb-Pb 2.76 TeV



# Approaching ultracentral Pb+Pb events

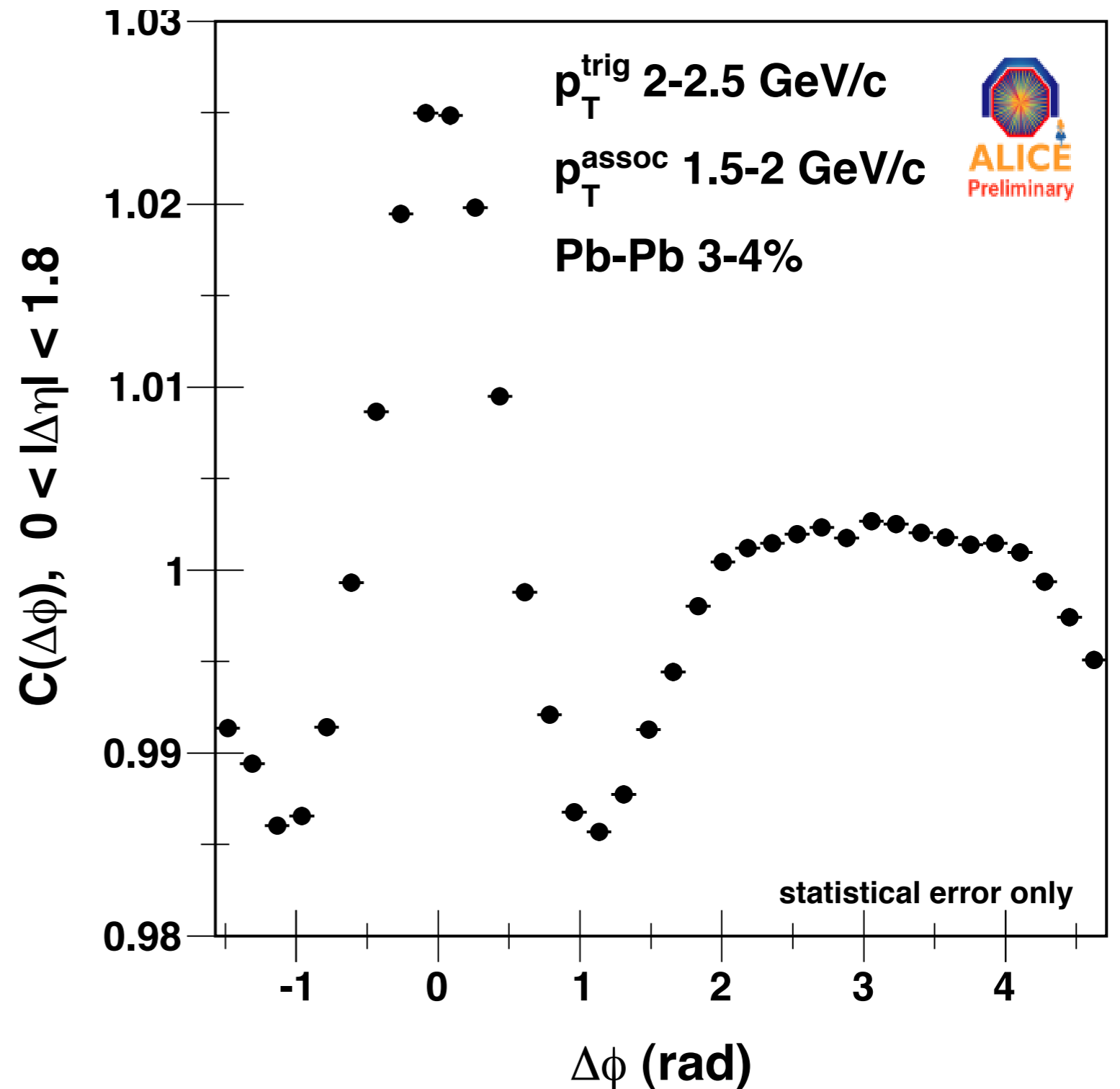
At 1-3 GeV/c, a dramatic shape evolution is observed within a small centrality range.



No background subtracted

# Approaching ultracentral Pb+Pb events

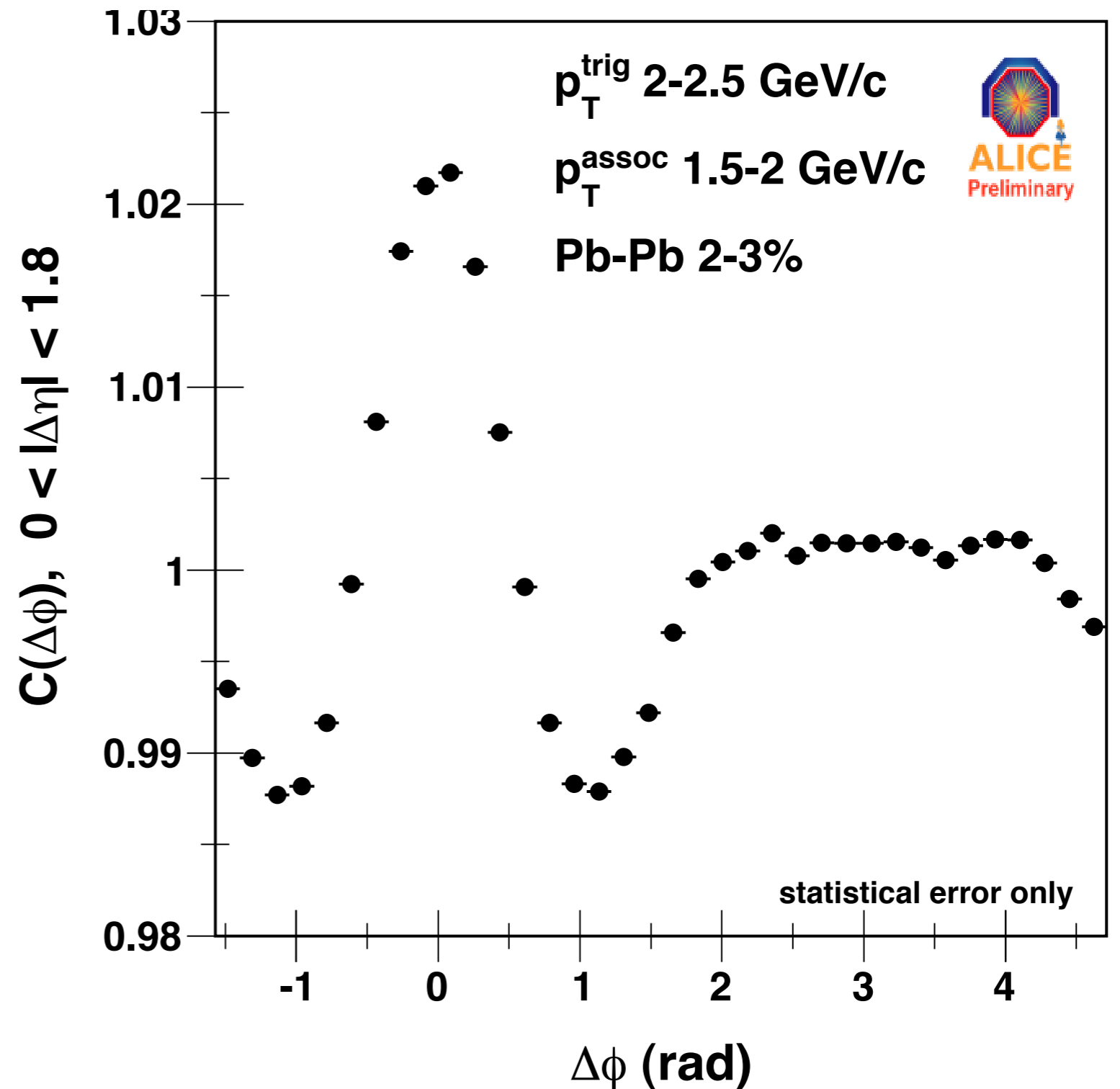
At 1-3 GeV/c, a dramatic shape evolution is observed within a small centrality range.



No background subtracted

# Approaching ultracentral Pb+Pb events

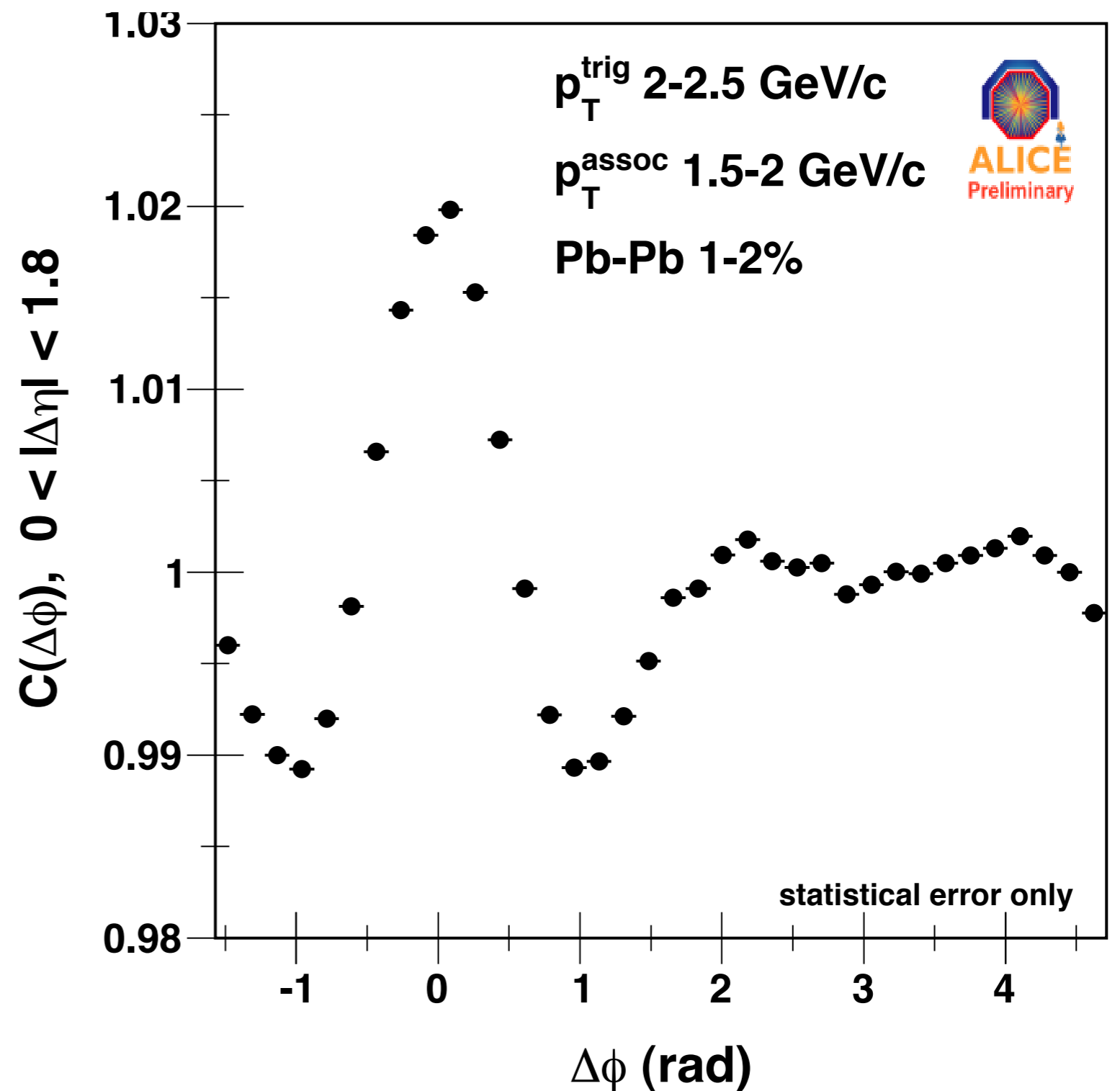
At 1-3 GeV/c, a dramatic shape evolution is observed within a small centrality range.



No background subtracted

# Approaching ultracentral Pb+Pb events

At 1-3 GeV/c, a dramatic shape evolution is observed within a small centrality range.



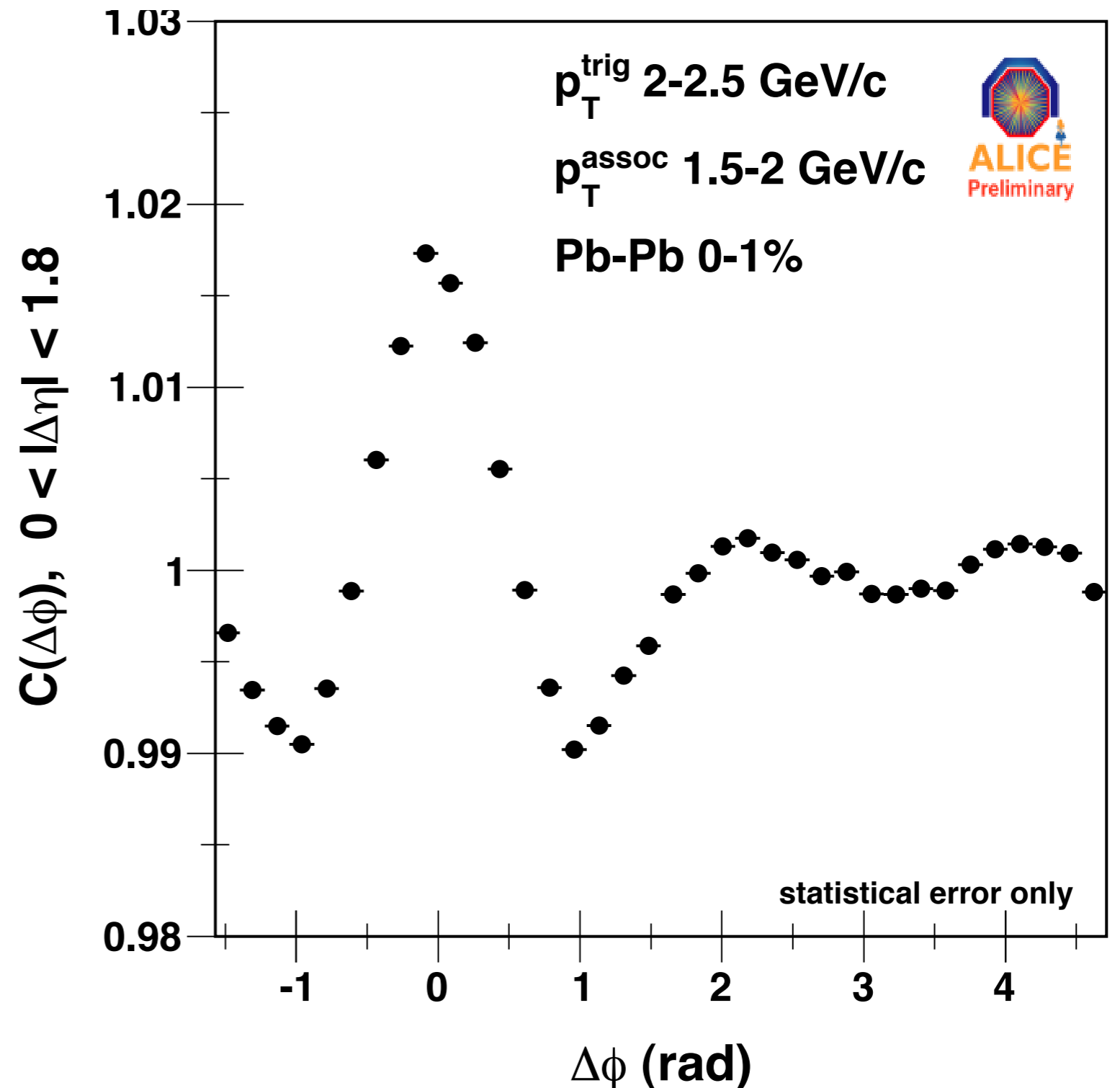
No background subtracted



# Approaching ultracentral Pb+Pb events

At 1-3 GeV/c, a dramatic shape evolution is observed within a small centrality range.

Double-peak away side structure in 1% most-central events

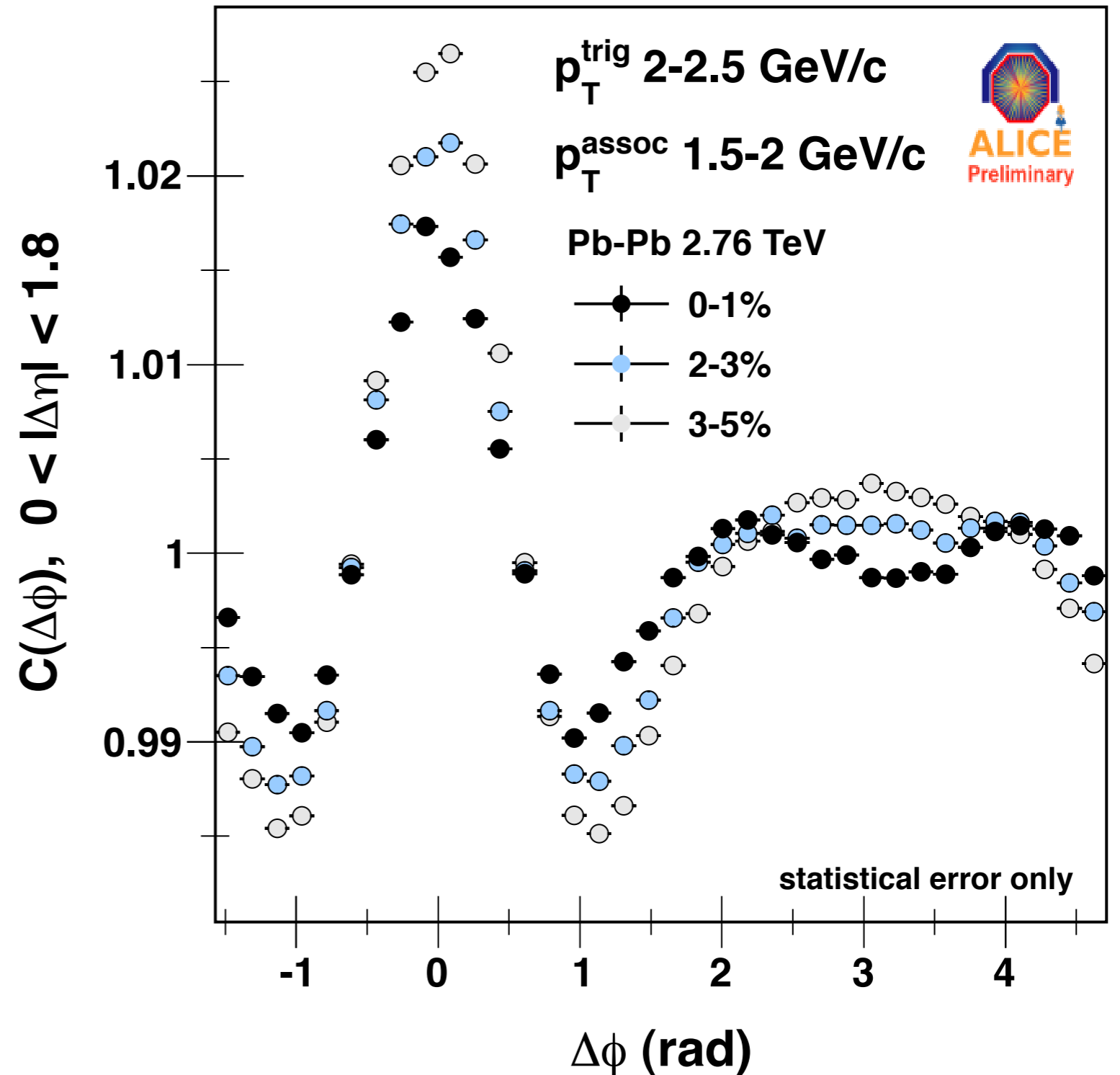


No background subtracted

# Approaching ultracentral Pb+Pb events

At 1-3 GeV/c, a dramatic shape evolution is observed within a small centrality range.

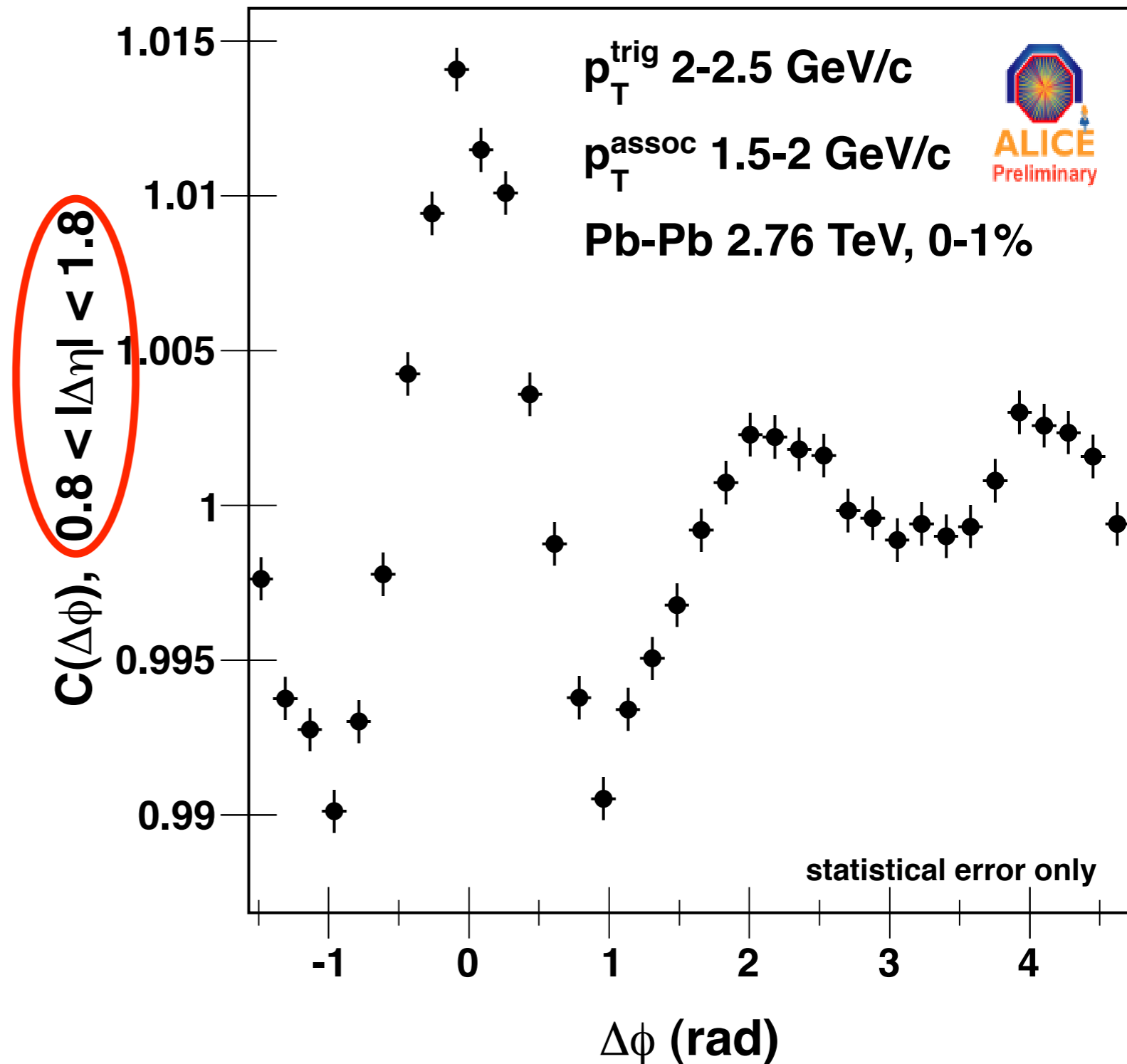
Double-peak away side structure in 1% most-central events



No background subtracted

# Fourier analysis at large $\Delta\eta$ , moderate $p_T$

Near side jet excluded by  
 $|\Delta\eta| > 0.8$  gap  
 Ridge at  $\Delta\phi=0$  remains

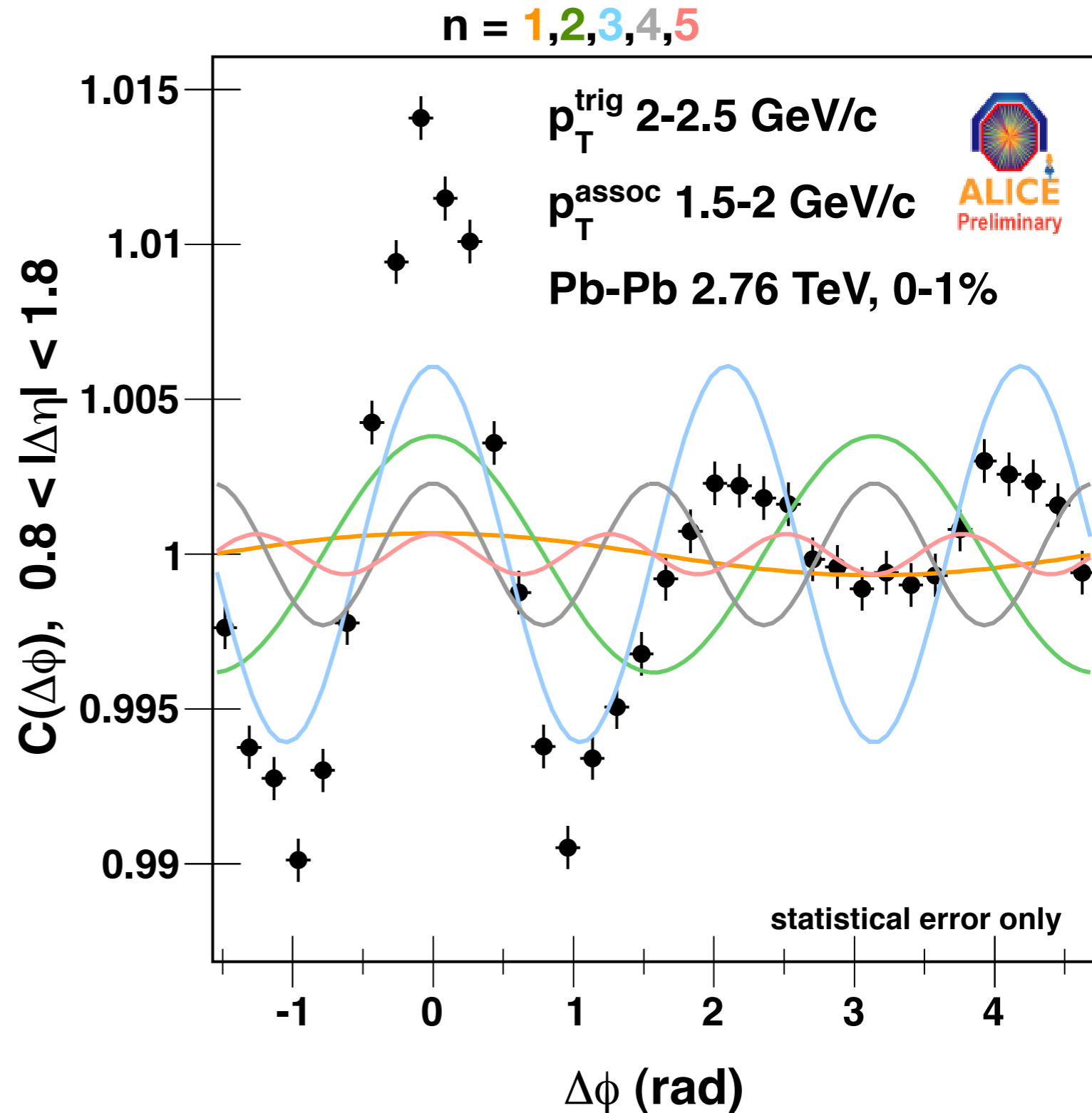


# Fourier analysis at large $\Delta\eta$ , moderate $p_T$

Near side jet excluded by  
 $|\Delta\eta| > 0.8$  gap  
 Ridge at  $\Delta\phi=0$  remains

2-particle Fourier coeffs.  
 Extract directly from  $C(\Delta\phi)$ :

$$\langle \cos n\Delta\phi \rangle = \frac{\int d\Delta\phi C(\Delta\phi) \cos n\Delta\phi}{\int d\Delta\phi C(\Delta\phi)}$$



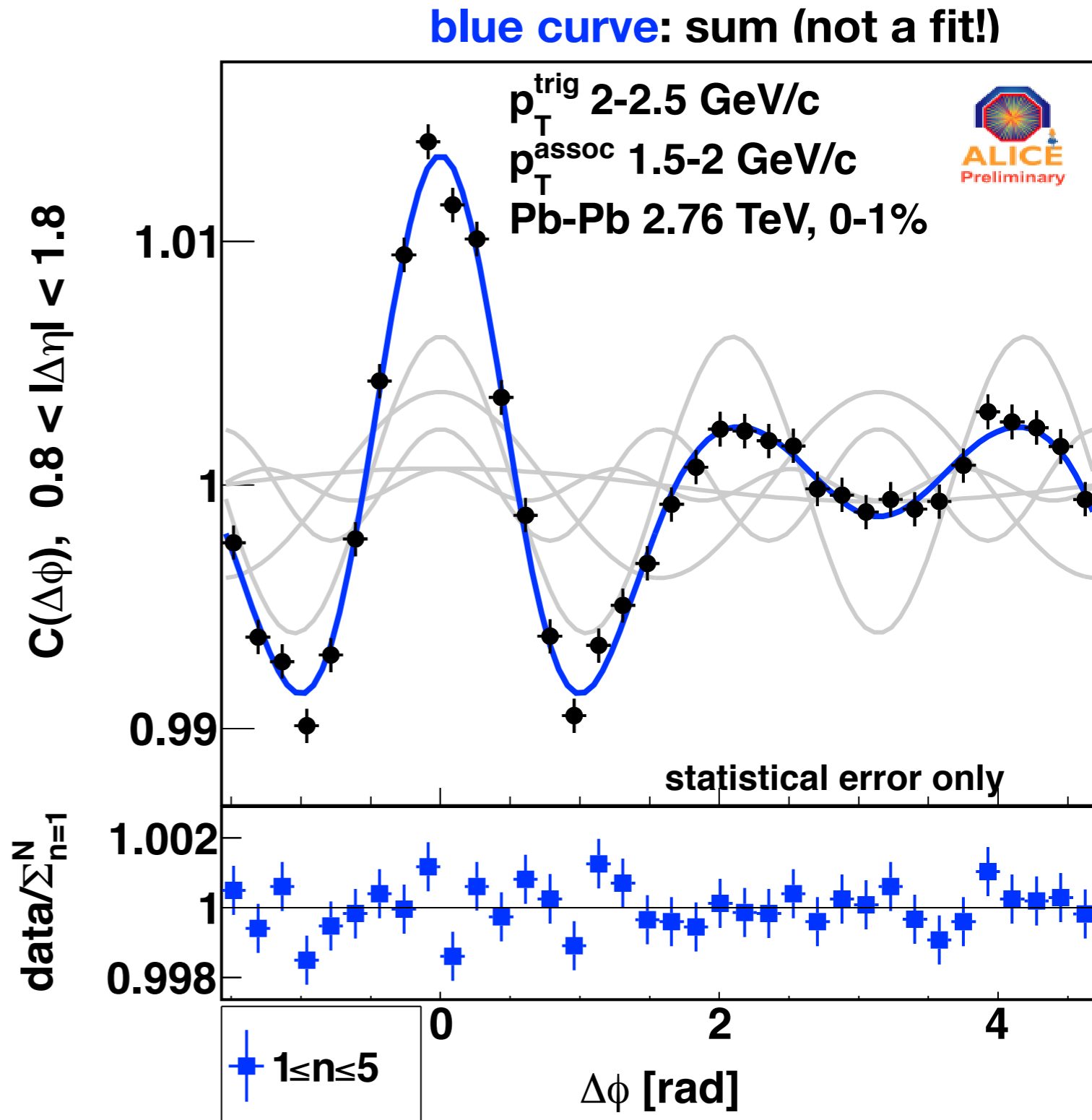
# Fourier analysis at large $\Delta\eta$ , moderate $p_T$

Near side jet excluded by  
 $|\Delta\eta| > 0.8$  gap  
 Ridge at  $\Delta\phi=0$  remains

2-particle Fourier coeffs.  
 Extract directly from  $C(\Delta\phi)$ :

$$\langle \cos n\Delta\phi \rangle = \frac{\int d\Delta\phi C(\Delta\phi) \cos n\Delta\phi}{\int d\Delta\phi C(\Delta\phi)}$$

Here, the first 5 moments describe shape at per-mille level.



# Fourier analysis at large $\Delta\eta$ , moderate $p_T$

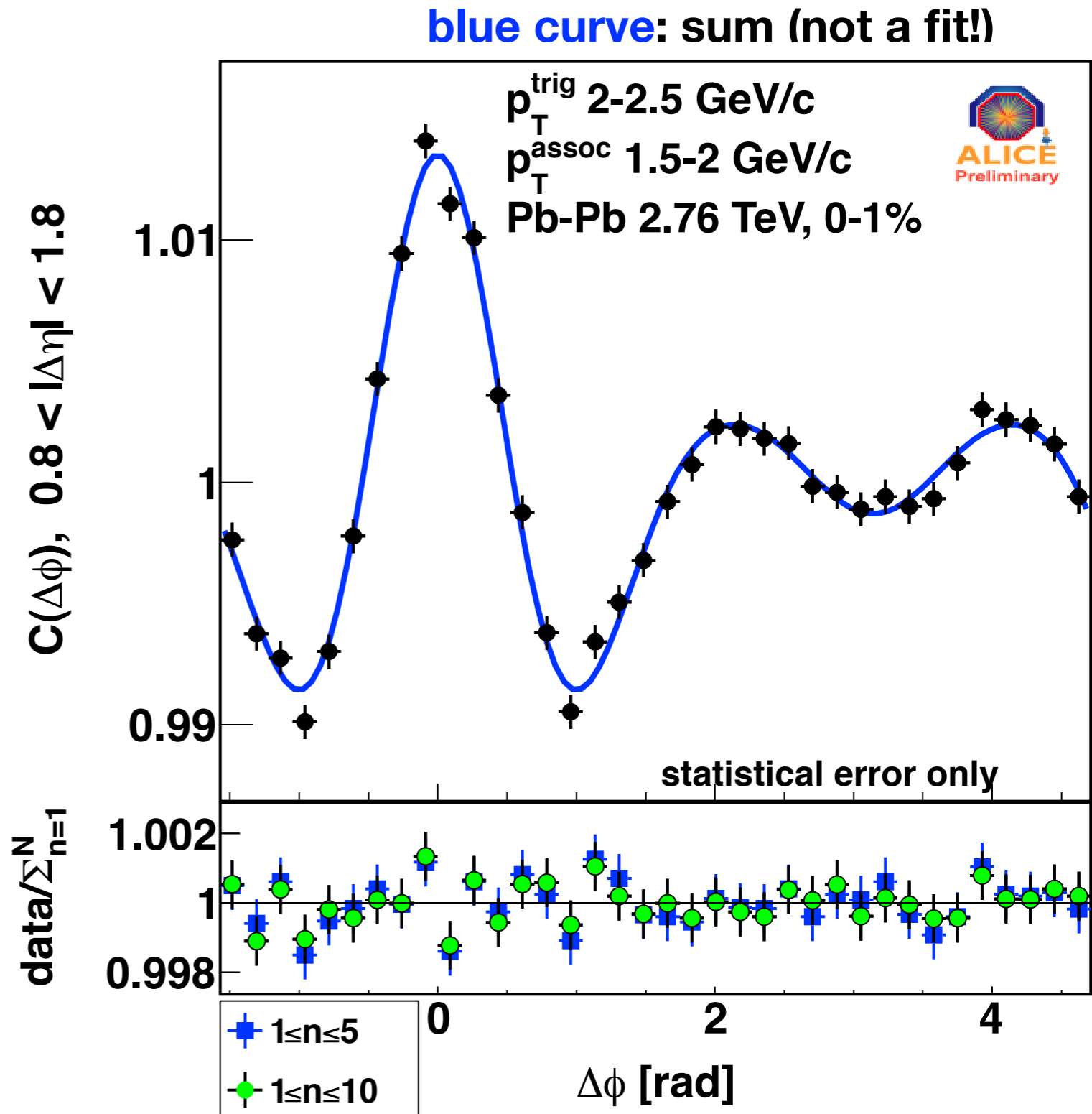
Near side jet excluded by  
 $|\Delta\eta| > 0.8$  gap  
 Ridge at  $\Delta\phi=0$  remains

2-particle Fourier coeffs.  
 Extract directly from  $C(\Delta\phi)$ :

$$\langle \cos n\Delta\phi \rangle = \frac{\int d\Delta\phi C(\Delta\phi) \cos n\Delta\phi}{\int d\Delta\phi C(\Delta\phi)}$$

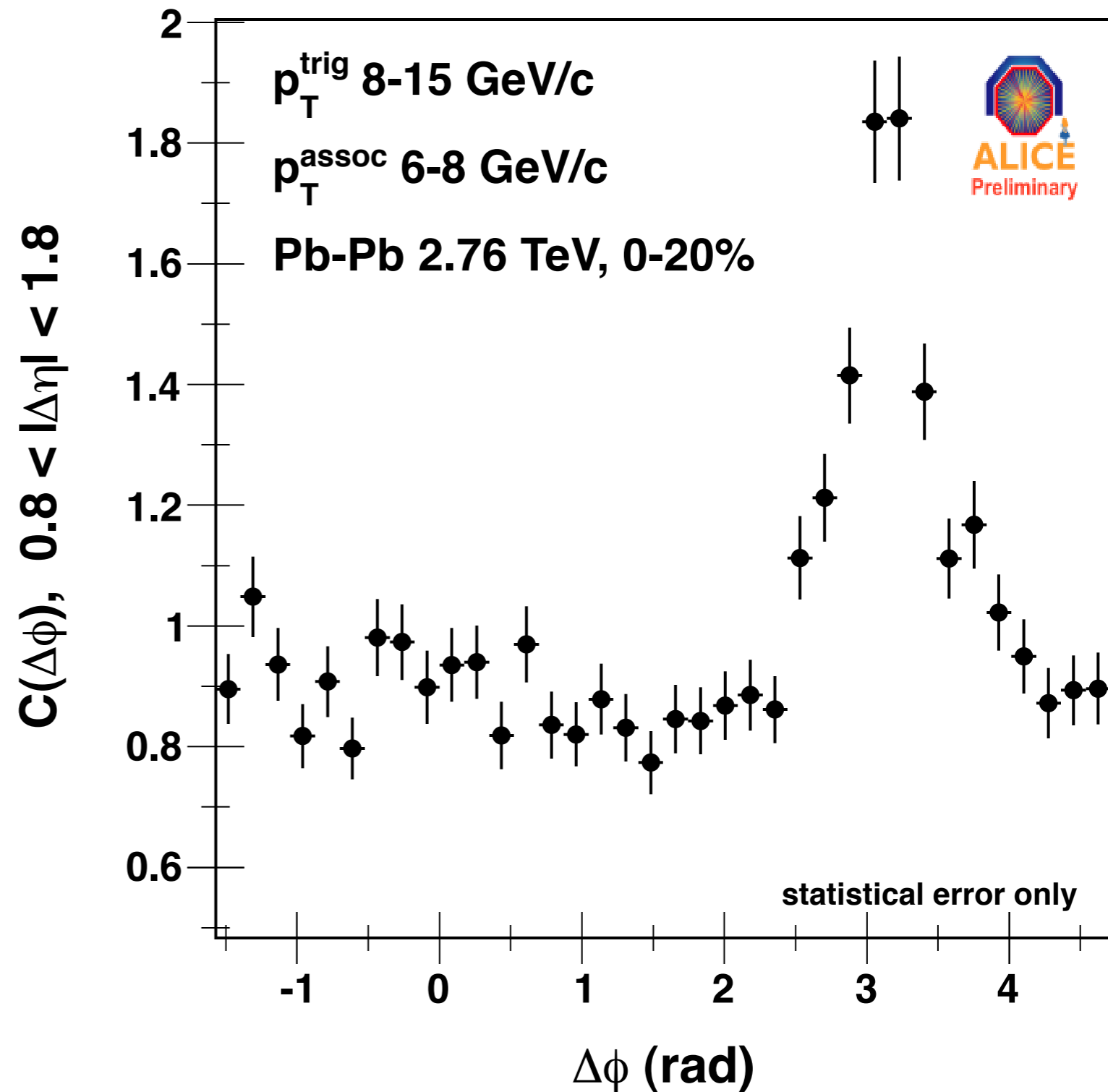
Here, the first 5 moments describe shape at per-mille level.

Little gained by using **10-term** series vs.  $1 < n < 5$ .



# Fourier analysis at large $\Delta\eta$ , higher $p_T$

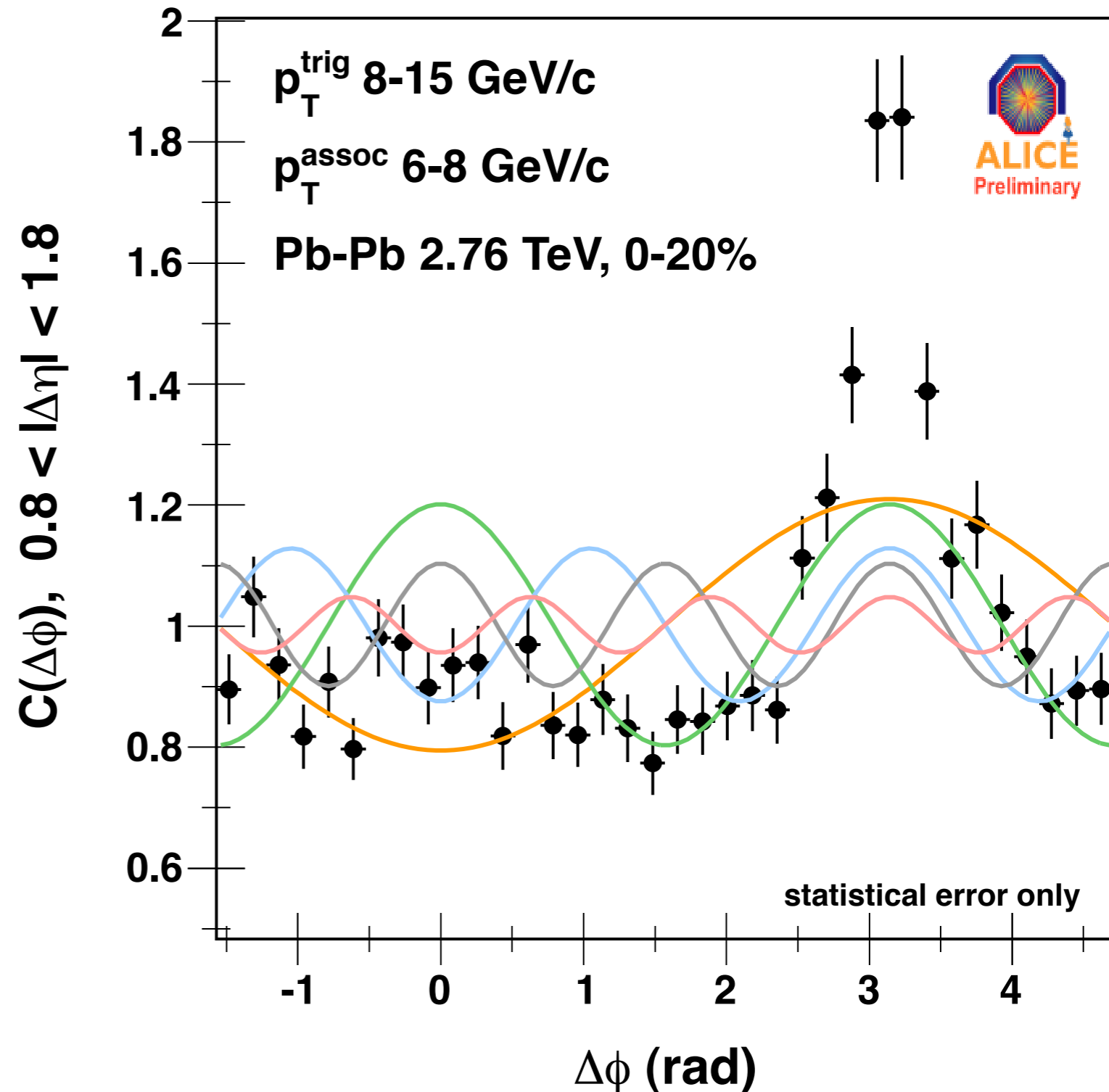
Correlation at  $|\Delta\eta| > 0.8$   
dominated by recoil jet.



# Fourier analysis at large $\Delta\eta$ , higher $p_T$

Correlation at  $|\Delta\eta| > 0.8$   
dominated by recoil jet.

Fourier decomposition  
always possible, but less  
natural here.

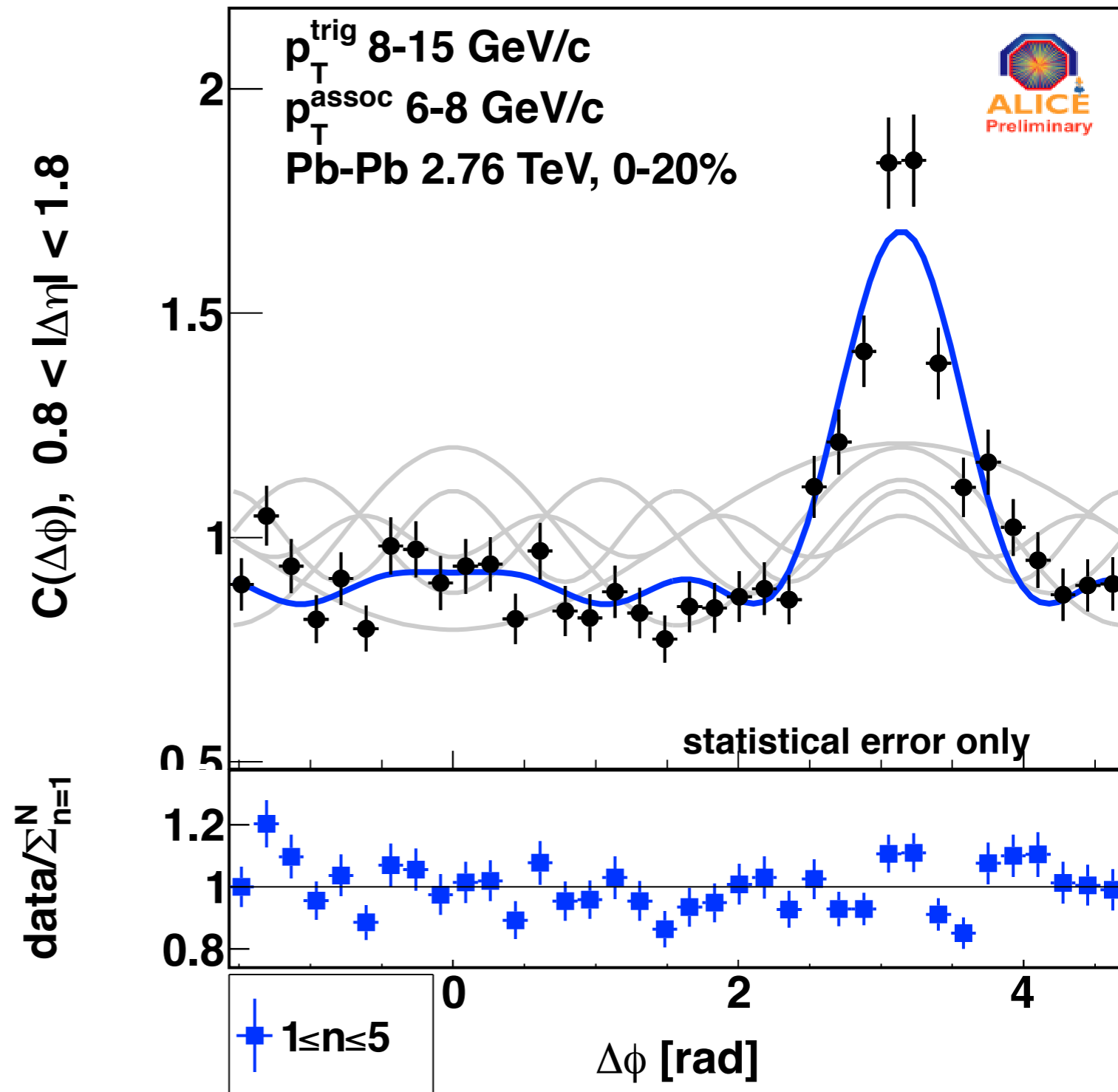




# Fourier analysis at large $\Delta\eta$ , higher $p_T$

Correlation at  $|\Delta\eta| > 0.8$   
dominated by recoil jet.

Fourier decomposition  
always possible, but less  
natural here.



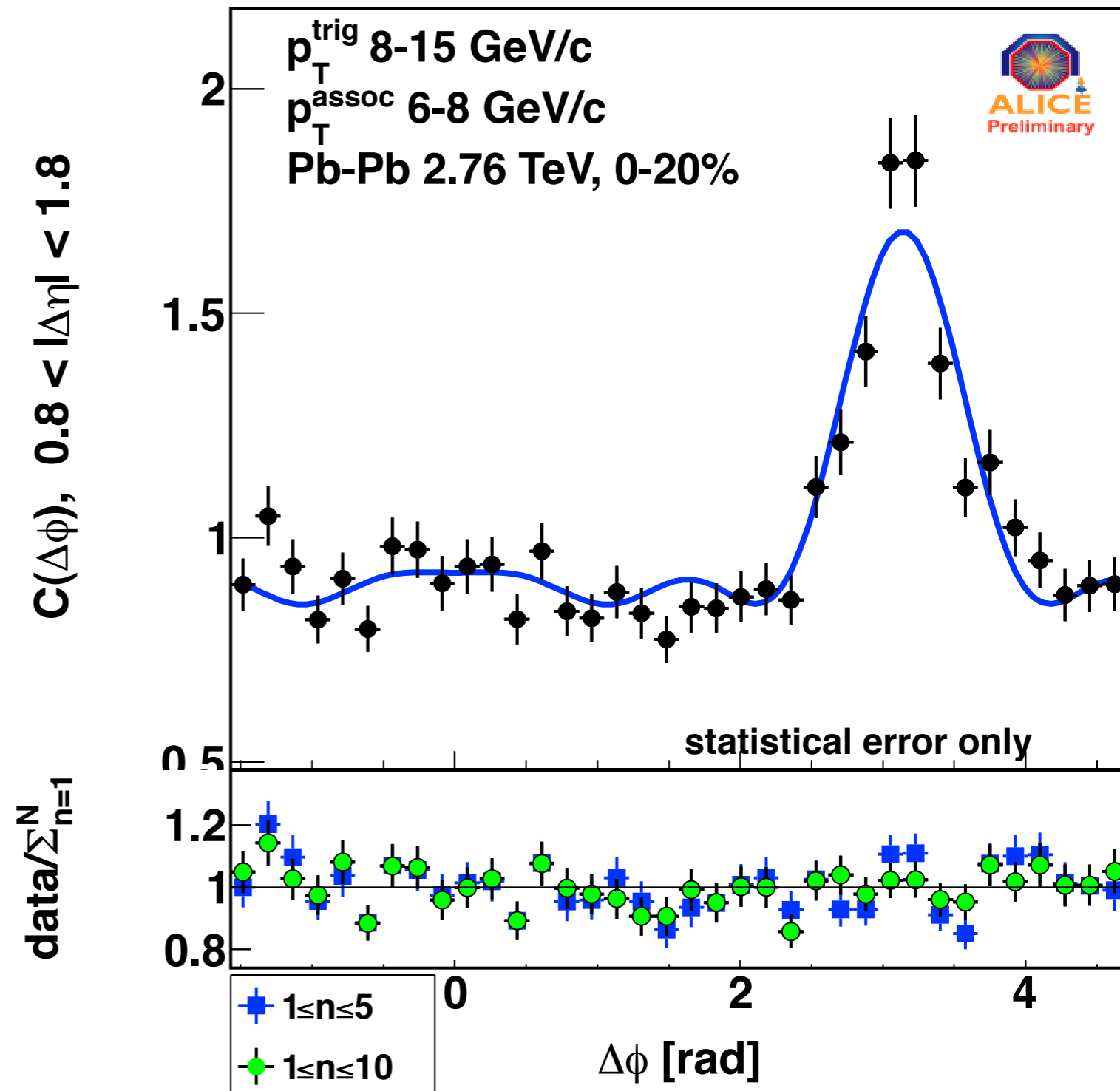
# Fourier analysis at large $\Delta\eta$ , higher $p_T$

Correlation at  $|\Delta\eta| > 0.8$   
dominated by recoil jet.

Fourier decomposition  
always possible, but less  
natural here.

Including  $1 \leq n \leq 10$  improves  
description vs  $1 \leq n \leq 5$ .

Sharp features require higher  
moments



# Flow vs. non-flow correlations

---

## Collective effects

Flow-related effects imply correlation through a plane of symmetry  $\psi_n$ .

# Flow vs. non-flow correlations

---

## Collective effects

Flow-related effects imply correlation through a plane of symmetry  $\psi_n$ .

Flow-dominated correlations should factorize:

$$\begin{aligned}
 \langle \cos n\Delta\varphi \rangle &= \langle \cos n(\varphi_{\text{trig}} - \varphi_{\text{assoc}}) \rangle \\
 &= \langle \cos n(\varphi_{\text{trig}} - \psi_n) \rangle \langle \cos n(\varphi_{\text{assoc}} - \psi_n) \rangle \\
 &= v_n(p_{T\text{trig}}) v_n(p_{T\text{assoc}})
 \end{aligned}$$

Pair coefficients are just products of familiar single-particle  $v_n$ s.

# Flow vs. non-flow correlations

## Collective effects

Flow-related effects imply correlation through a plane of symmetry  $\psi_n$ .

Flow-dominated correlations should factorize:

$$\begin{aligned} \langle \cos n\Delta\varphi \rangle &= \langle \cos n(\varphi_{\text{trig}} - \varphi_{\text{assoc}}) \rangle \\ &= \langle \cos n(\varphi_{\text{trig}} - \psi_n) \rangle \langle \cos n(\varphi_{\text{assoc}} - \psi_n) \rangle \\ &= v_n(p_{T\text{trig}}) v_n(p_{T\text{assoc}}) \end{aligned}$$

Pair coefficients are just products of familiar single-particle  $v_n$ s.

## Jet-related effects

A few energetic particles are highly correlated by fragmentation, but not directly through  $\psi_n$ .

**Caveat:** there can be indirect correlations, i.e. length-dependent quenching.

**Would be largest w.r.t.  $\psi_2$  since it reflects the collision geometry.**

# Flow vs. non-flow correlations

## Collective effects

Flow-related effects imply correlation through a plane of symmetry  $\psi_n$ .

Flow-dominated correlations should factorize:

$$\begin{aligned} \langle \cos n\Delta\varphi \rangle &= \langle \cos n(\varphi_{\text{trig}} - \varphi_{\text{assoc}}) \rangle \\ &= \langle \cos n(\varphi_{\text{trig}} - \psi_n) \rangle \langle \cos n(\varphi_{\text{assoc}} - \psi_n) \rangle \\ &= v_n(p_{T\text{trig}}) v_n(p_{T\text{assoc}}) \end{aligned}$$

Pair coefficients are just products of familiar single-particle  $v_n$ s.

## Jet-related effects

A few energetic particles are highly correlated by fragmentation, but not directly through  $\psi_n$ .

**Caveat:** there can be indirect correlations, i.e. length-dependent quenching.

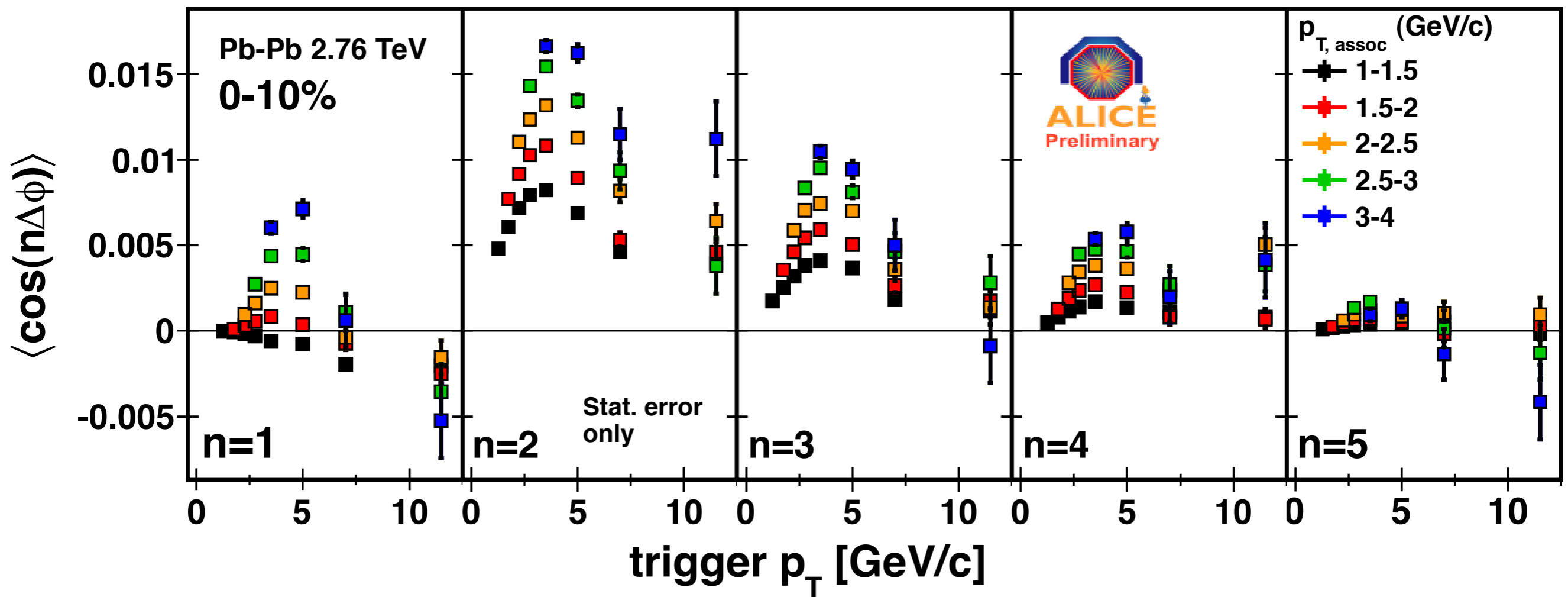
Would be largest w.r.t.  $\psi_2$  since it reflects the collision geometry.

The collectivity relation

$$\langle \cos n\Delta\varphi \rangle \stackrel{?}{=} v_n(p_{T\text{trig}}) v_n(p_{T\text{assoc}})$$

is a quantitative hypothesis that can be tested!

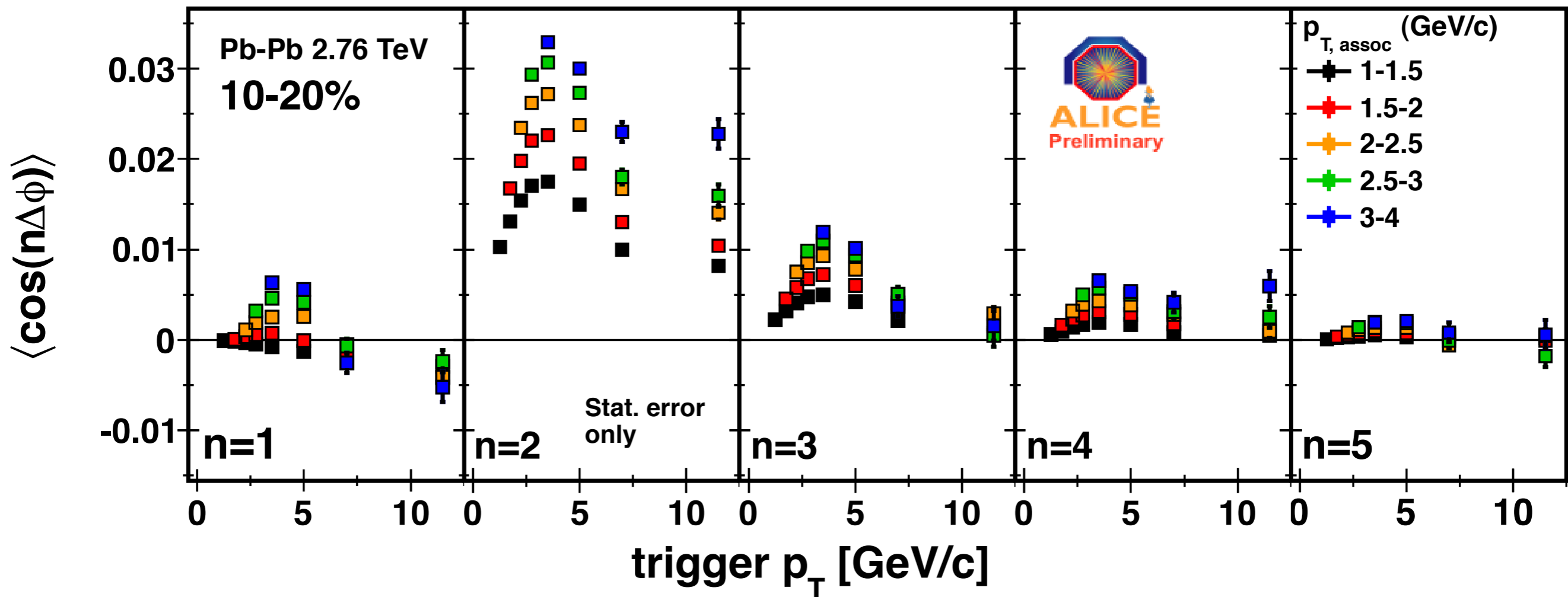
# Fourier coefficients vs. trigger $p_T$



With rising associated  $p_T$ ...

Anisotropy rises at all orders in central events.

# Fourier coefficients vs. trigger $p_T$



With rising associated  $p_T$ ...

Anisotropy rises at all orders in central events.

With increasing centrality...

$n=2$  amplitudes:

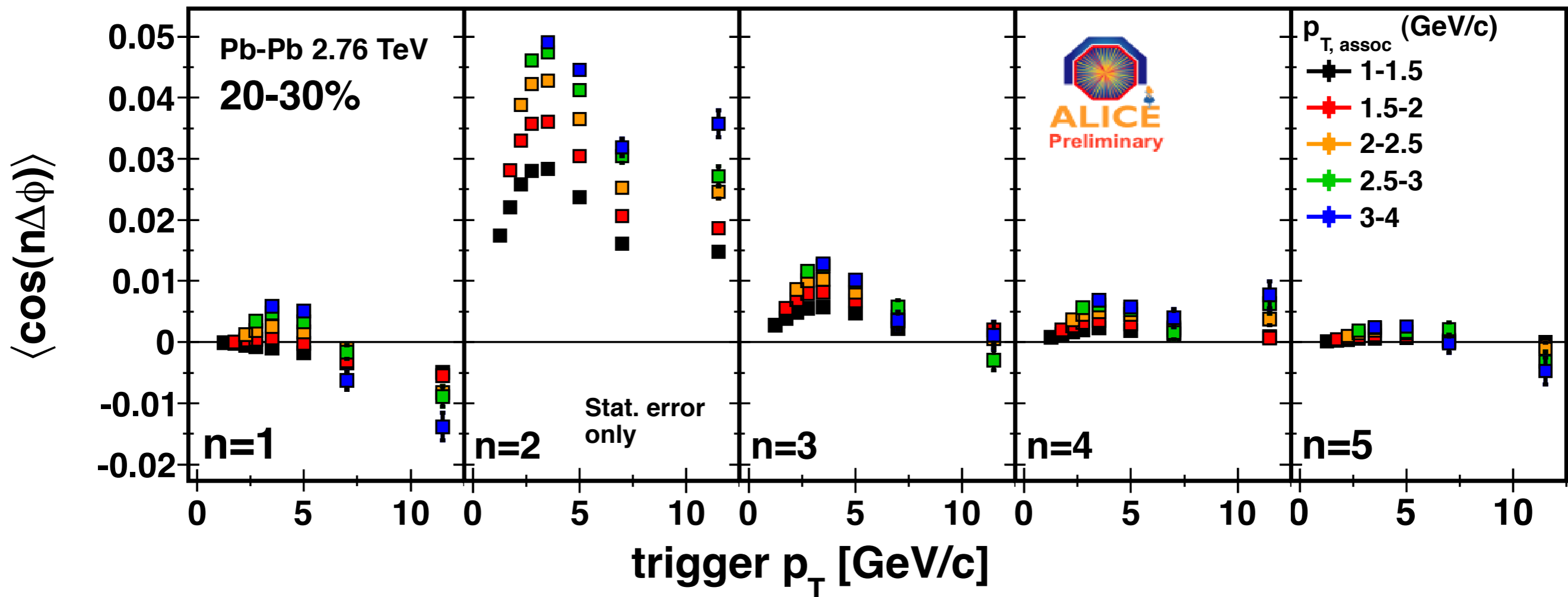
Comparable to other terms in central events, but dominant in mid-central...reasonable.

Odd terms become negative with rising  $p_T$ , centrality

Due to the away-side jet



# Fourier coefficients vs. trigger $p_T$



With rising associated  $p_T$ ...

Anisotropy rises at all orders in central events.

With increasing centrality...

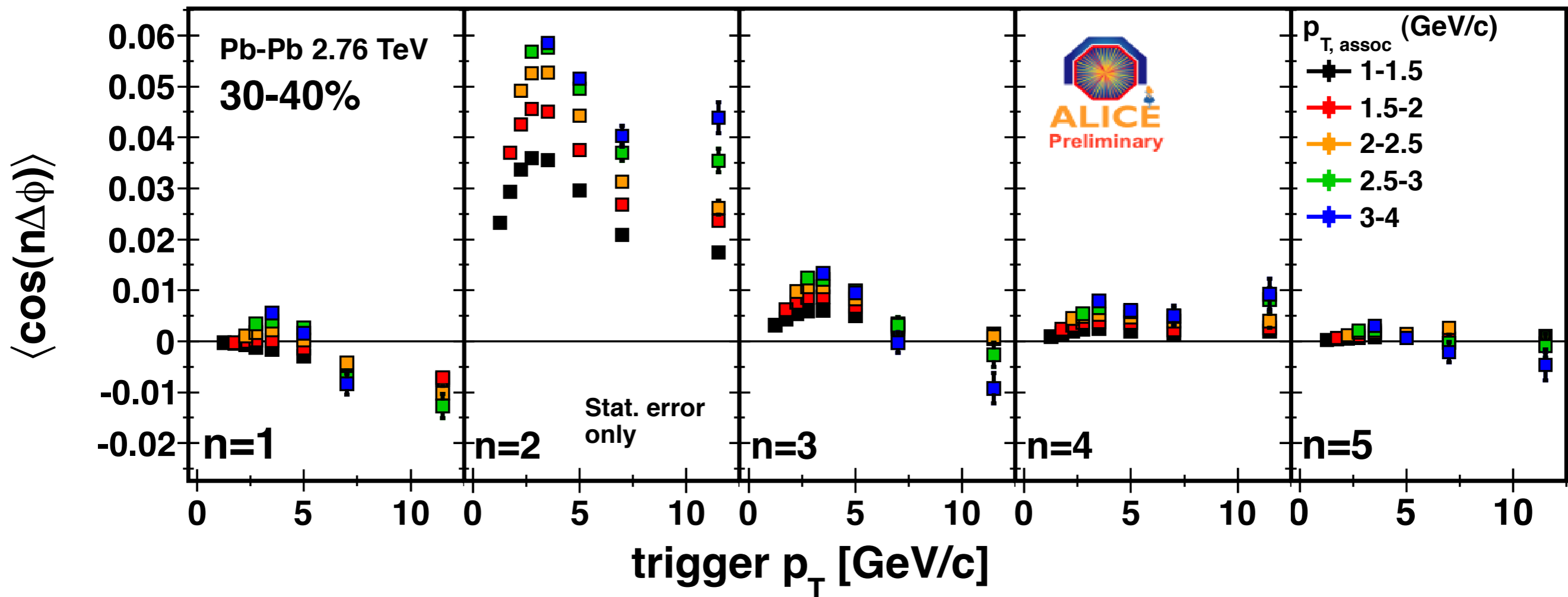
$n=2$  amplitudes:

Comparable to other terms in central events, but dominant in mid-central...reasonable.

Odd terms become negative with rising  $p_T$ , centrality

Due to the away-side jet

# Fourier coefficients vs. trigger $p_T$



With rising associated  $p_T$ ...

Anisotropy rises at all orders in central events.

With increasing centrality...

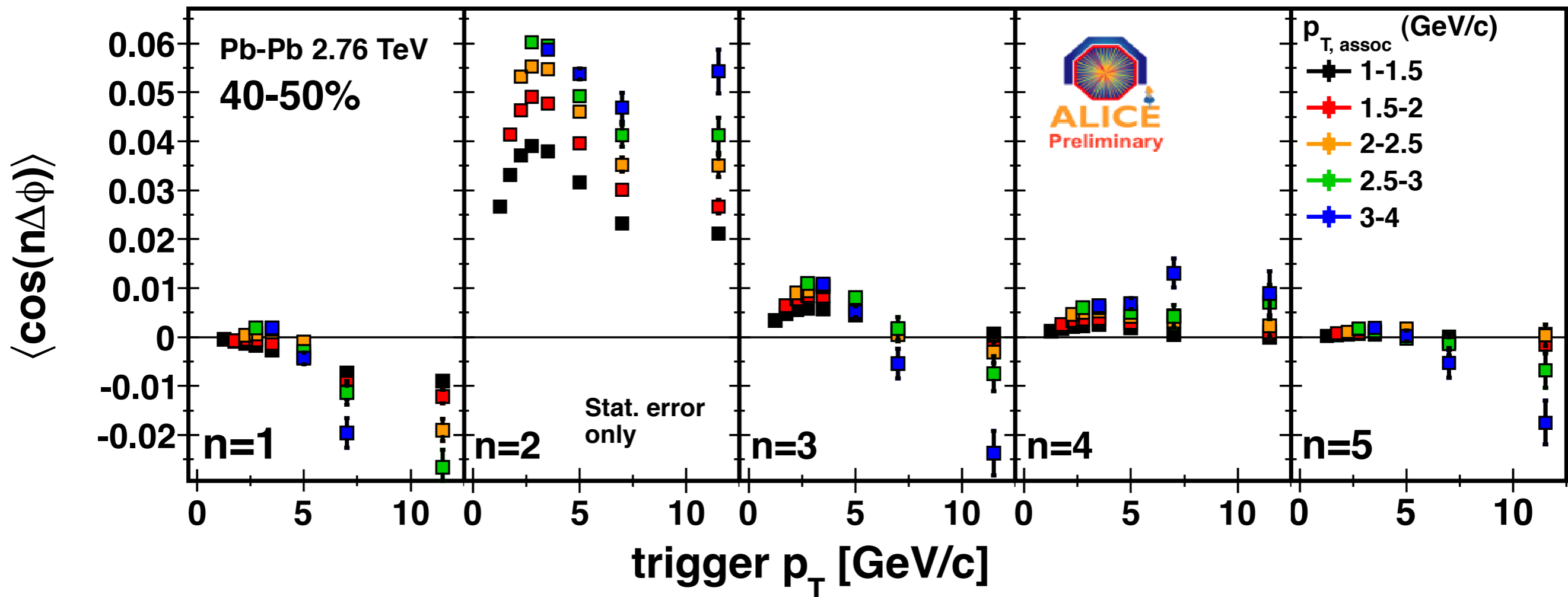
$n=2$  amplitudes:

Comparable to other terms in central events, but dominant in mid-central...reasonable.

Odd terms become negative with rising  $p_T$ , centrality

Due to the away-side jet

# Fourier coefficients vs. trigger $p_T$



With rising associated  $p_T$ ...

Anisotropy rises at all orders in central events.

With increasing centrality...

$n=2$  amplitudes:

Comparable to other terms in central events, but dominant in mid-central...reasonable.

Odd terms become negative with rising  $p_T$ , centrality

Due to the away-side jet

# Global fit of 2-particle Fourier moments

Find best  $v_n(p_T)$

Fit  $\langle \cos n\Delta\phi \rangle$  for all  $p_T$   
bins simultaneously

Fit function:  $V_{n\Delta} = v_n^t v_n^a$ .

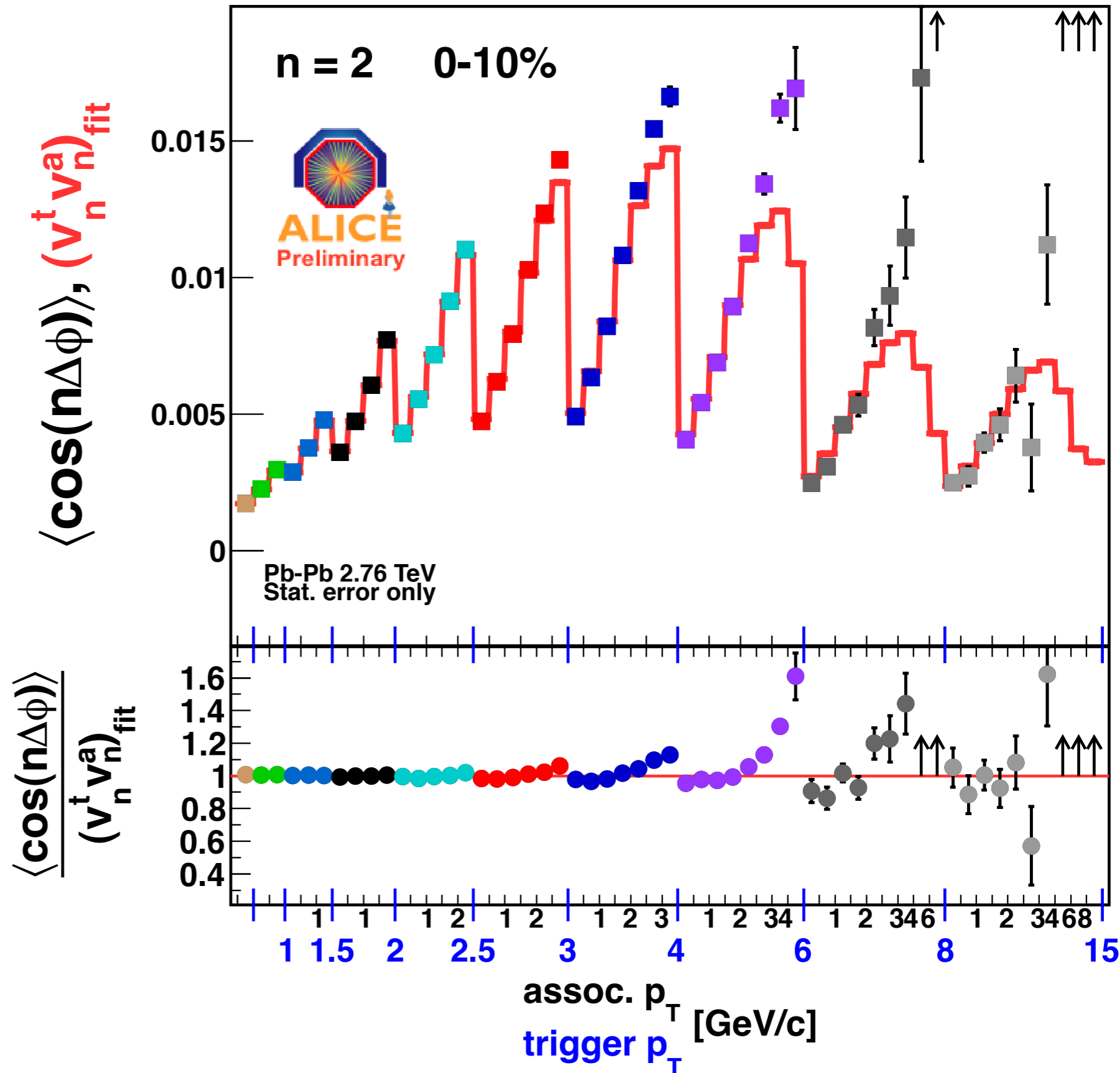
Fit breaks at high  $p_T$ ,  
where jets dominate.

**Key idea**

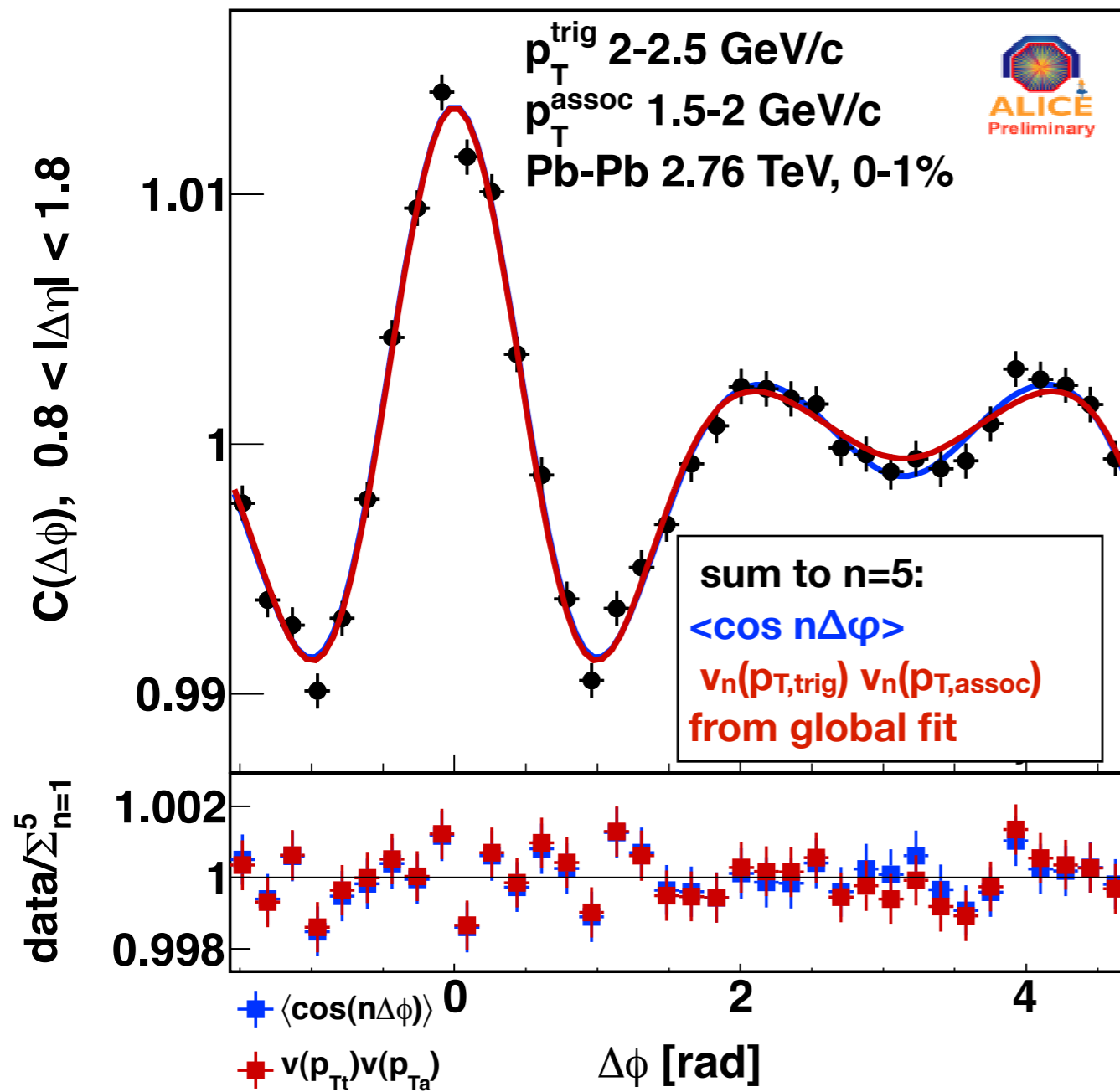
If fit matches data  
suggests flow-type  
correlations

If fit diverges  
collective description less  
appropriate.

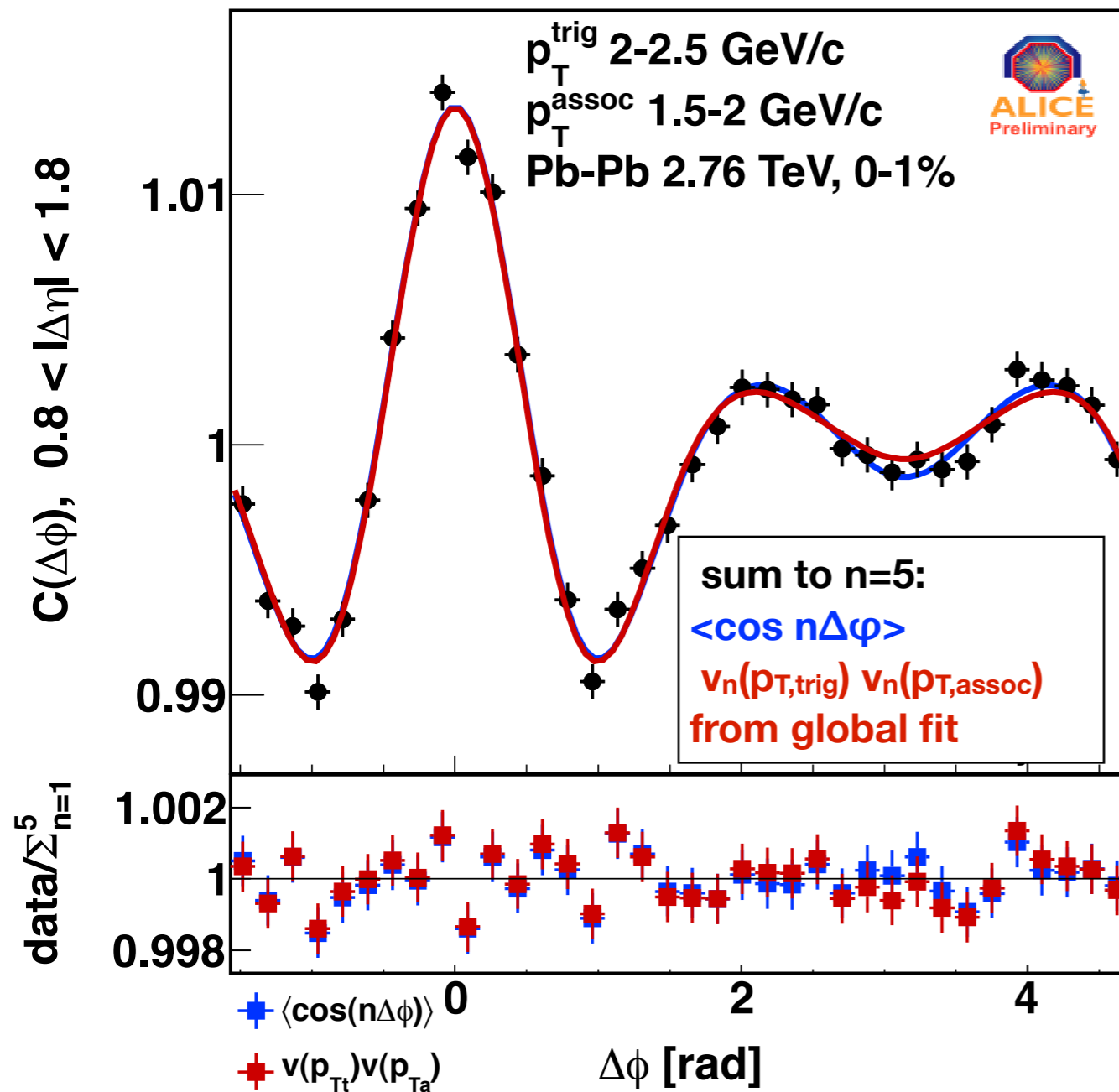
Transition between cases  
follows clear trends.



# Large- $\Delta\eta$ global fit results

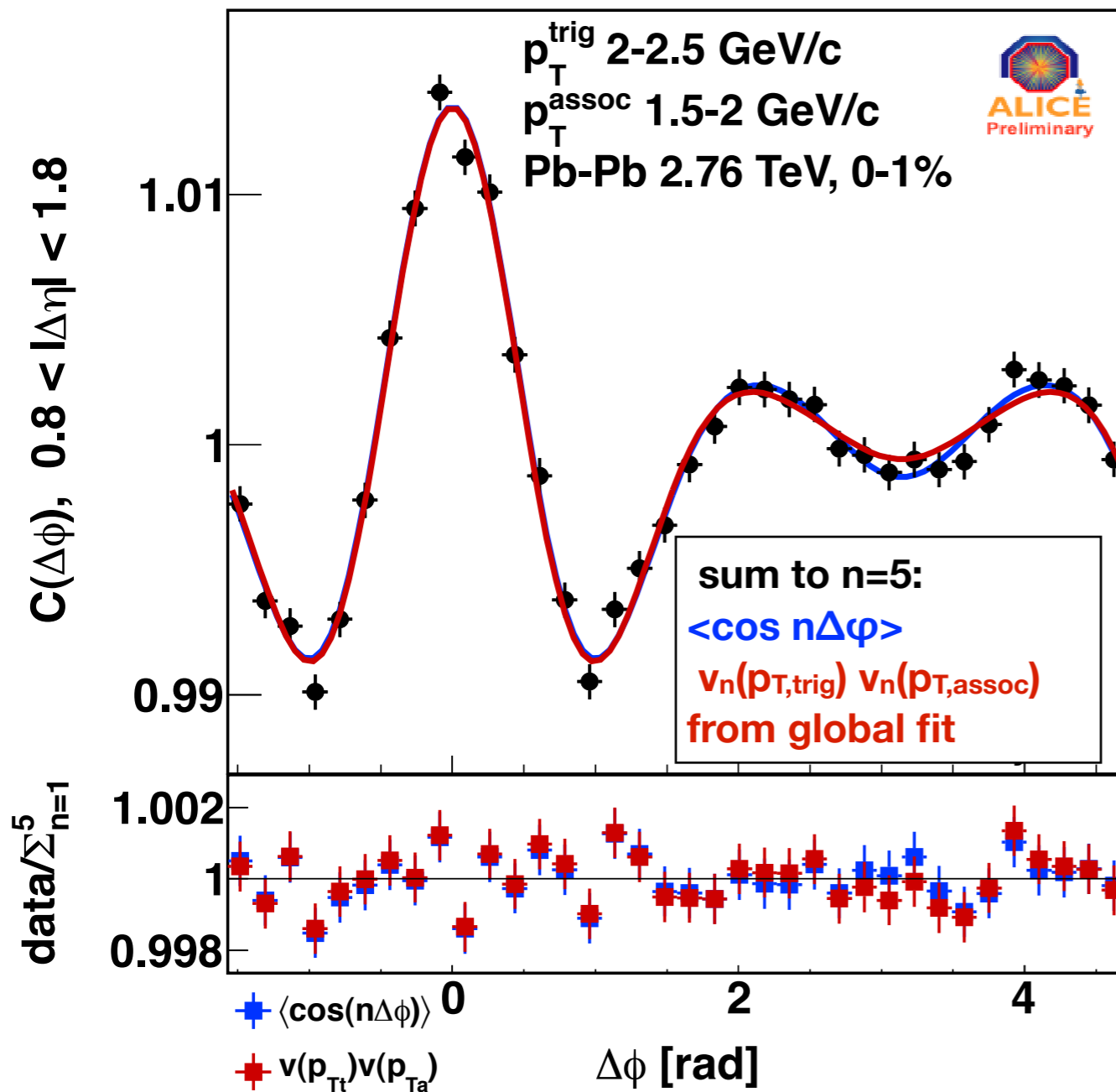


# Large- $\Delta\eta$ global fit results

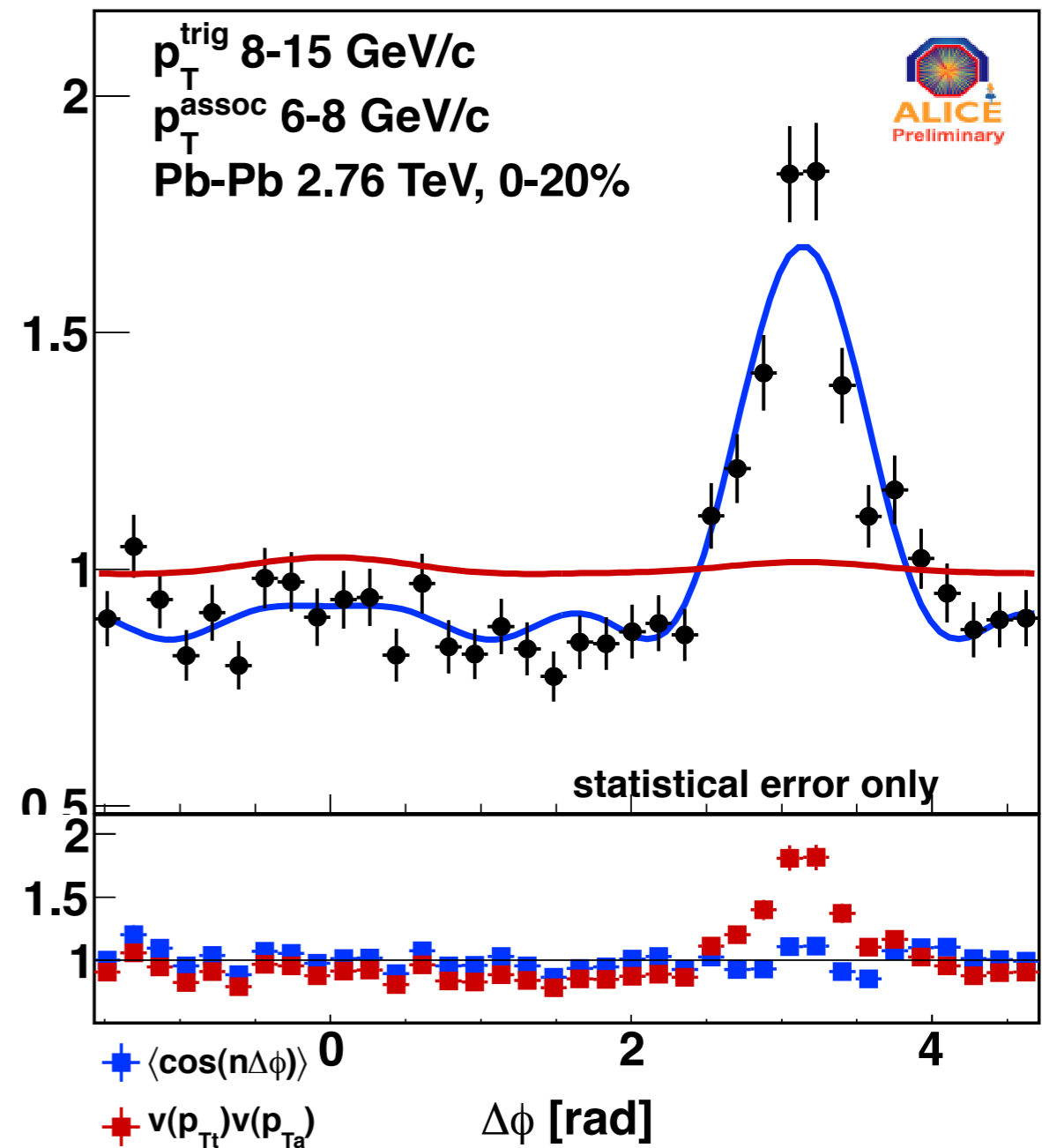


**Good description for  
 central, low/intermediate  $p_T$   
 correlations.**

# Large- $\Delta\eta$ global fit results



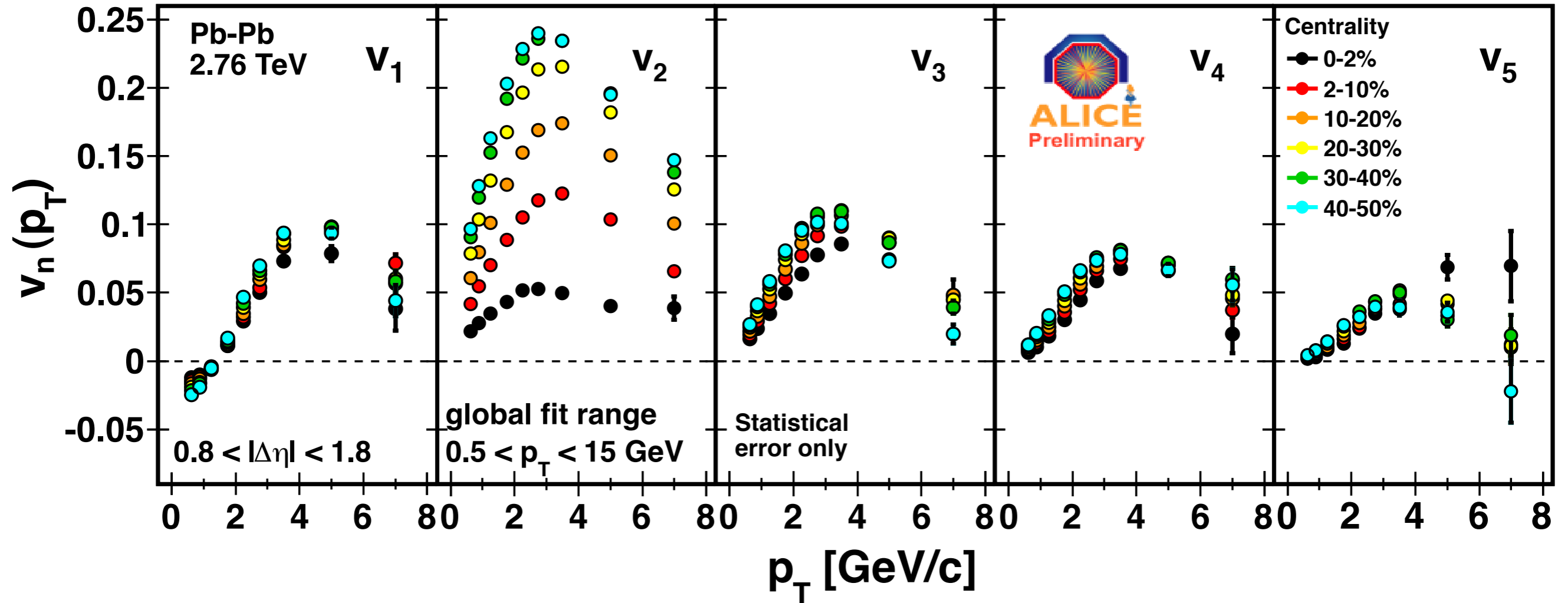
Good description for central, low/intermediate  $p_T$  correlations.



Not even close at high  $p_T$ , where away-side jet dominates.

# Global fit results: $v_n\{GF\}$ vs. $p_T$

A new  $v_n$  determination with high statistical precision



Comparable magnitudes for central events

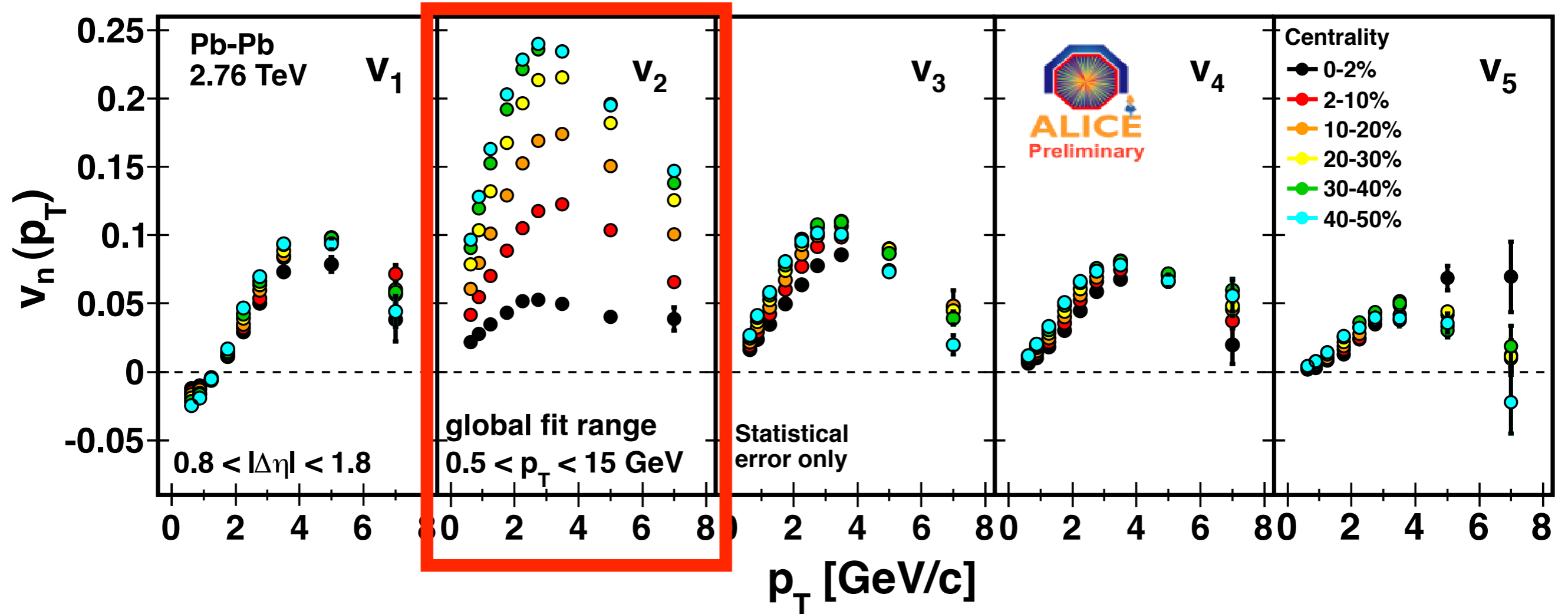
$v_2$  dominates in mid-central events - reflects collision geometry

For 0-2%,  $v_3 > v_2$ : natural description of away-side double hump



# Global fit results: $v_n\{GF\}$ vs. $p_T$

A new  $v_n$  determination with high statistical precision



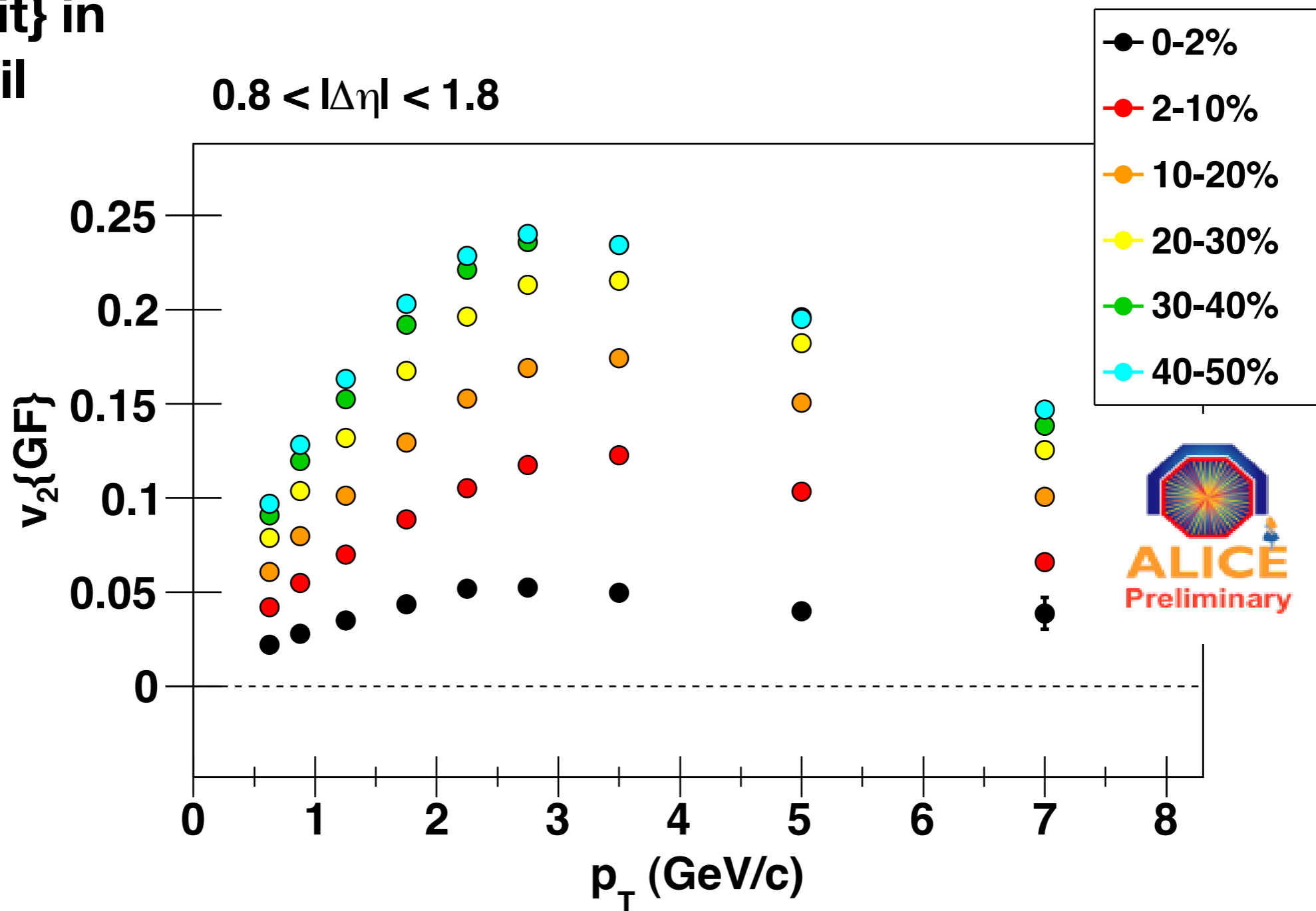
Comparable magnitudes for central events

$v_2$  dominates in mid-central events - reflects collision geometry

For 0-2%,  $v_3 > v_2$ : natural description of away-side double hump

# Comparison with conventional $v_2$ results

$v_2$ {global fit} in  
more detail



# Comparison with conventional $v_2$ results

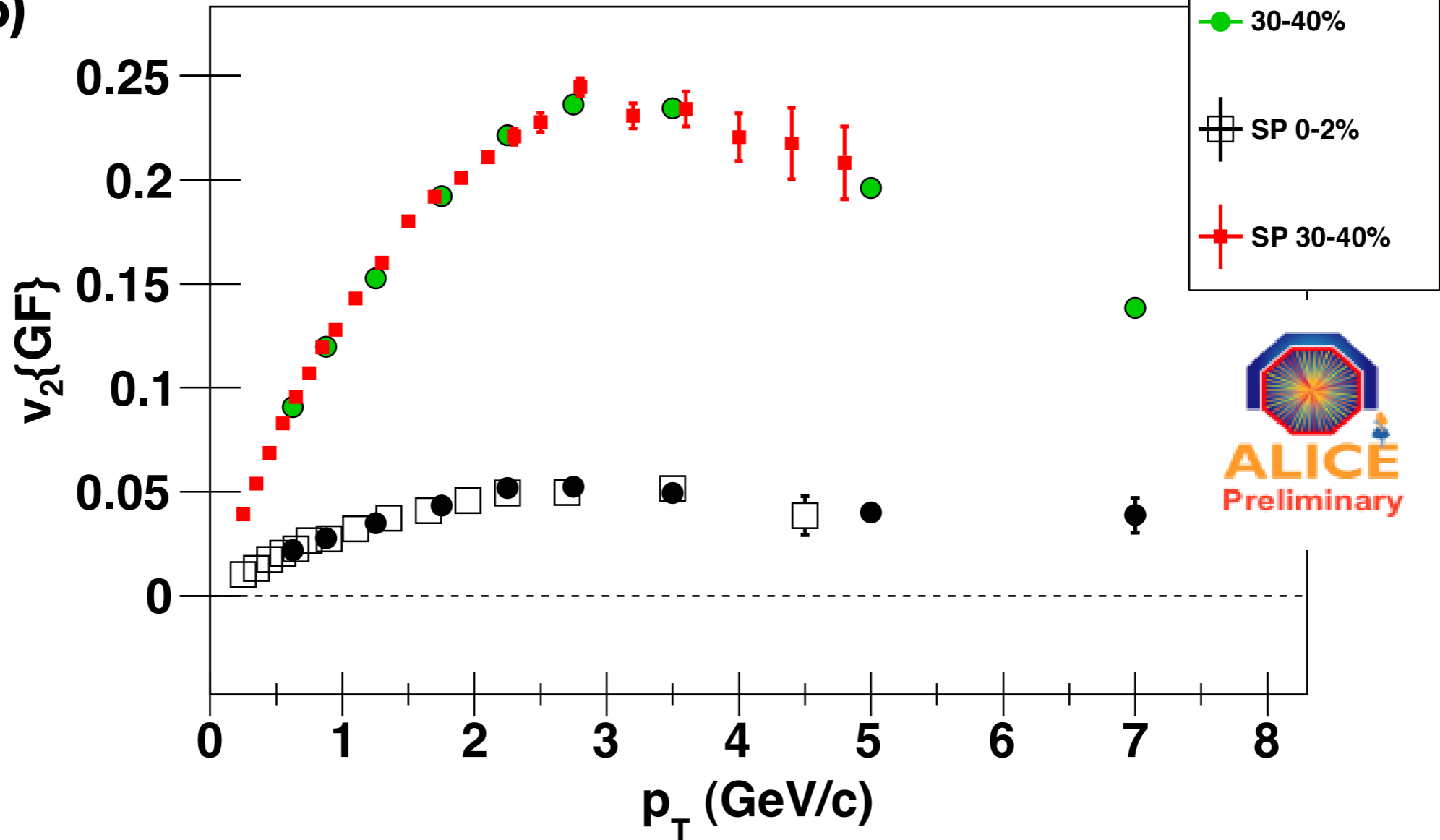
With new ALICE  
measurement  
(1105.3865)

Global fit

$0.8 < |\Delta\eta| < 1.8$

S.P. (CERN-PH-EP-2011-073)

$1.0 < |\Delta\eta| < 1.6$

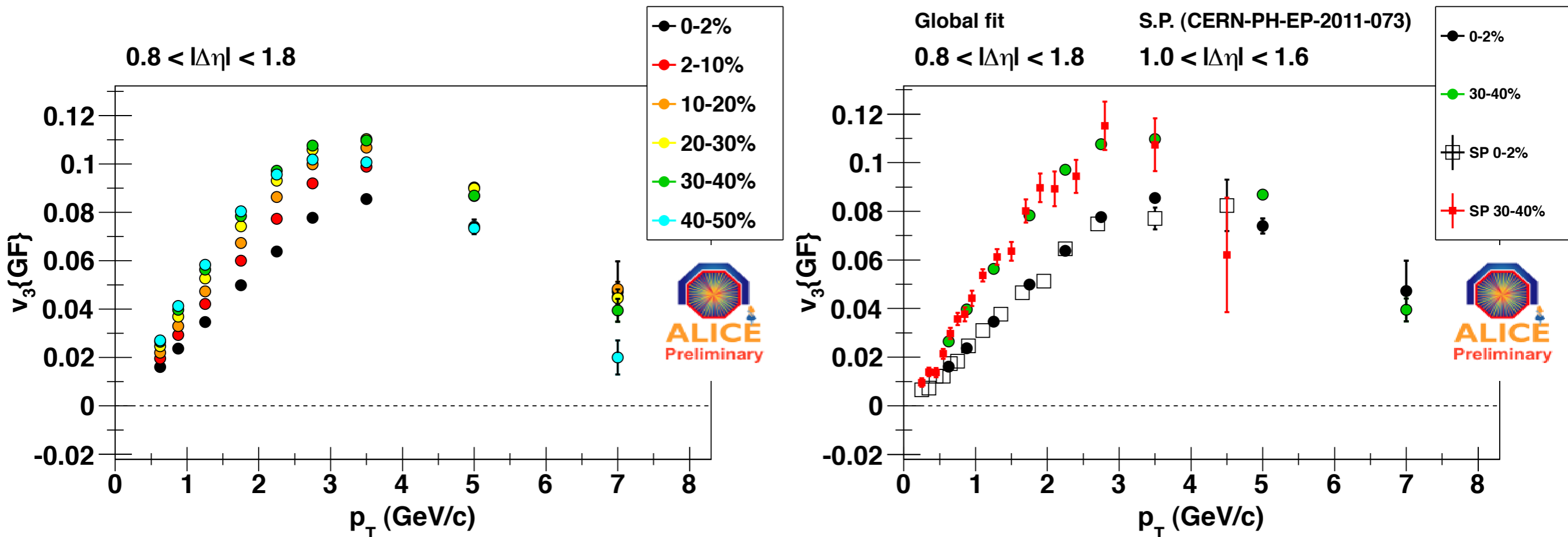


**Global fit gives excellent agreement with scalar-product method**

**At moderate  $p_T$ , large  $|\Delta\eta|$  correlations appear completely dominated by flow!**

# Comparison with conventional $v_n$ results

$v_3$  also agrees closely!



$v_3$  from large  $\Delta\eta$  correlations matches established flow methods

Great care is taken to control nonflow in scalar-product result

Hydro naturally describes the double hump--no need for conical emission

Agreement persists for  $v_4$  and  $v_5$ .

# Yield modification: $I_{CP}$ and $I_{AA}$

Compare  $1/N_{trig} dN/d\Delta\phi$  in Pb+Pb with:  
 peripheral for  $I_{CP}$   
 p+p for  $I_{AA}$

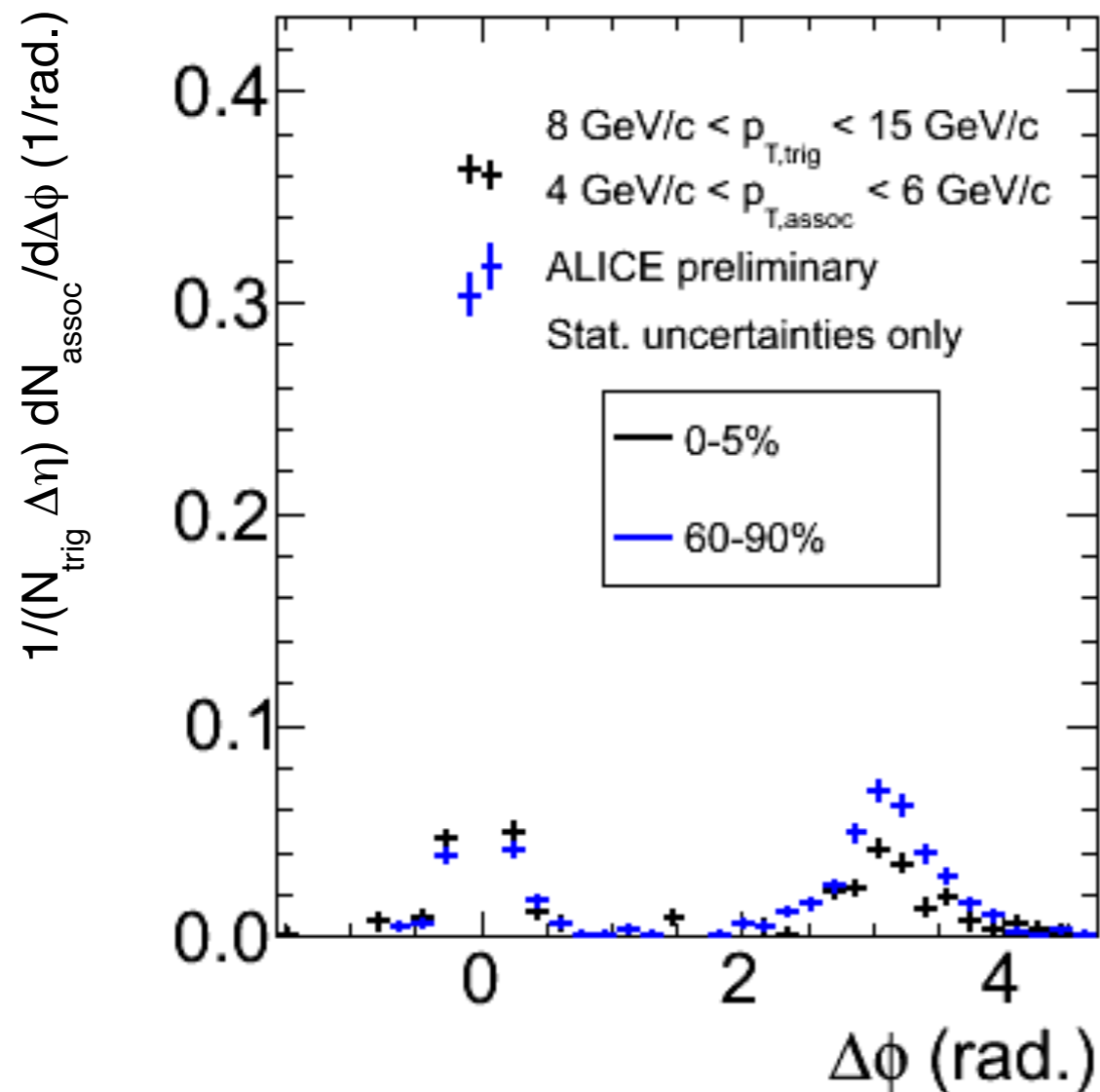
Integrate yields in selected  $\Delta\phi$  range

Here,  $0 (\pi) \pm 0.7$  for near (away) side

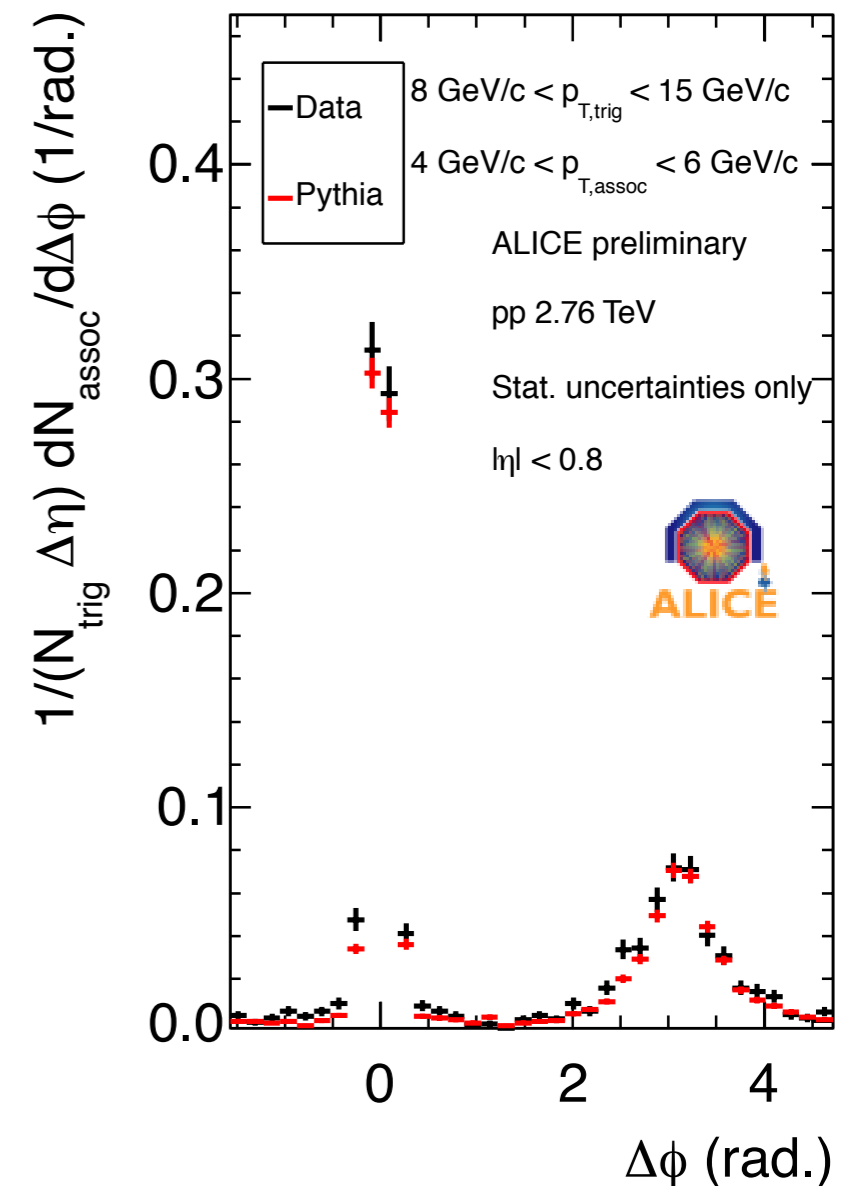
$$I_{AA}(p_{T,trig}; p_{T,assoc}) = \frac{Y^{AA}(p_{T,trig}; p_{T,assoc})}{Y^{PP}(p_{T,trig}; p_{T,assoc})}$$

$$I_{CP}(p_{T,trig}; p_{T,assoc}) = \frac{Y_{central}^{AA}(p_{T,trig}; p_{T,assoc})}{Y_{peripheral}^{AA}(p_{T,trig}; p_{T,assoc})}$$

**Pb+Pb**



**p+p**



# Yield modification: $I_{CP}$ and $I_{AA}$

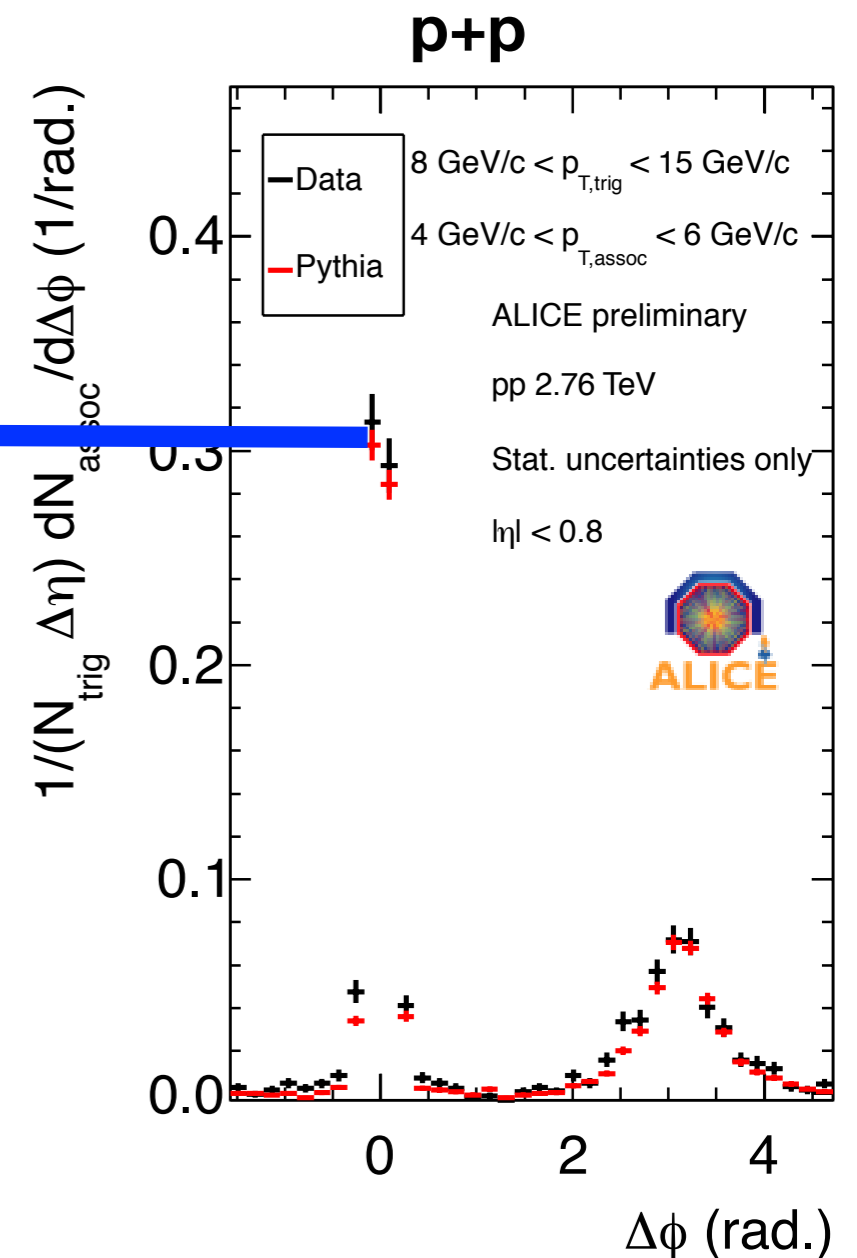
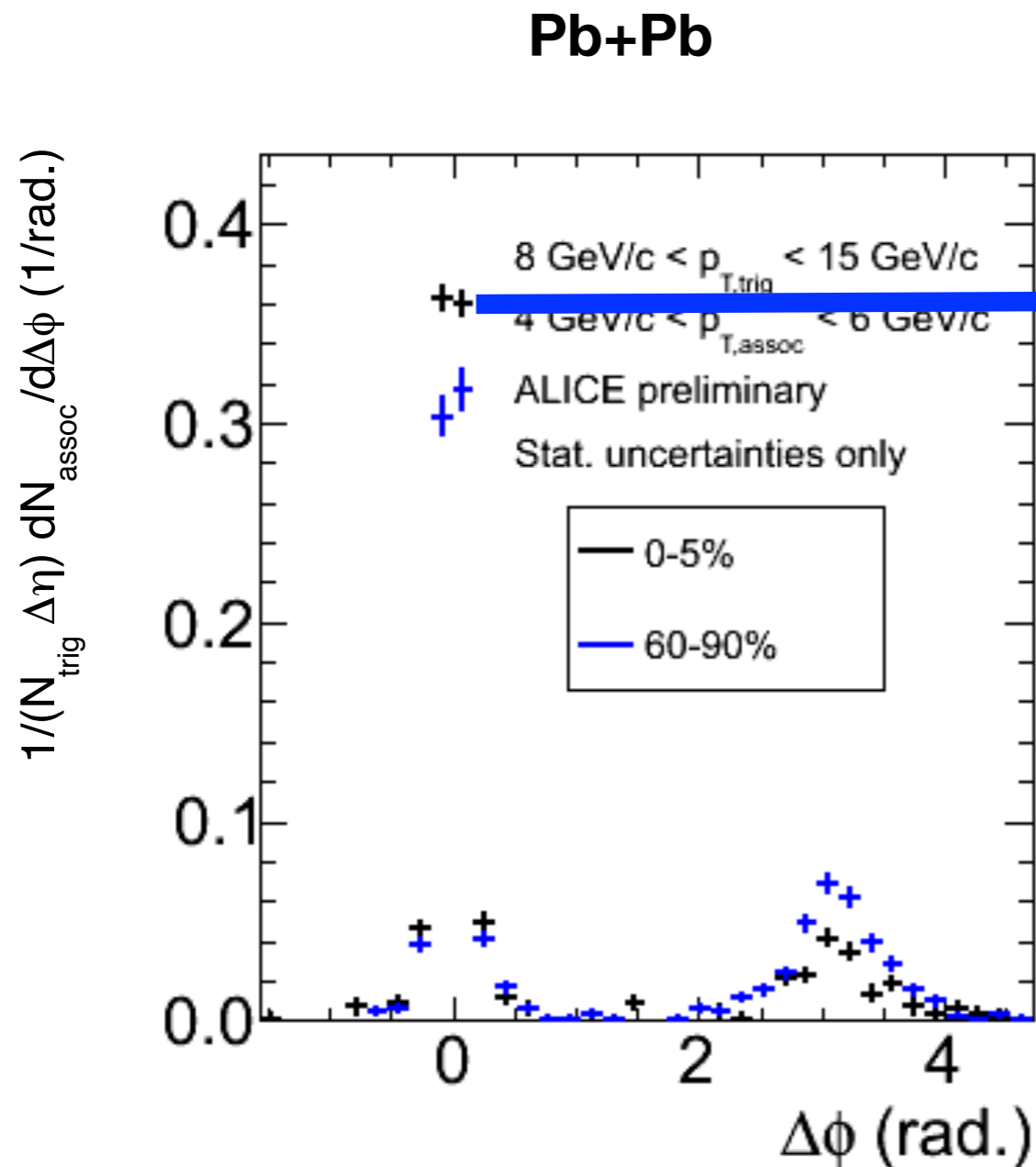
Compare  $1/N_{trig} dN/d\Delta\phi$  in Pb+Pb with:  
 peripheral for  $I_{CP}$   
 p+p for  $I_{AA}$

Integrate yields in selected  $\Delta\phi$  range

Here,  $0 (\pi) \pm 0.7$  for near (away) side

$$I_{AA}(p_{T,trig}; p_{T,assoc}) = \frac{Y^{AA}(p_{T,trig}; p_{T,assoc})}{Y^{PP}(p_{T,trig}; p_{T,assoc})}$$

$$I_{CP}(p_{T,trig}; p_{T,assoc}) = \frac{Y_{central}^{AA}(p_{T,trig}; p_{T,assoc})}{Y_{peripheral}^{AA}(p_{T,trig}; p_{T,assoc})}$$



# Yield modification: $I_{CP}$ and $I_{AA}$

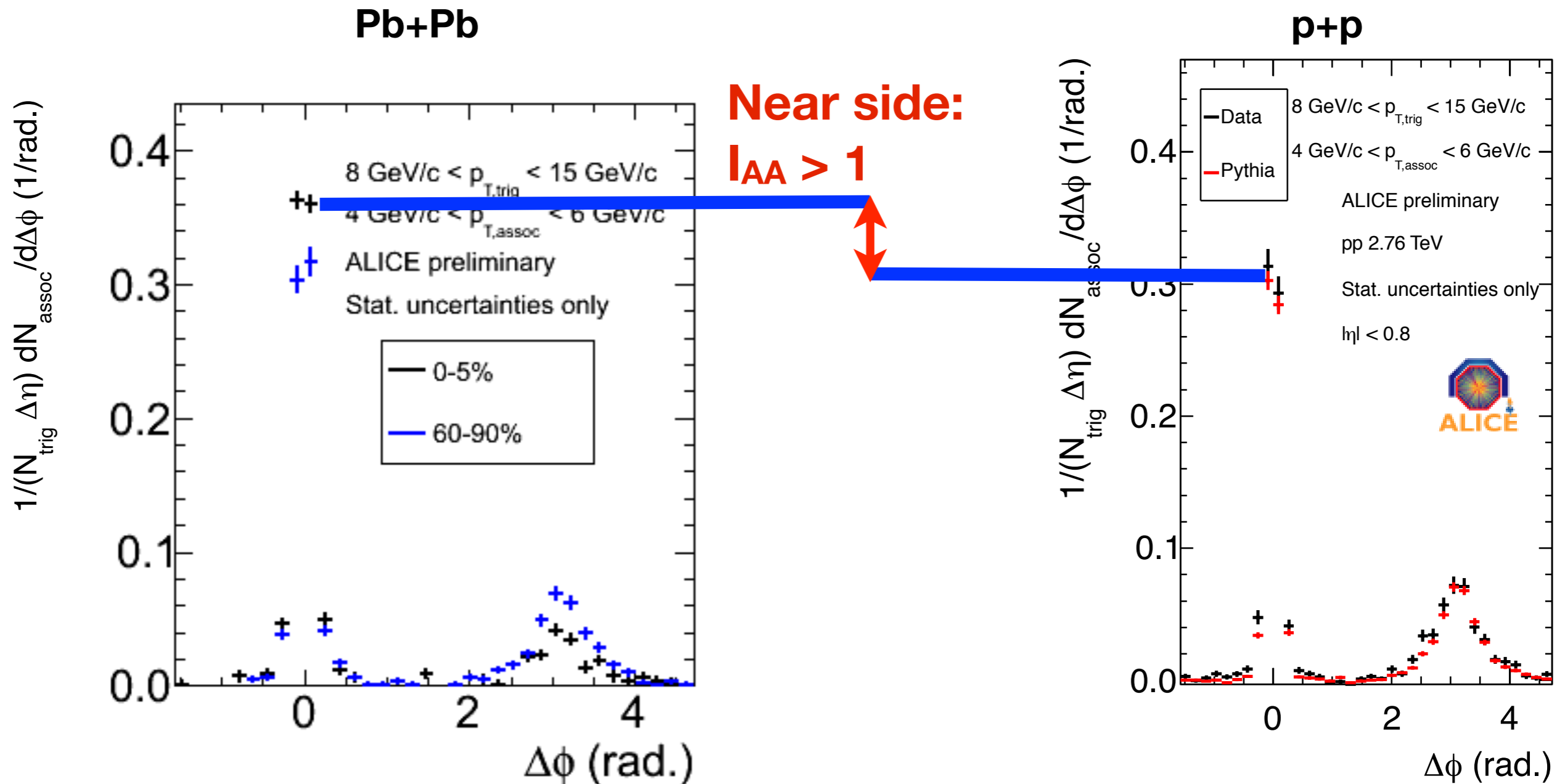
Compare  $1/N_{trig} dN/d\Delta\phi$  in Pb+Pb with:  
 peripheral for  $I_{CP}$   
 p+p for  $I_{AA}$

Integrate yields in selected  $\Delta\phi$  range

Here,  $0 (\pi) \pm 0.7$  for near (away) side

$$I_{AA}(p_{T,trig}; p_{T,assoc}) = \frac{Y^{AA}(p_{T,trig}; p_{T,assoc})}{Y^{PP}(p_{T,trig}; p_{T,assoc})}$$

$$I_{CP}(p_{T,trig}; p_{T,assoc}) = \frac{Y_{central}^{AA}(p_{T,trig}; p_{T,assoc})}{Y_{peripheral}^{AA}(p_{T,trig}; p_{T,assoc})}$$



# Yield modification: $I_{CP}$ and $I_{AA}$

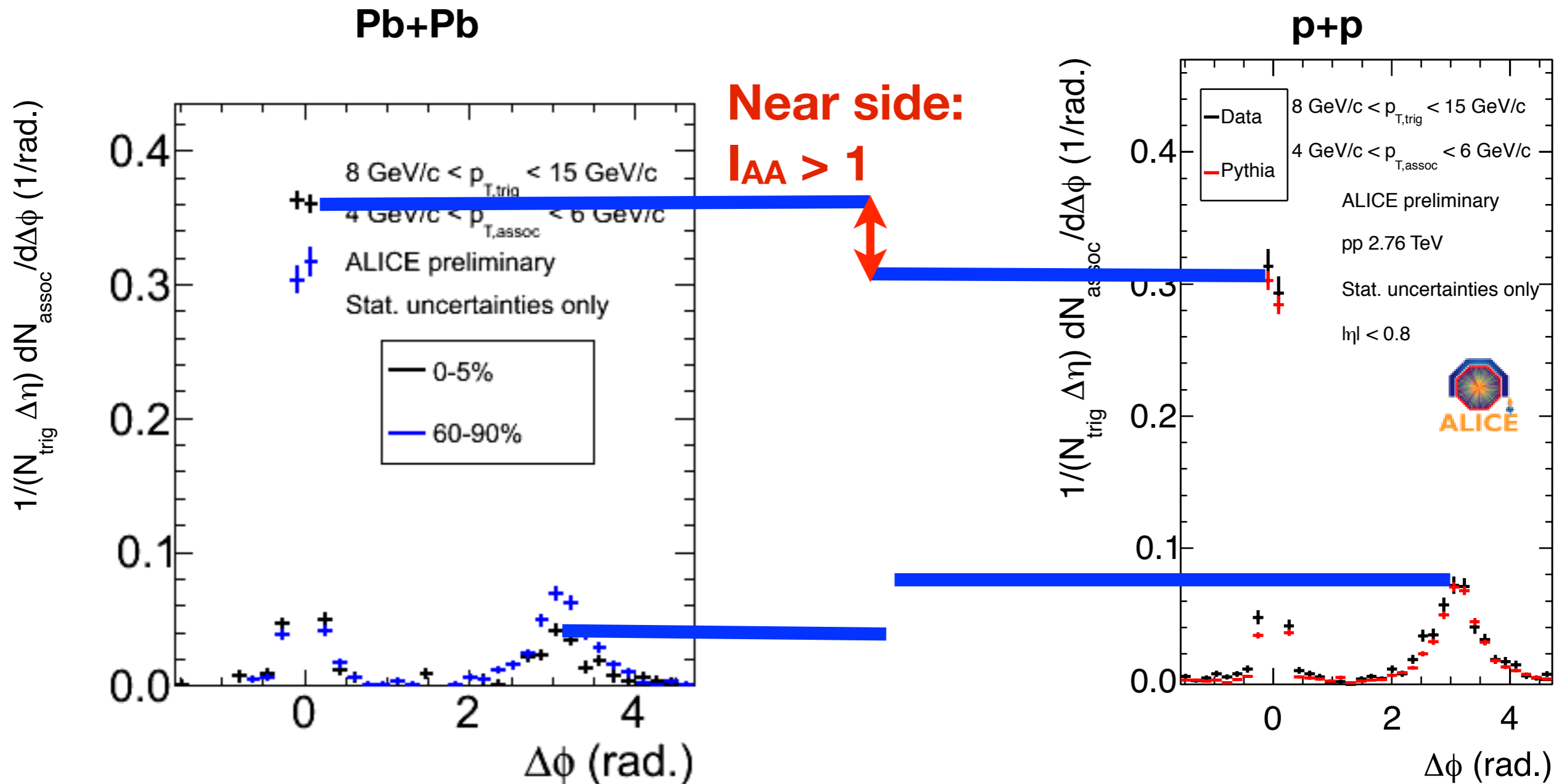
Compare  $1/N_{trig} dN/d\Delta\phi$  in Pb+Pb with:  
 peripheral for  $I_{CP}$   
 p+p for  $I_{AA}$

Integrate yields in selected  $\Delta\phi$  range

Here,  $0 (\pi) \pm 0.7$  for near (away) side

$$I_{AA}(p_{T,trig}; p_{T,assoc}) = \frac{Y^{AA}(p_{T,trig}; p_{T,assoc})}{Y^{PP}(p_{T,trig}; p_{T,assoc})}$$

$$I_{CP}(p_{T,trig}; p_{T,assoc}) = \frac{Y_{central}^{AA}(p_{T,trig}; p_{T,assoc})}{Y_{peripheral}^{AA}(p_{T,trig}; p_{T,assoc})}$$





# Yield modification: $I_{CP}$ and $I_{AA}$

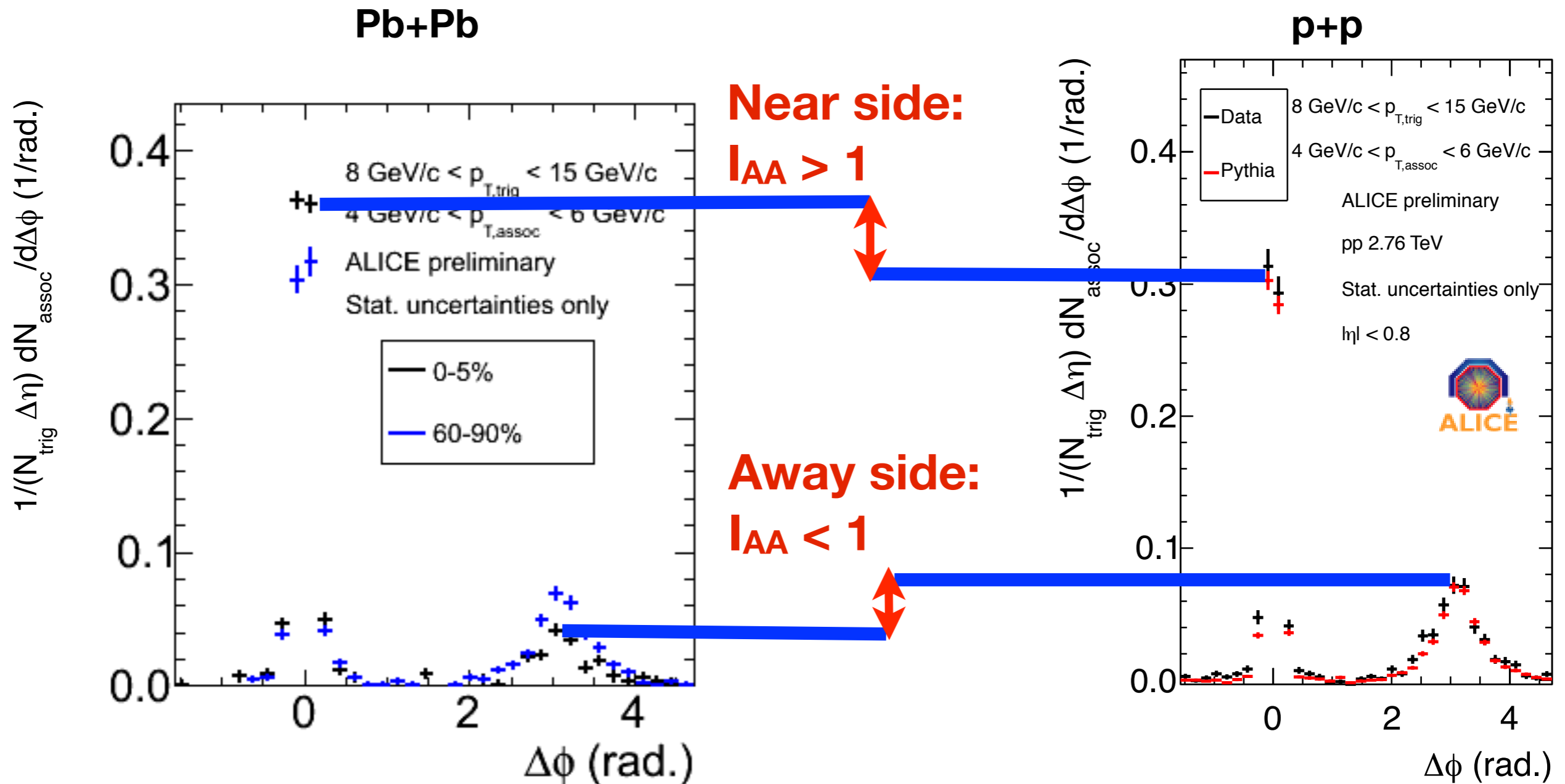
Compare  $1/N_{trig} dN/d\Delta\phi$  in Pb+Pb with:  
 peripheral for  $I_{CP}$   
 p+p for  $I_{AA}$

Integrate yields in selected  $\Delta\phi$  range

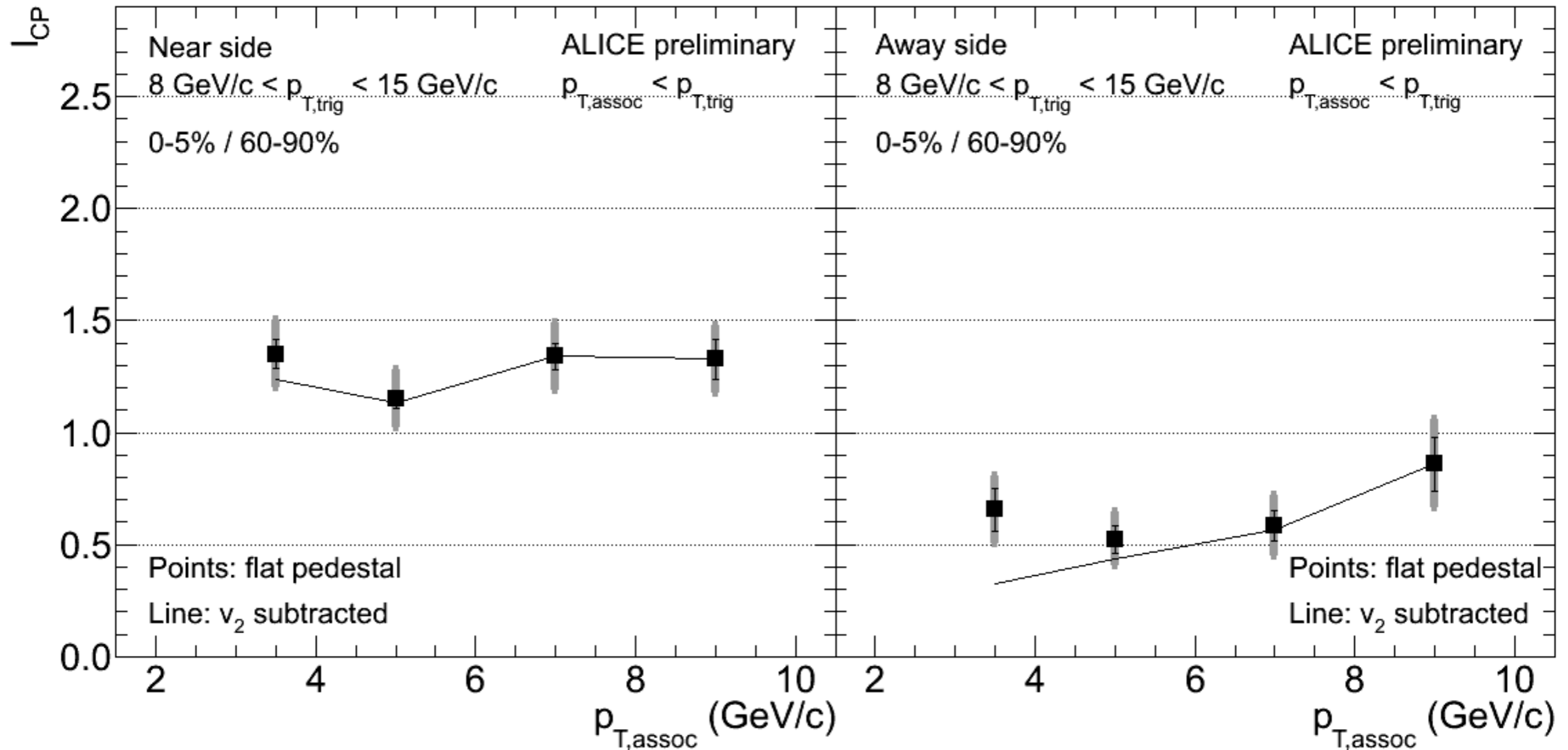
Here,  $0 (\pi) \pm 0.7$  for near (away) side

$$I_{AA}(p_{T,trig}; p_{T,assoc}) = \frac{Y^{AA}(p_{T,trig}; p_{T,assoc})}{Y^{PP}(p_{T,trig}; p_{T,assoc})}$$

$$I_{CP}(p_{T,trig}; p_{T,assoc}) = \frac{Y_{central}^{AA}(p_{T,trig}; p_{T,assoc})}{Y_{peripheral}^{AA}(p_{T,trig}; p_{T,assoc})}$$



# $I_{CP}$ on near and away side



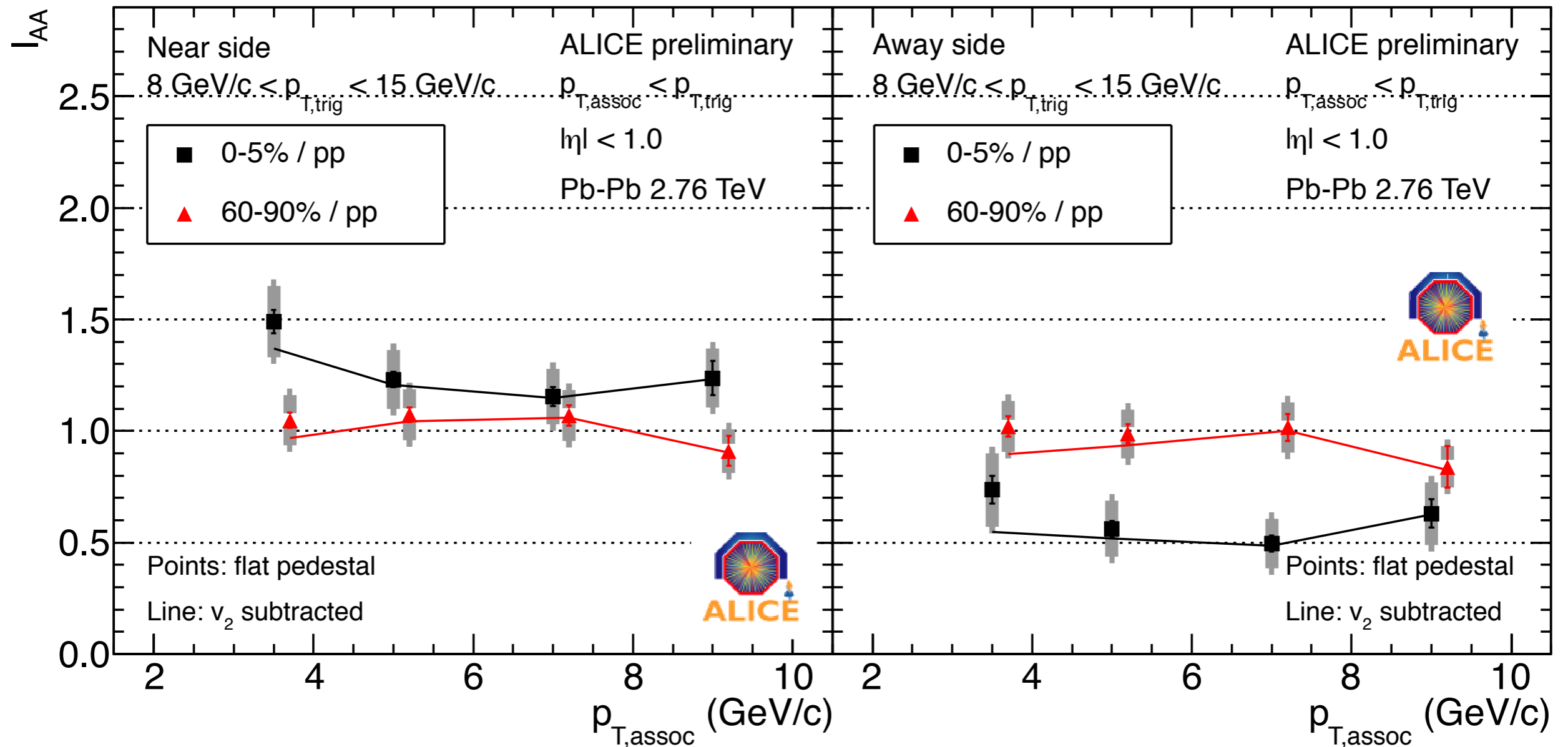
**Enhancement on near side, suppression on away side**

**Flat or  $v_2$ -only bkg. assumptions give same results above 5 GeV**

**Away side  $I_{AA} \sim 0.6$  at intermediate  $p_T$**

**Note on rise at last point:  $p_{T, \text{trig}} > p_{T, \text{assoc}}$  requirement in overlapping  $p_T$  bin influences kinematics: interpret with care.**

# $I_{AA}$ at 2.76 TeV



## Observations

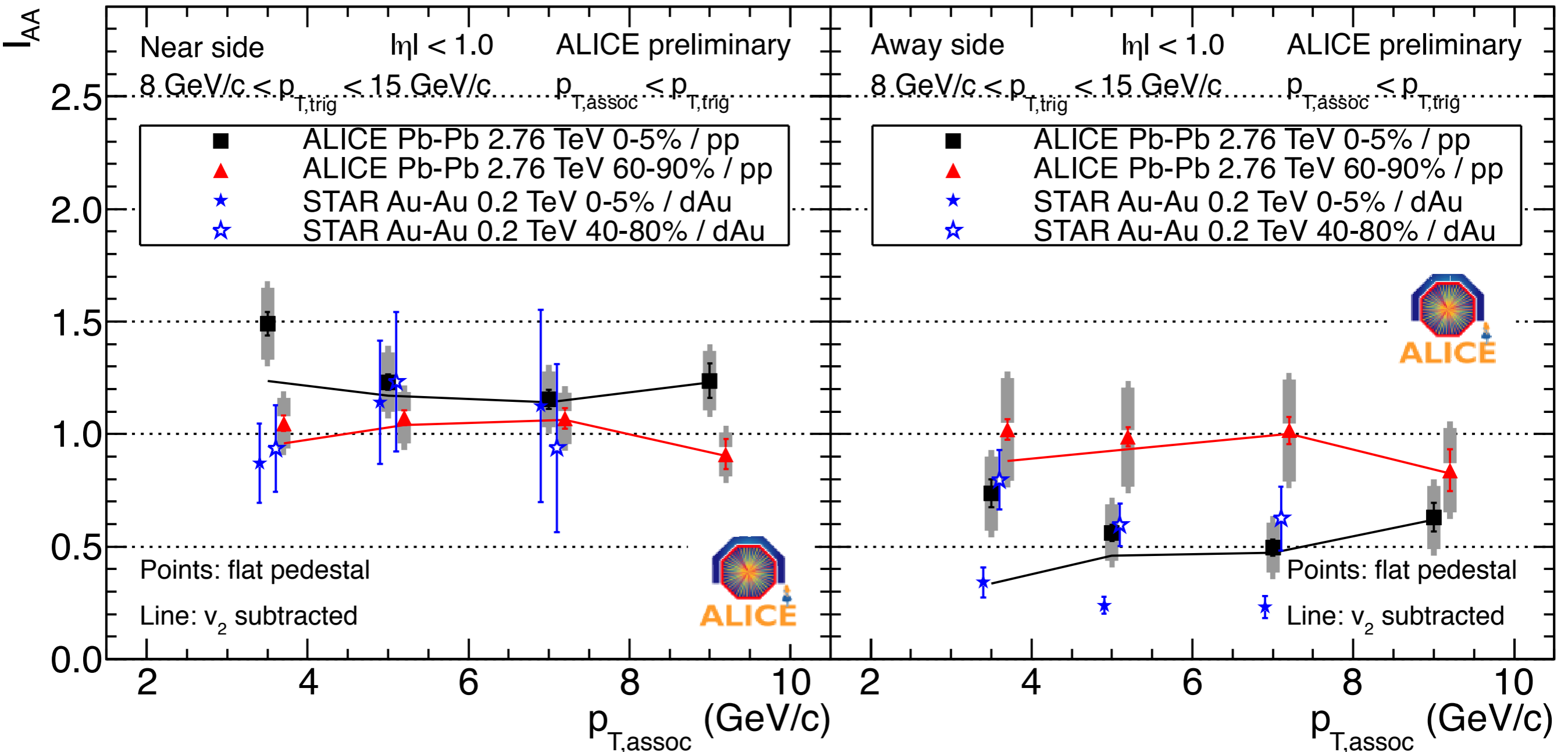
**Near side yields enhanced by 1.2-1.3 for  $p_{T,assoc} > 3$  GeV/c in central events**

**Some peripheral data consistent with 1**

**Away side 0.5-0.6 for central,  $\sim 1$  for peripheral**

# RHIC comparison

$I_{AA}$  consistent with STAR on both near and away side



# In summary:

---

**Ultracentral 2-peak away-side structure**

**Fully described by Fourier moments**

**No need to invoke conical emission**

**Long-range anisotropy**

**Low pt: fully consistent w/ std. flow techniques**

**High pt: break from collective behavior --> Recoil jet**

**First LHC  $I_{AA}$ ,  $I_{CP}$**

**Near side: moderate enhancement**

**Away-side: significant suppression**

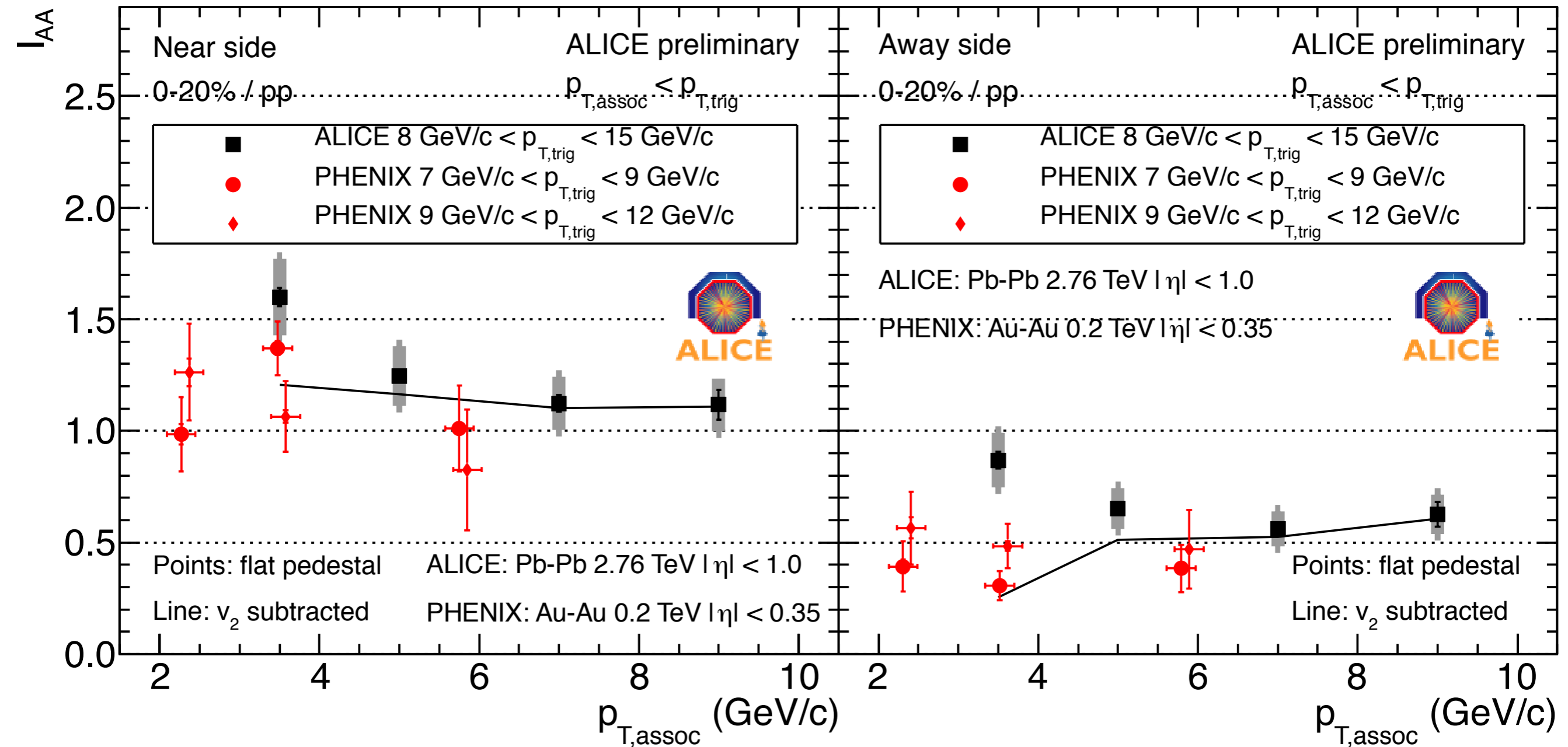
**Consistent with RHIC**

# Backups

---

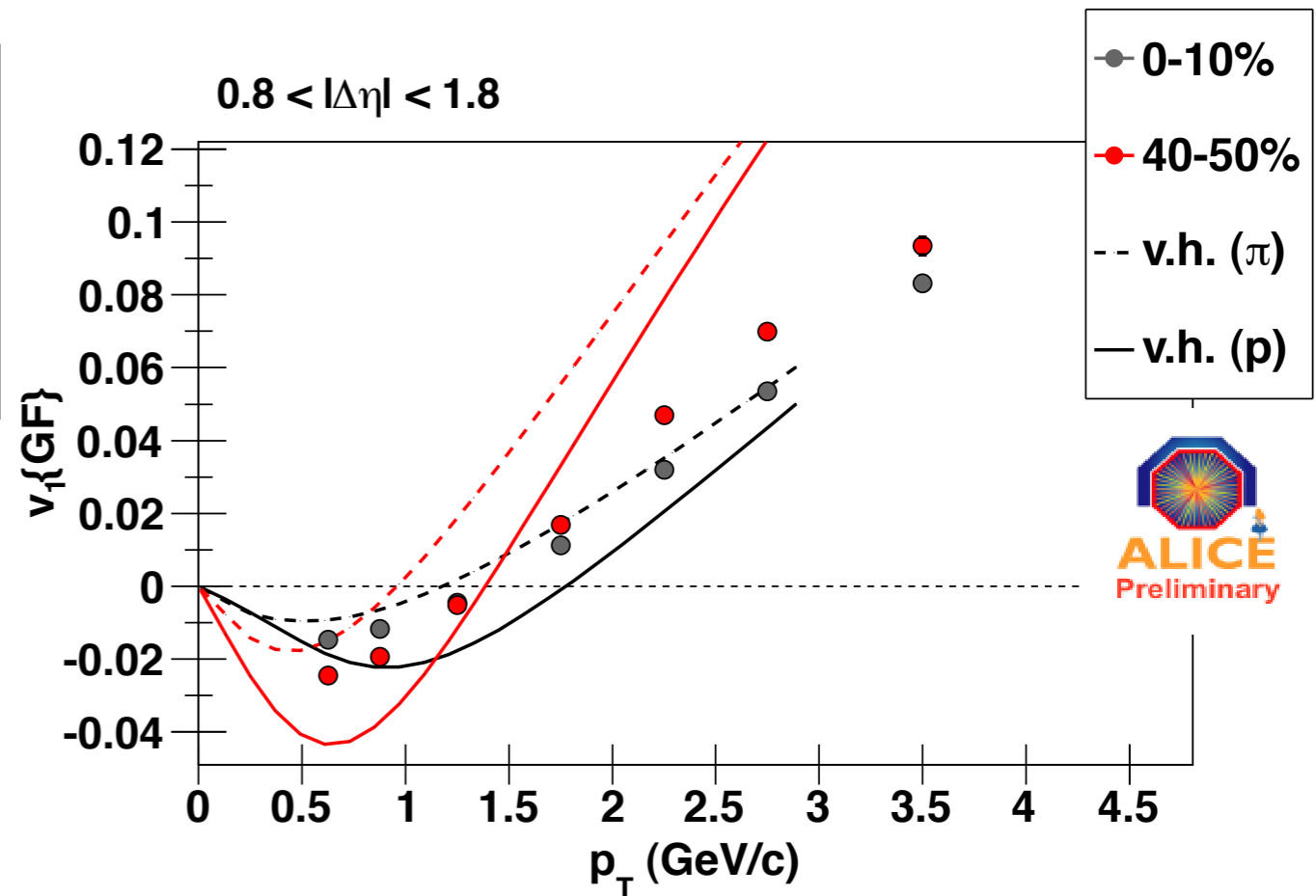
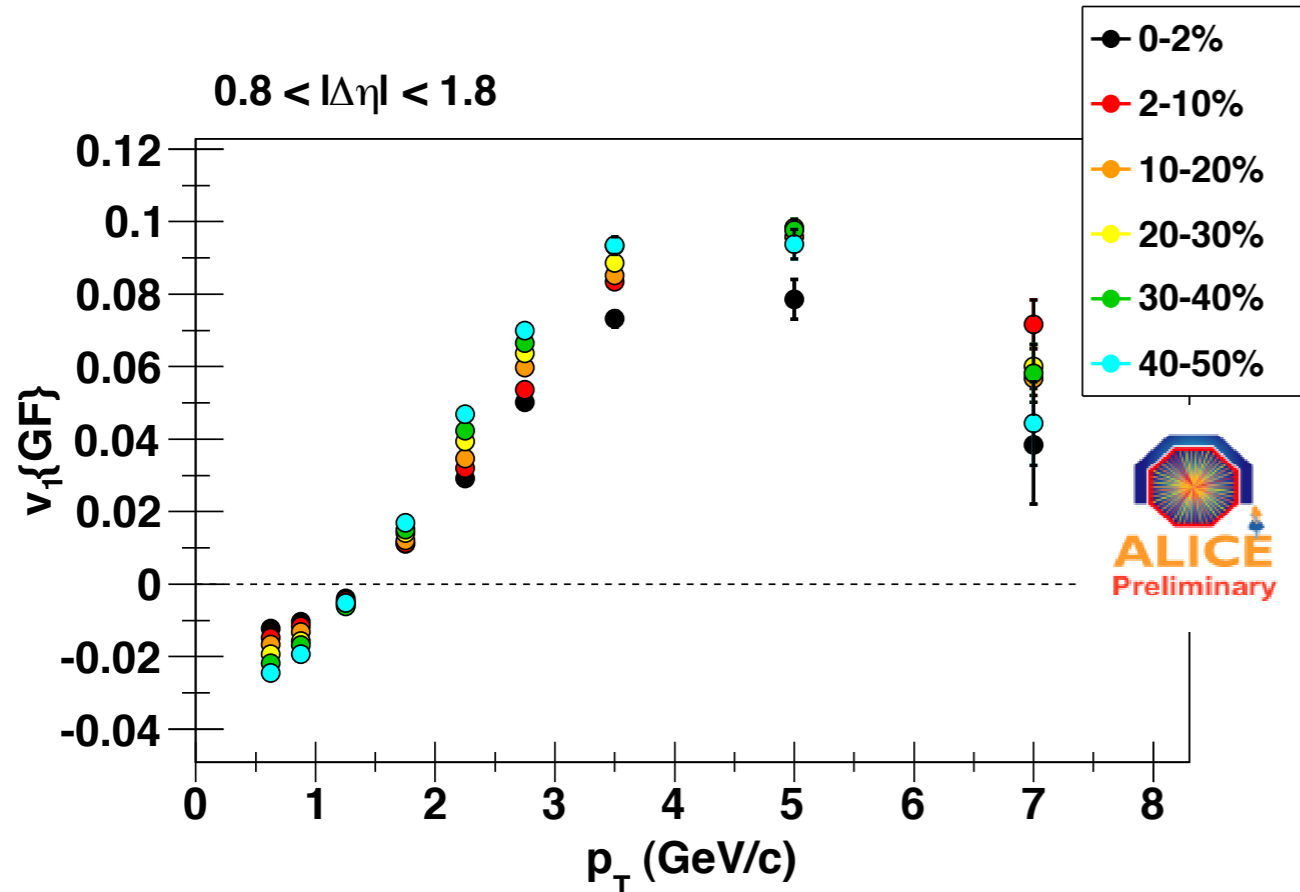
# PHENIX comparisons

$I_{AA}$  moderately higher than in PHENIX  
With limited statistical significance



# $v_1\{GF\}$ with $v_1$ hydro prediction

Very interesting, unfortunately no time



## Viscous hydro model by M. Luzum

Calculation from same framework as  $v_3$  result (arXiv:1007.5469)

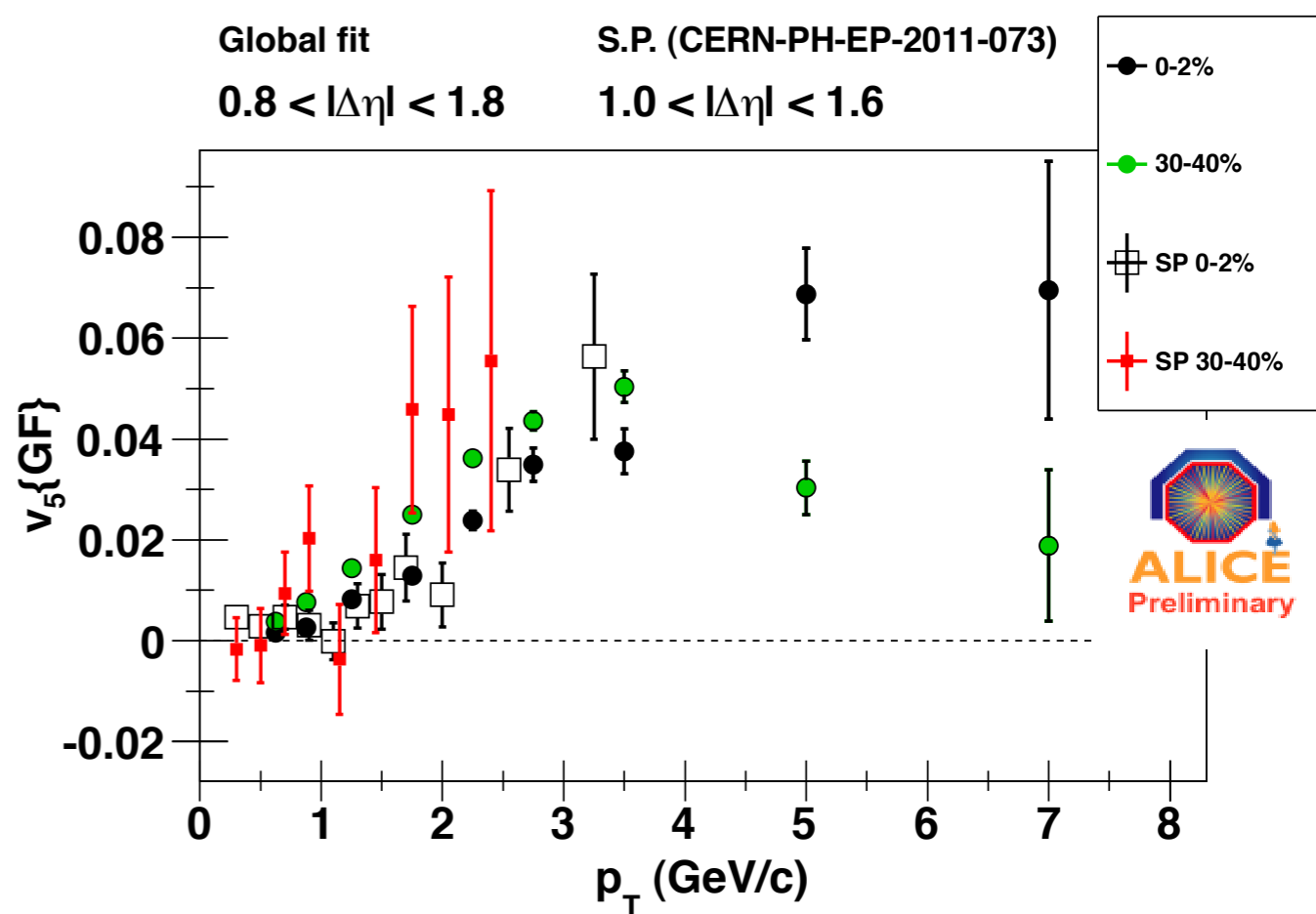
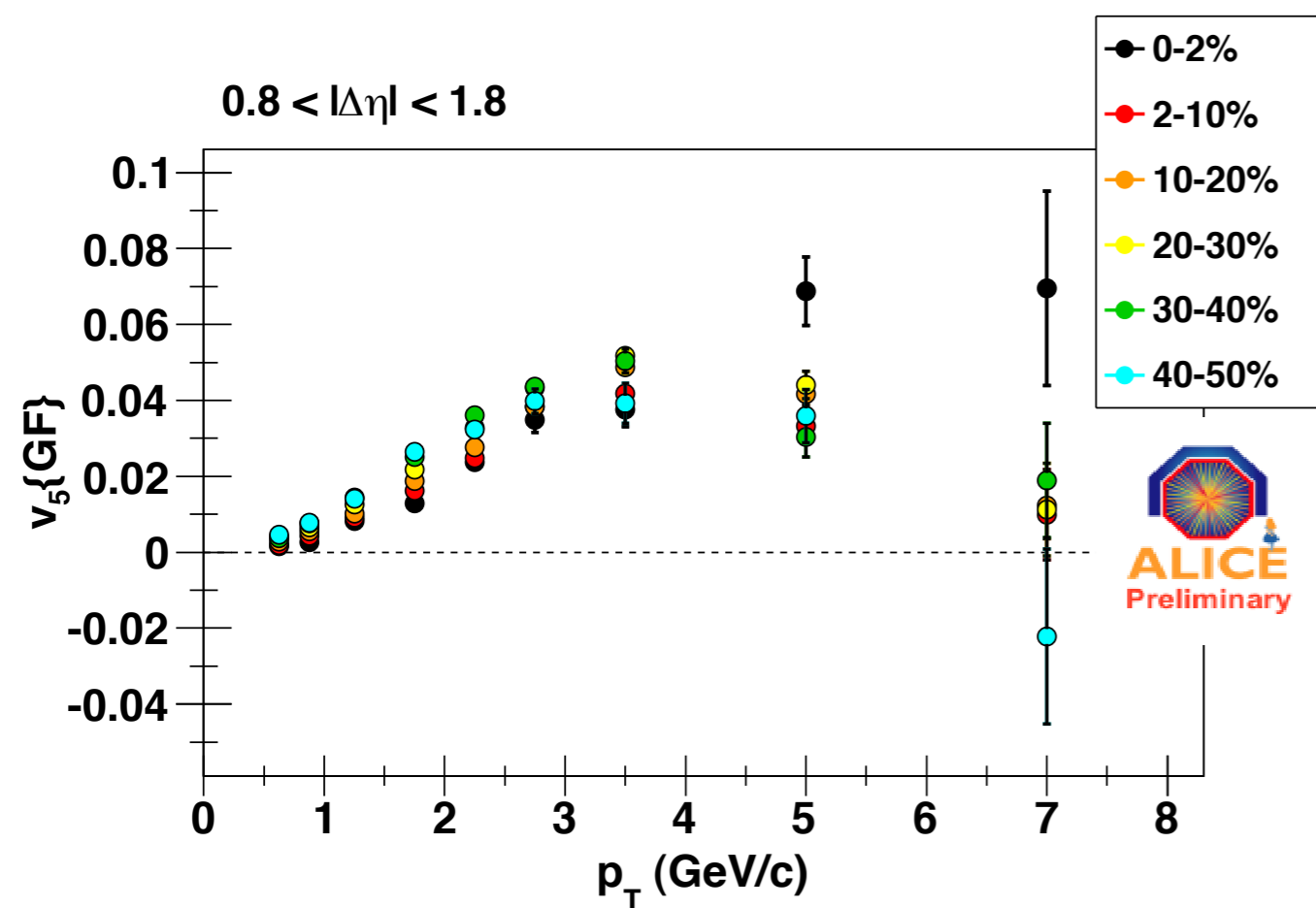
$\eta/s = 0.08$  for  $\pi$ , K (not shown), p using PHOBOS Glauber ICs

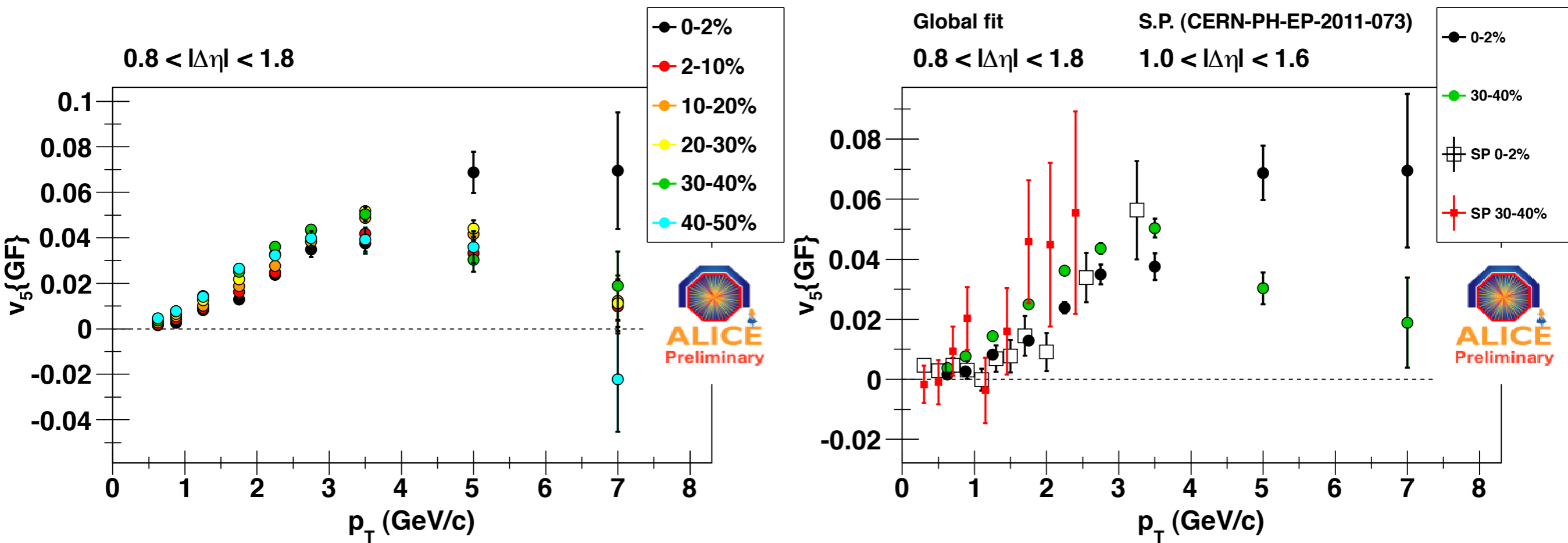
Good agreement for central data, less so for mid-central

Note: global fit includes particles only above 0.5 GeV, model uses all  $p_T$

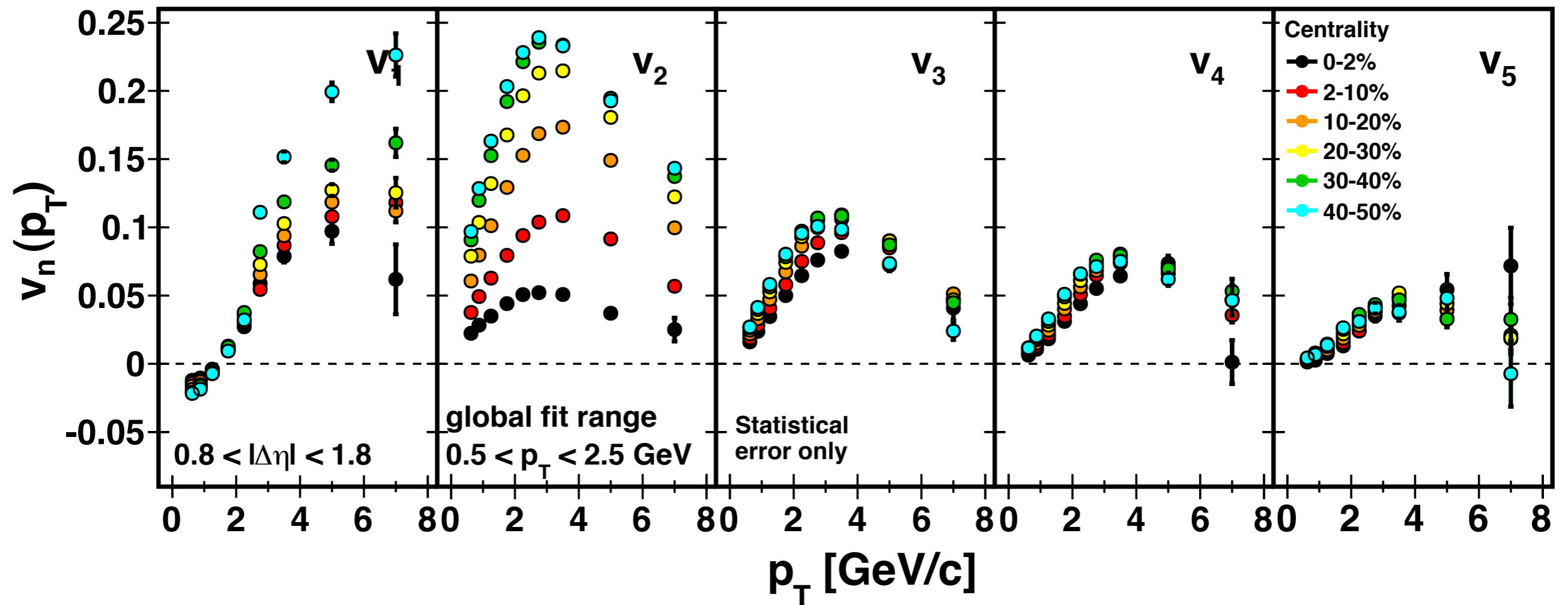


# $v_4\{GF\}$





# What if the high- $p_T$ points are excluded?

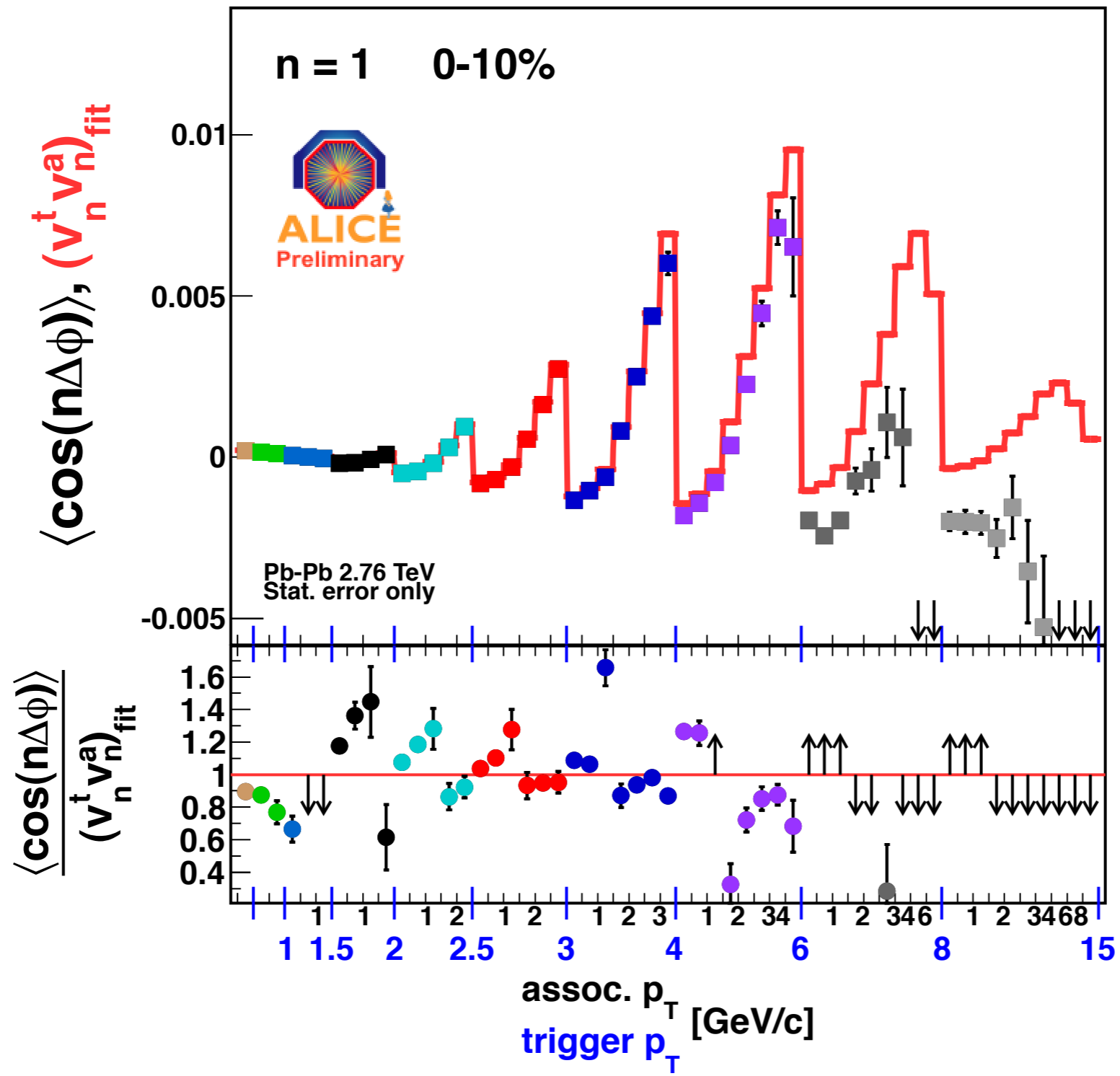


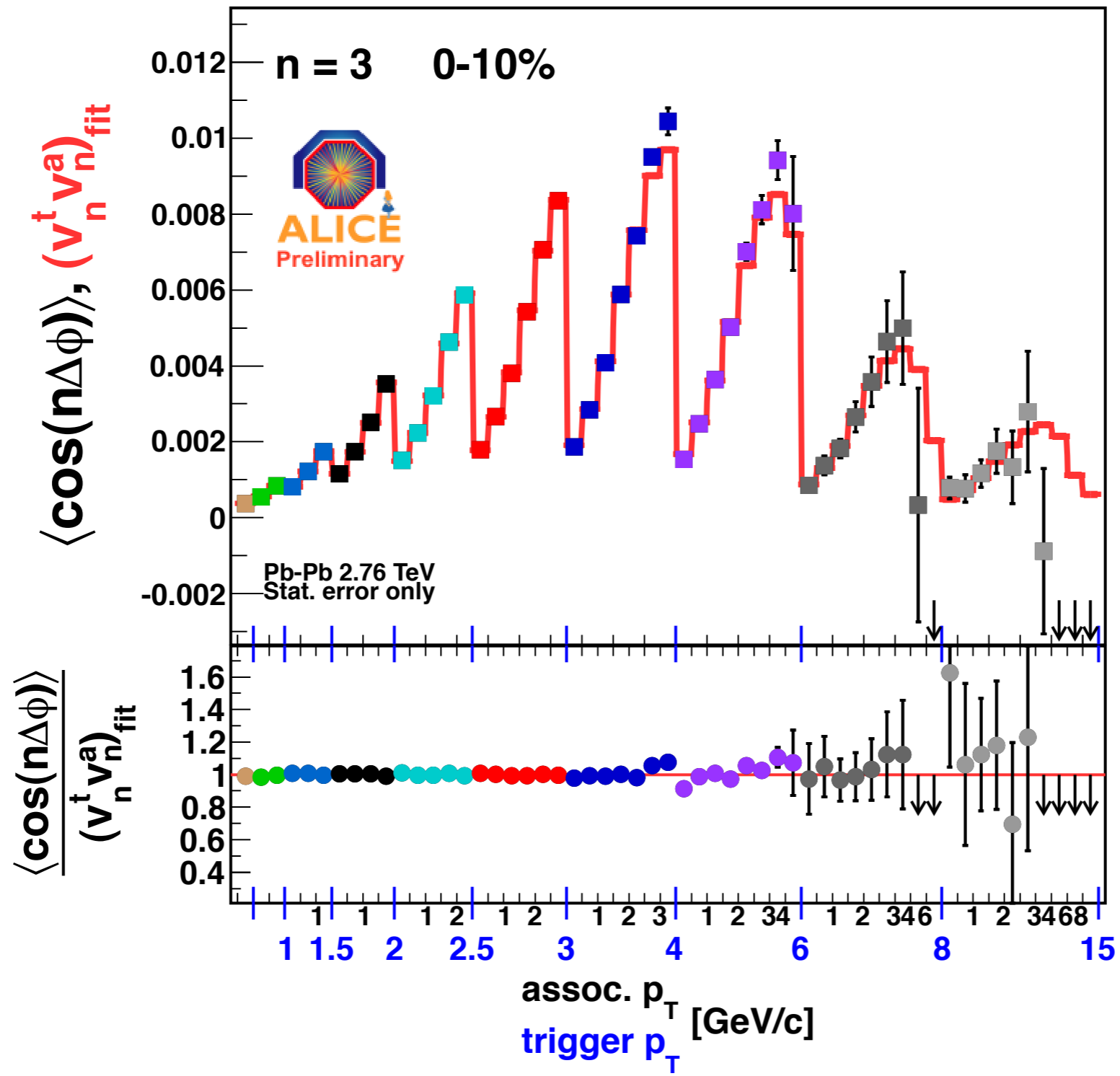
Here, information from  $p_T < 2.5$  GeV/c is used to constrain the fit.

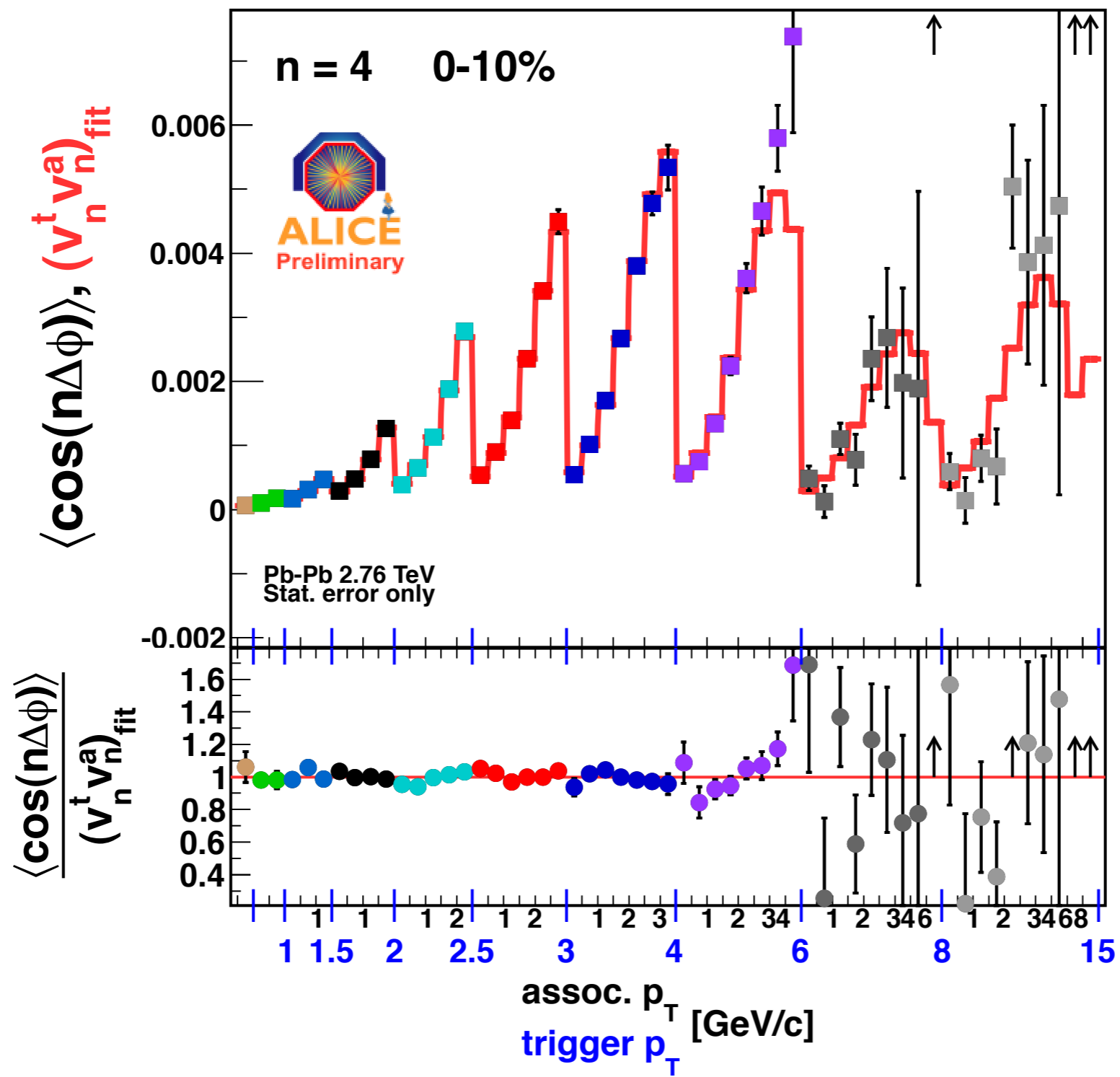
$v_2$ - $v_5$  only weakly affected

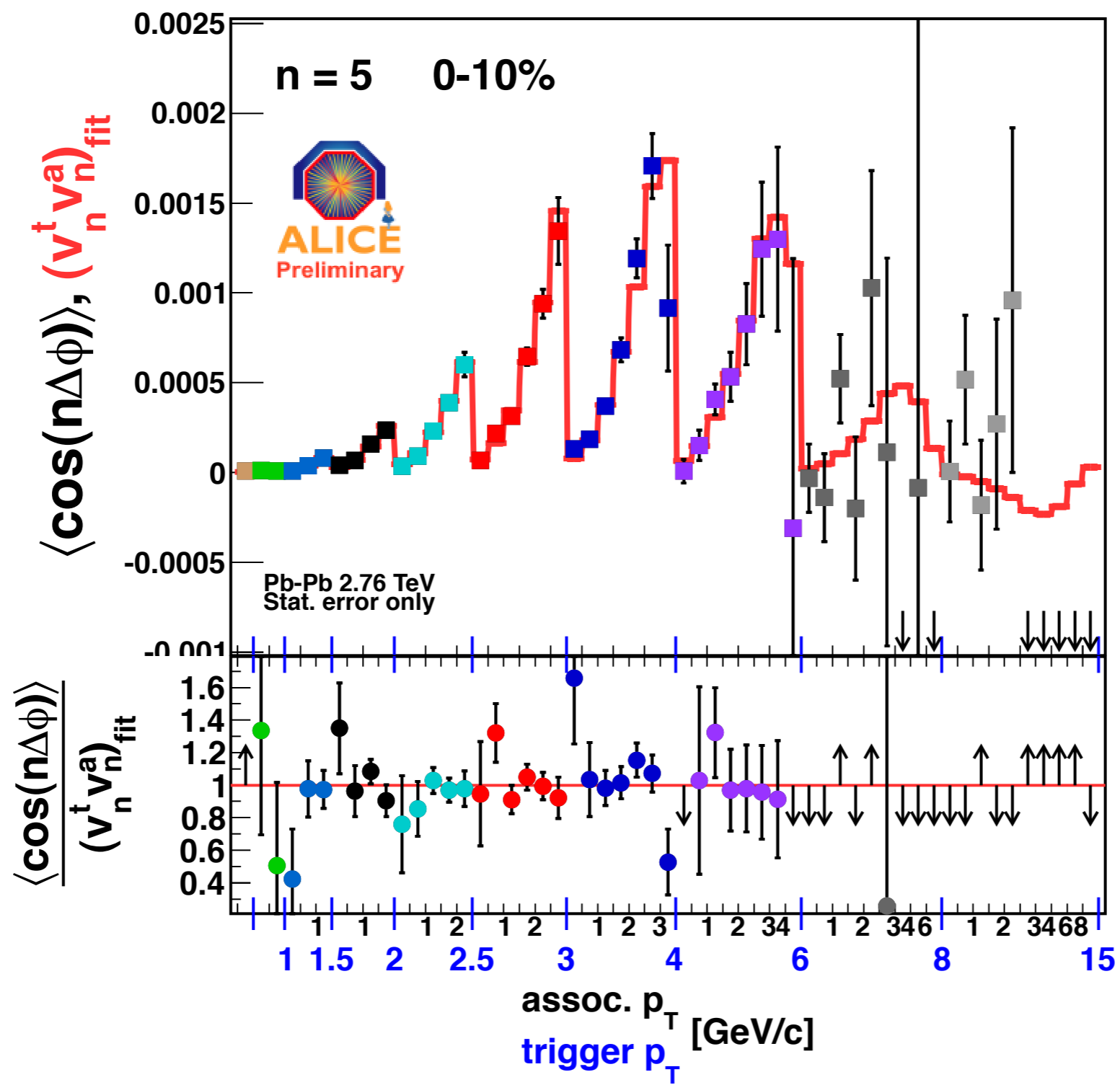
$v_1$  rises sharply at high  $p_T$

reflects momentum conservation?









# Understanding the near side

If  $\Delta E$  leads to  $I_{AA}^{\text{near}} > 1$ , then why wasn't this also seen at RHIC?

## 1. Phase space considerations

Steeper parton production at RHIC. There, high-pt triggers have larger  $z$ , lower assoc. yields.

## 2. Parton spectral shape:

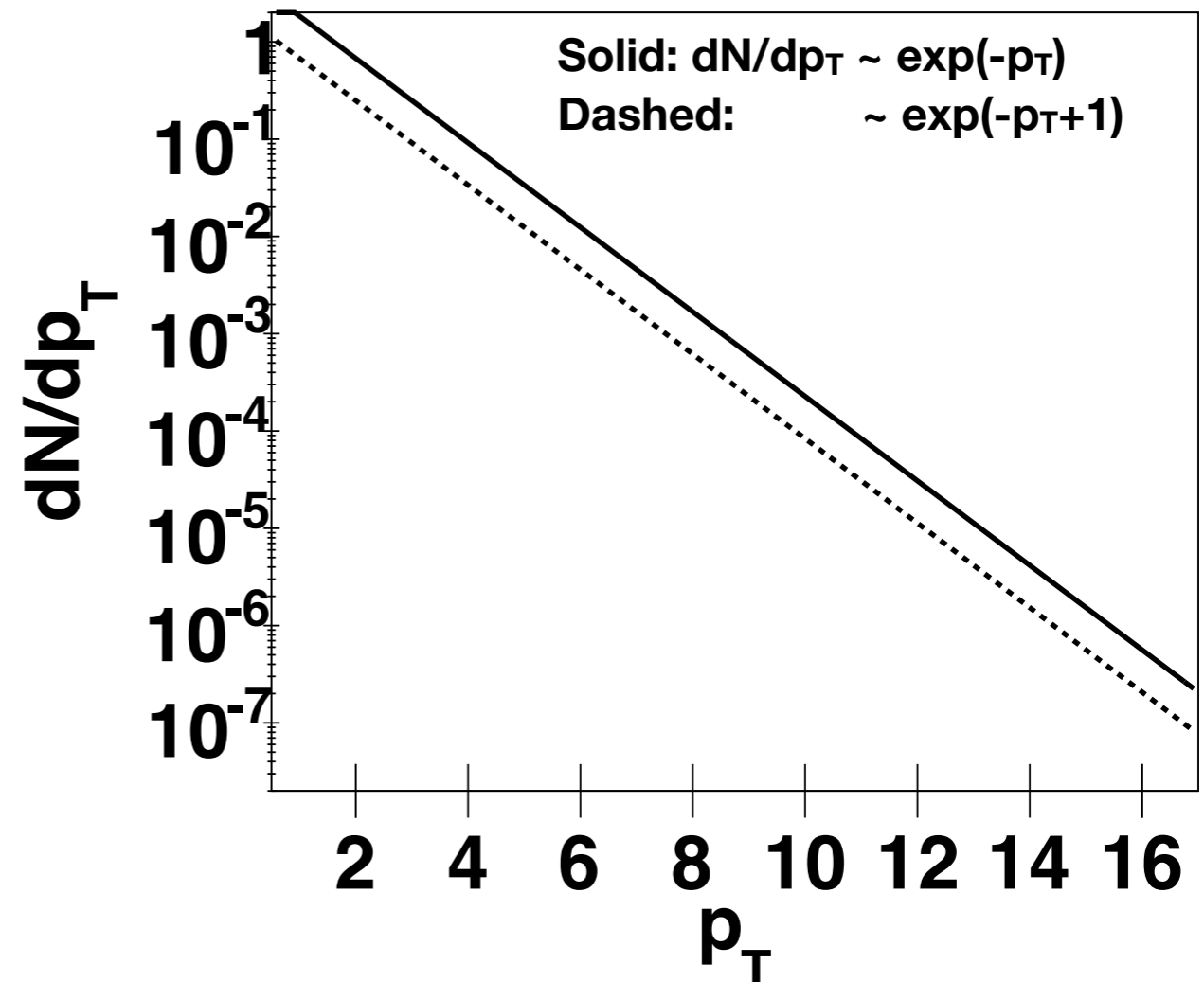
Consider a fixed  $\Delta E$

(i.e. every parton loses 1 GeV)

For an exponential, the slope is unchanged.  
Energy loss is independent of  $E$ .

Probing different parton energy by requiring a trigger particle does not change the associated per-trigger yield.

Thus  $I_{AA}$  can be 1 even for large  $\Delta E$ .  
Under these conditions, surface bias cannot be inferred from  $I_{AA}=1$ .





# Understanding the near side

If  $\Delta E$  leads to  $I_{AA}^{\text{near}} > 1$ , then why wasn't this also seen at RHIC?

## 1. Phase space considerations

Steeper parton production at RHIC. There, high-pt triggers have larger  $z$ , lower assoc. yields.

## 2. Parton spectral shape:

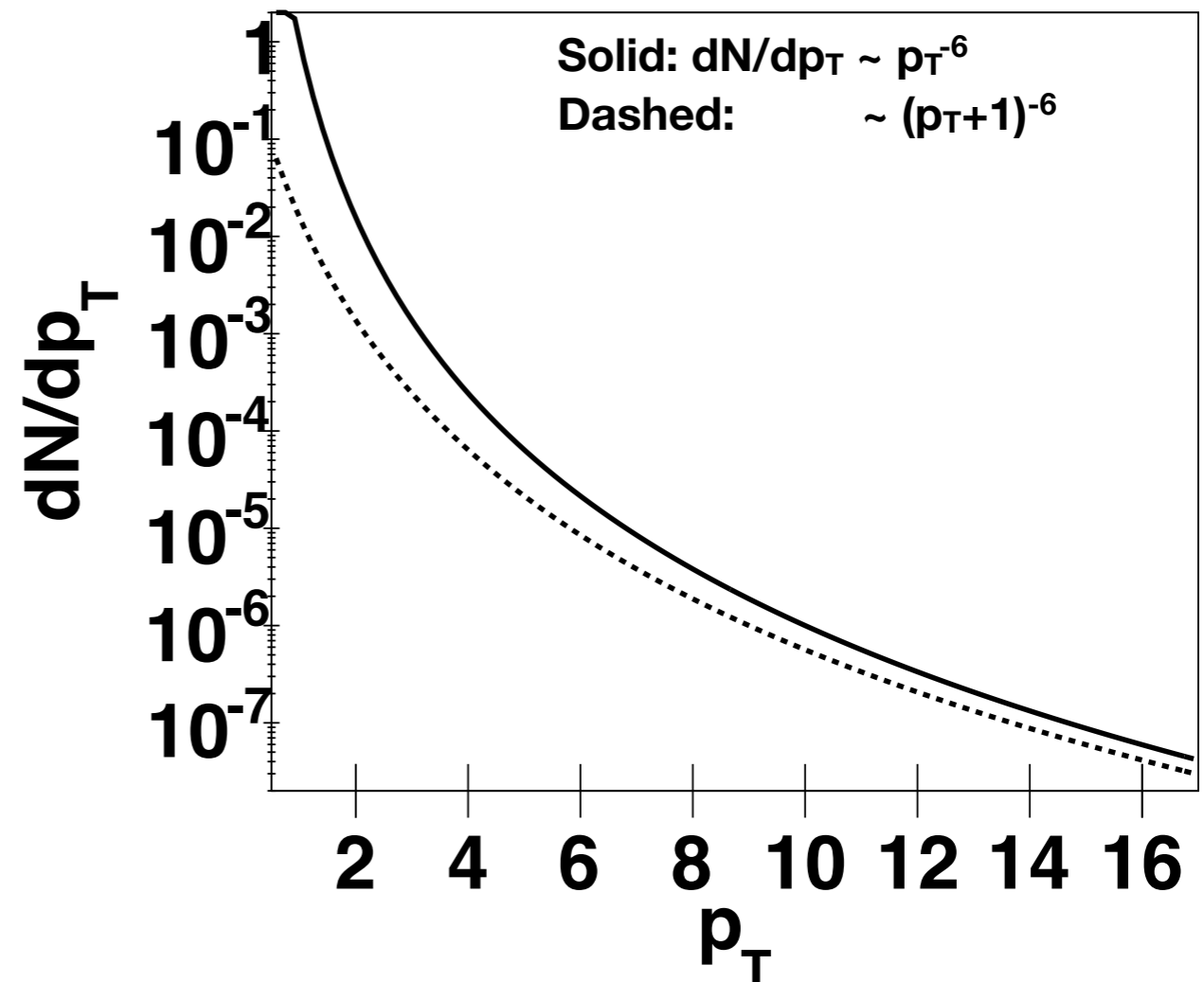
Consider a fixed  $\Delta E$

(i.e. every parton loses 1 GeV)

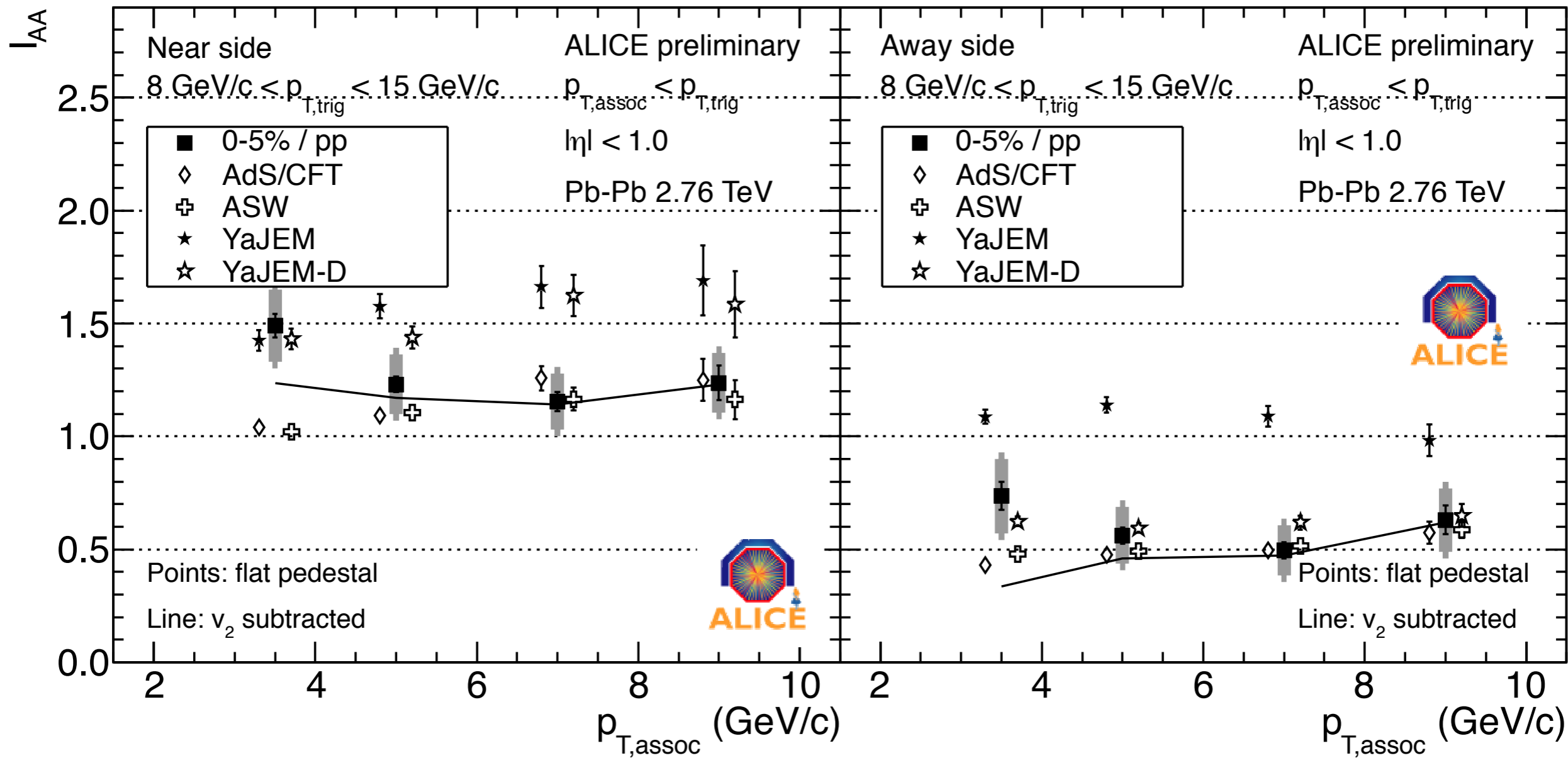
For a power law, the slope becomes flatter.

If phase space permits, the trigger requirement can lead to increased per-trigger associated yield.

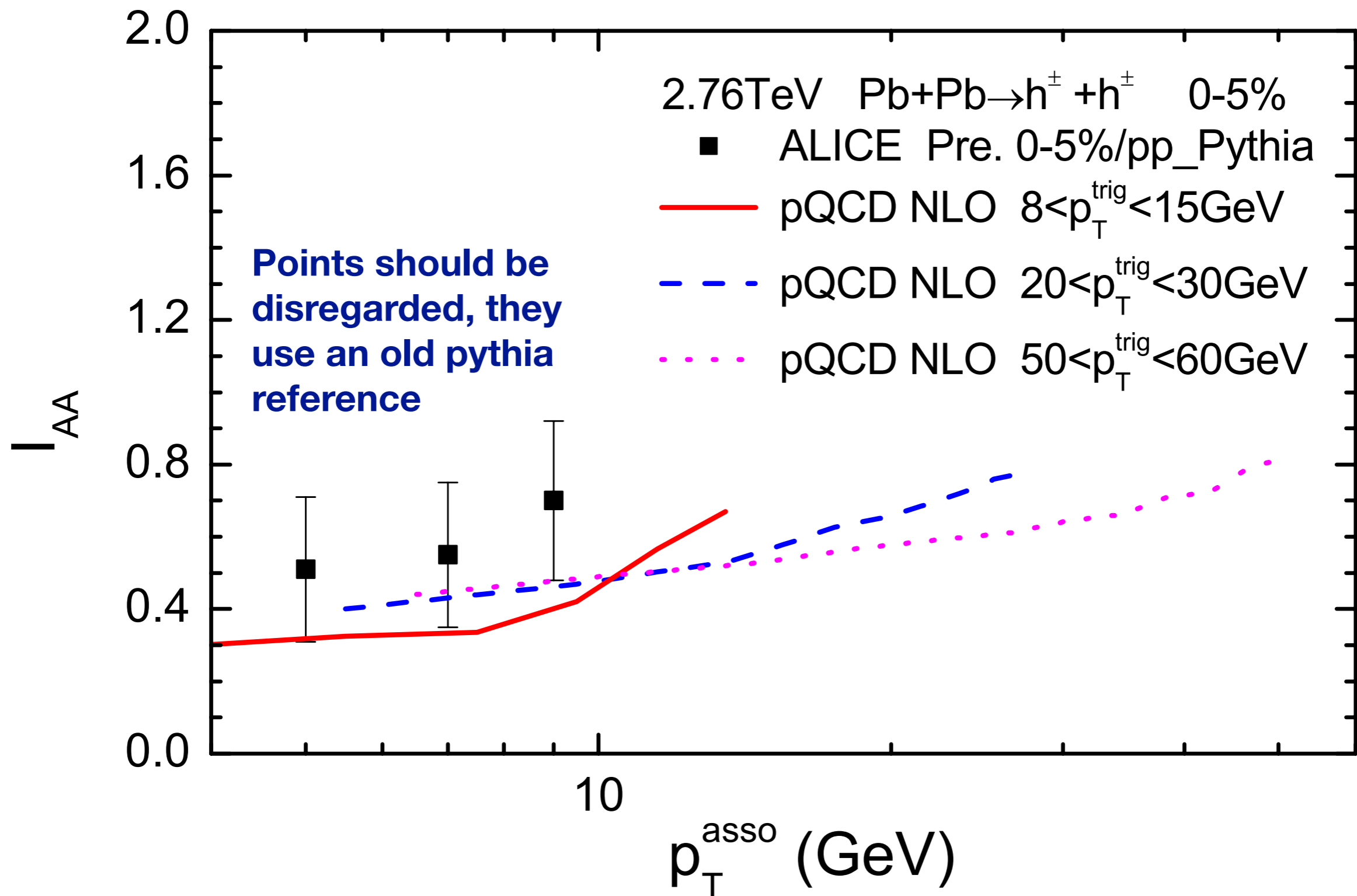
Thus  $I_{AA}$  can be  $> 1$ .



# YaJEM comparison



# From Xin-Nian Wang



# Jet yield extraction

## Handling background

The non-jet component must be characterized and removed

No known assumption-free methods...

Go to high pt for reduced bias

Trigger pt 8-15 GeV/c

Associated pt > 4 GeV/c, always with ptt > pta

Work with several bkg. shape/normalization schemes, compare

Differences gauge systematics

Ultimately ZYAM is used

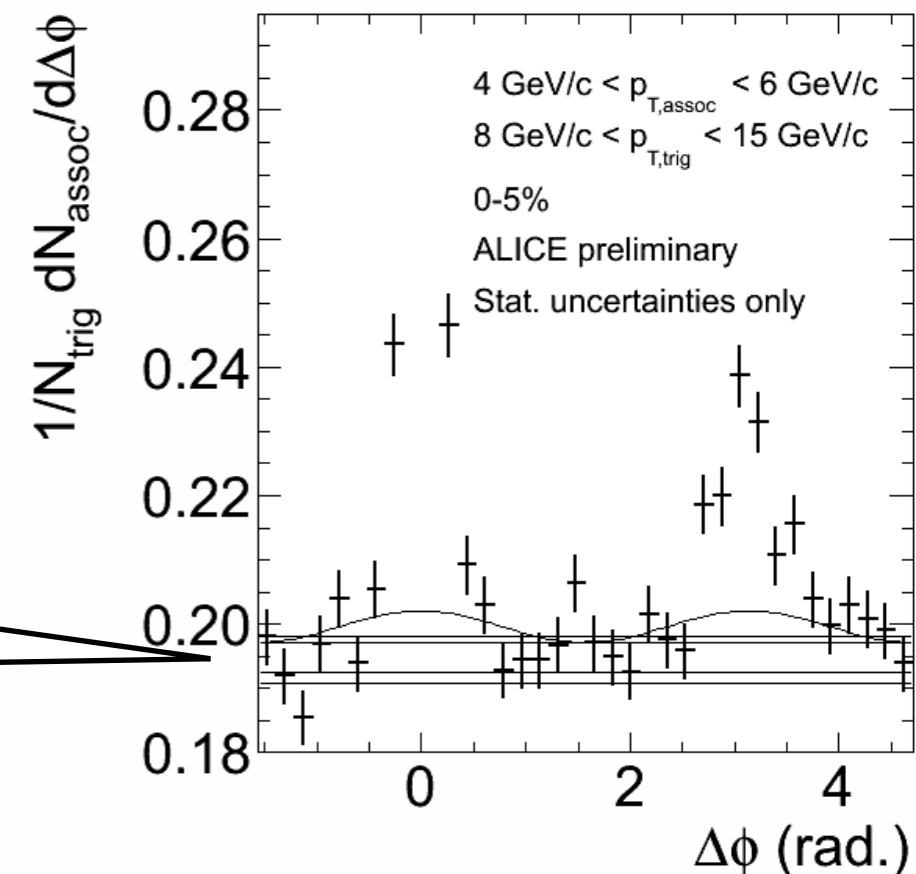
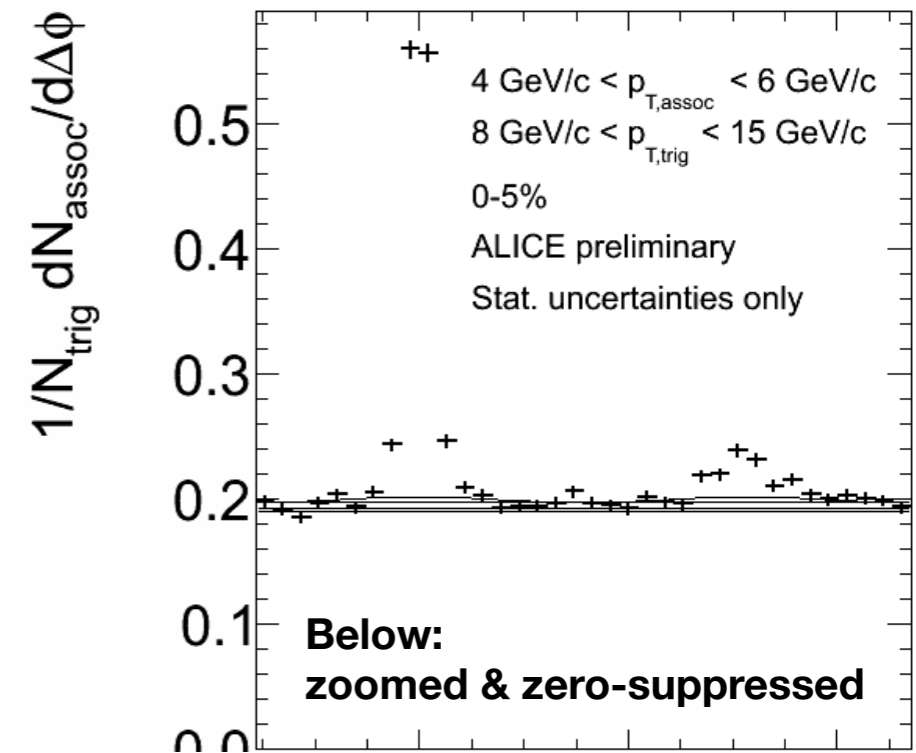
Different "M" definitions --> sys. uncertainty

### Different bkg shape ansatzes:

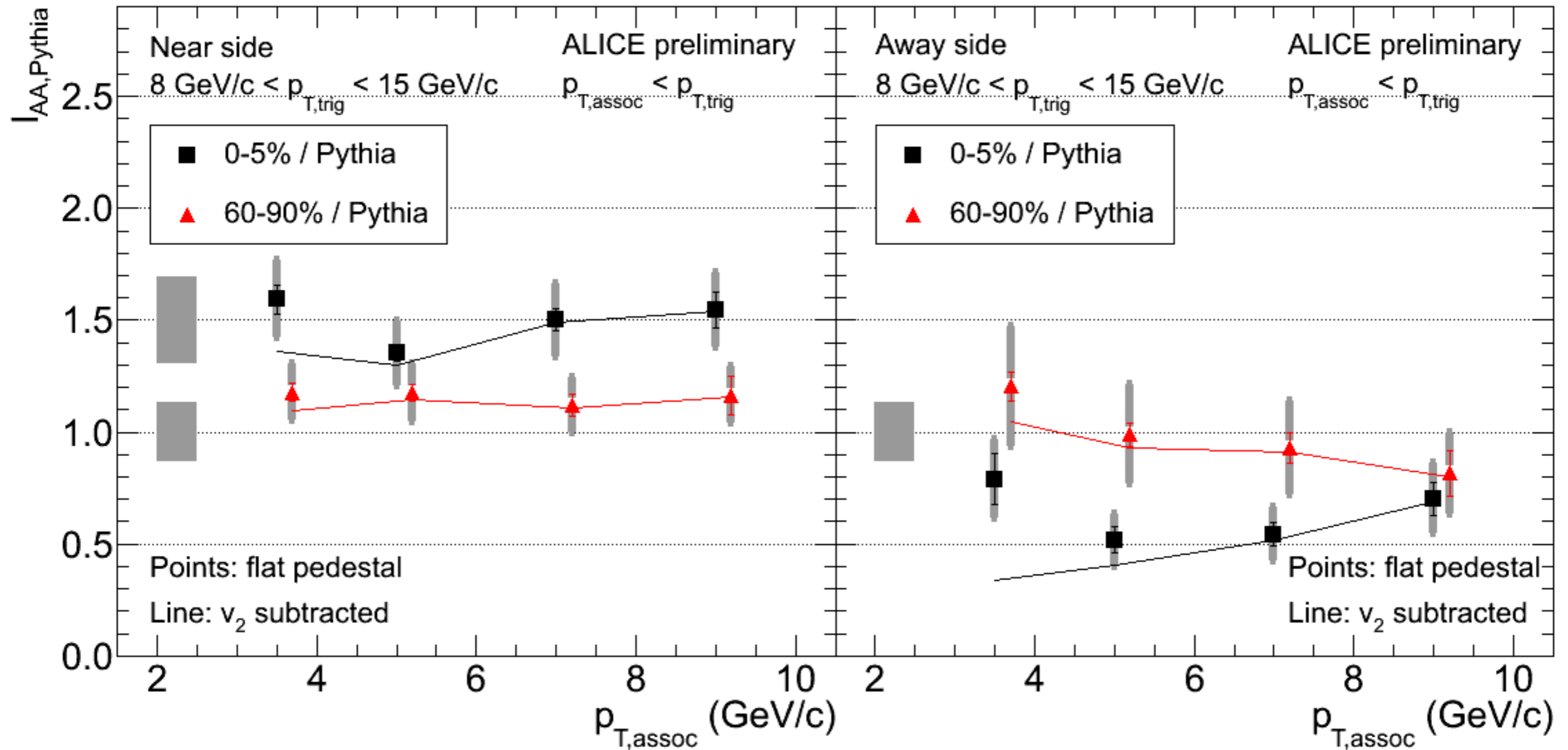
- v<sub>2</sub>-only
- flat pedestal

### Different ZYAM levels:

- n-lowest-bin averages
- const. fit over transverse region



# Utrecht :: $I_{AA}$ using pythia reference



## Observations

**Near side yields enhanced by 1.3-1.5 for  $p_{T,\text{assoc}} > 4 \text{ GeV/c}$  in central events**

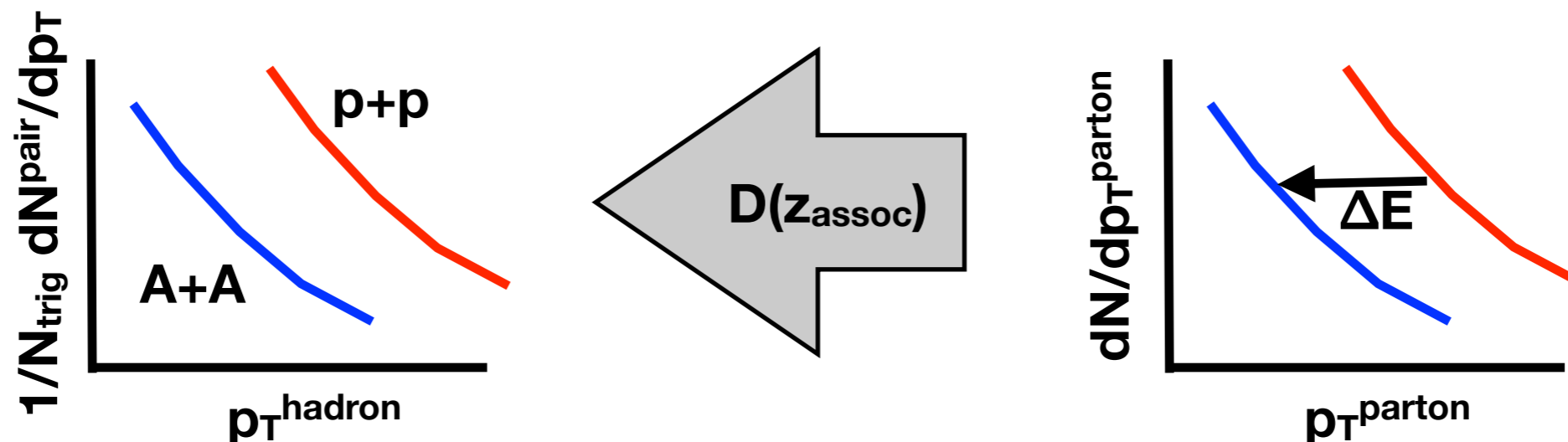
**Some enhancement measured even in peripheral data**

**Away side 0.5-0.7 for central,  $\sim 1$  for peripheral**

# Near-side vs. away-side $I_{AA}$

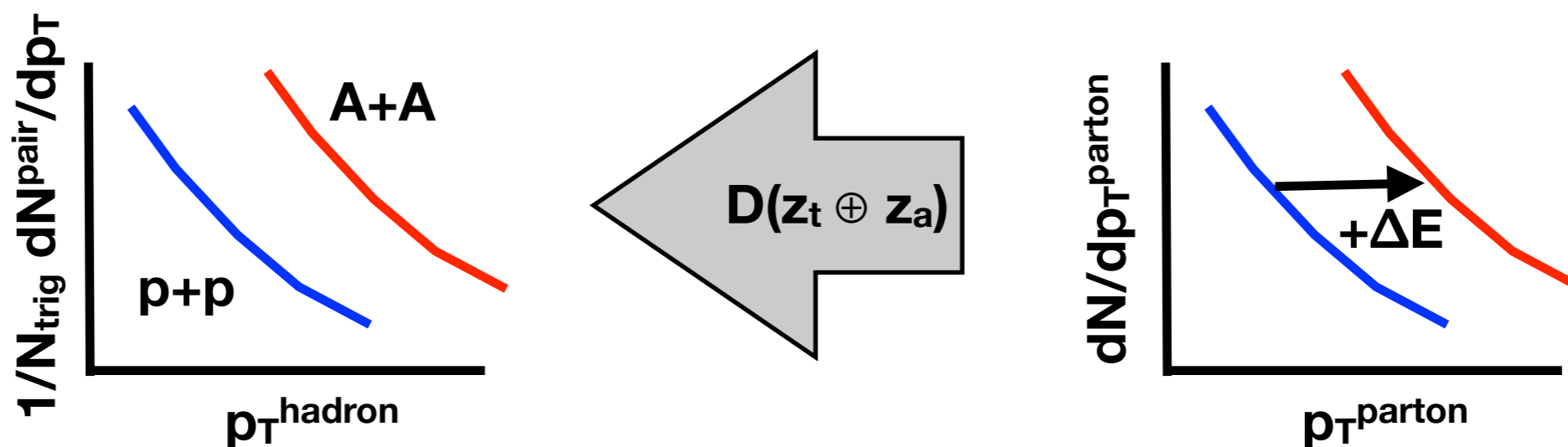
Consider partons losing  $\Delta E$ , then fragmenting in vacuum.

Away side:



$\Delta E$  lowers parton  $\langle p_T \rangle \Rightarrow$  fewer pairs/trigger in  $A+A$  on away side.

Near side:



Including the trigger particle requires partons at higher initial energies.

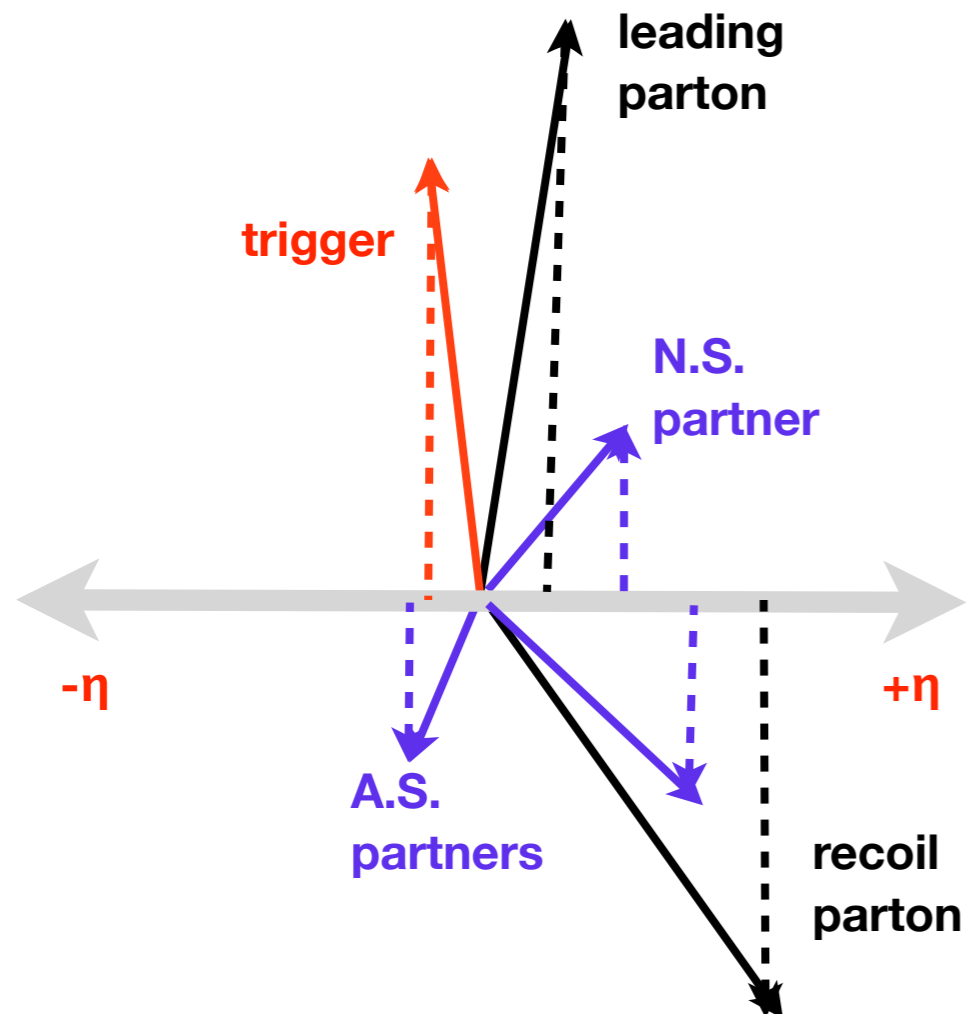
# Kinematics at the LHC vs. RHIC

## Near-side correlations

Requiring a trigger particle means  $p_{T,\text{parton}} > p_{T,\text{trig}} + p_{T,\text{assoc.}}$

## On the recoil side

No trigger:  $p_{T,\text{parton}} > p_{T,\text{assoc.}}$



# Kinematics at the LHC vs. RHIC

## Near-side correlations

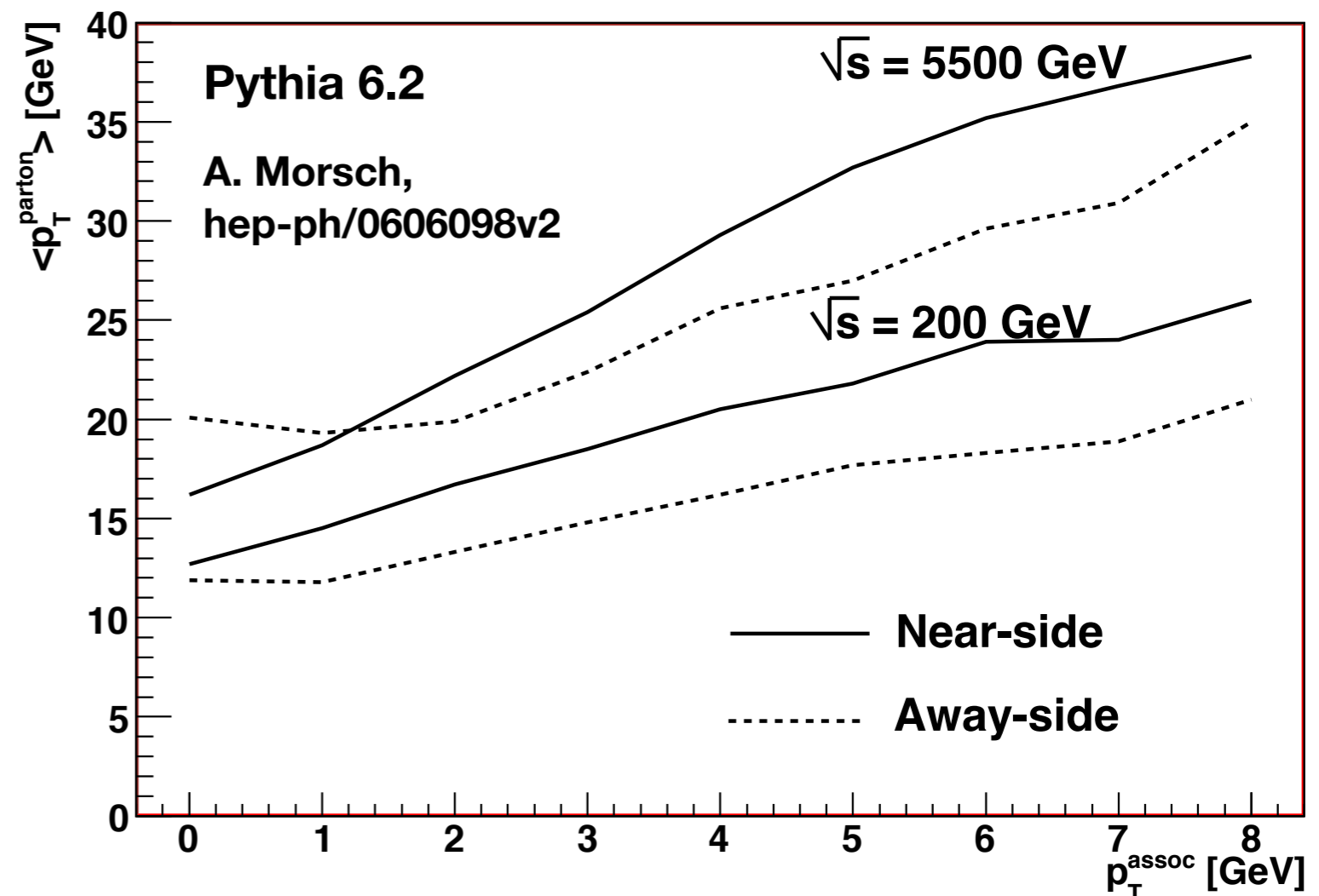
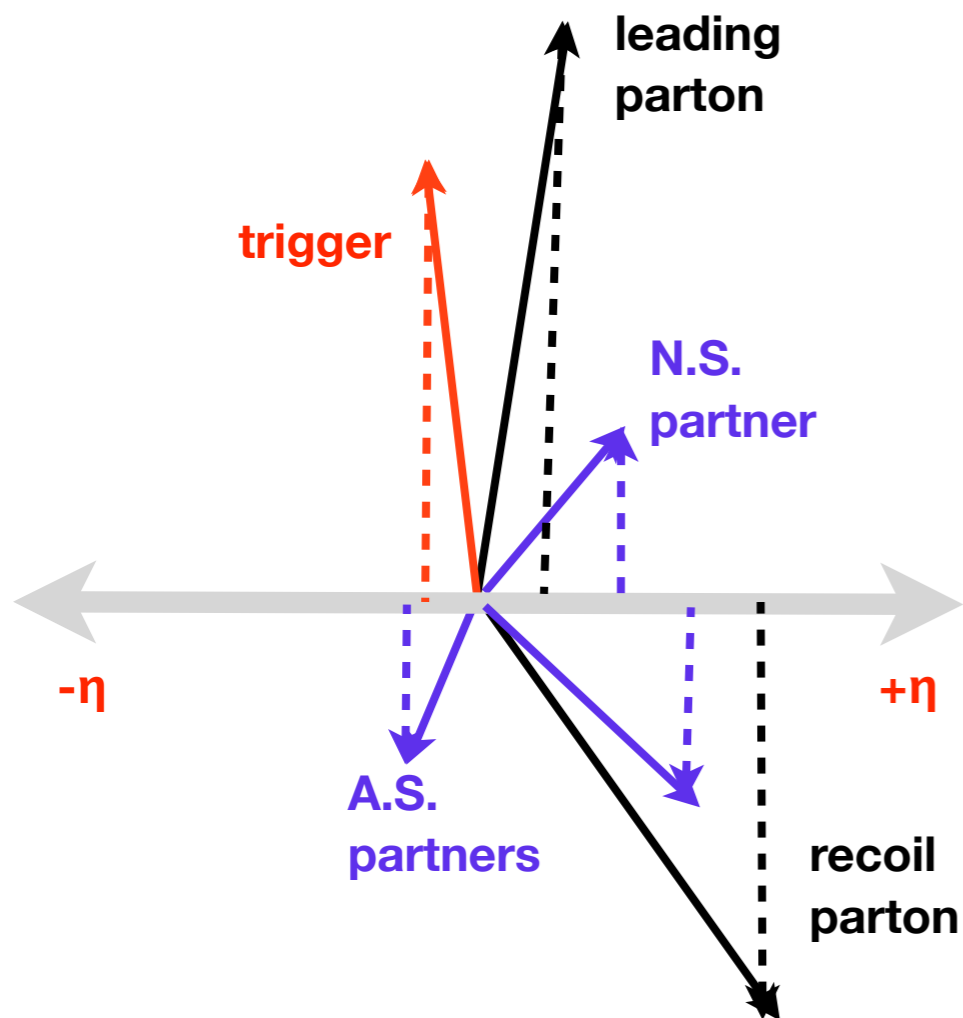
Requiring a trigger particle means  $p_{T,\text{parton}} > p_{T,\text{trig}} + p_{T,\text{assoc}}$ .

## On the recoil side

No trigger:  $p_{T,\text{parton}} > p_{T,\text{assoc}}$ .

## Parton $p_T$ vs. associated $p_T - p_{T,\text{trig}} > 8 \text{ GeV}/c$ :

- Near side samples higher  $p_{T,\text{parton}}$  than away side
- At fixed  $p_{T,\text{trig}}$  &  $p_{T,\text{assoc}}$ , much larger  $p_{T,\text{parton}}$  at LHC







## Systematic Uncertainties

- Detector efficiency and two-track effects
- Different detectors for centrality determination
- $p_T$  resolution
  - Fold associated  $p_T$  distribution with momentum resolution
- Different pedestal determination schemes
- Integration window (between  $\pm 0.5$  rad. and  $\pm 0.9$  rad.)

Detector efficiency	5-8%
Centrality selection	2-8%
$p_T$ resolution	3%
Pedestal calculation	7-20%
Integration window	0-3%

Ranges indicate different values for  $I_{CP}^{AA,Pythia}$  and near/away side